

University of Windsor

Scholarship at UWindor

Electronic Theses and Dissertations

Theses, Dissertations, and Major Papers

1979

THE METABOLISM OF 3-DEOXY-3-FLUORO-D-GLUCOSE BY LOCUSTA MIGRATORIA.

ALEXANDER DIMITRI. ROMASCHIN
University of Windsor

Follow this and additional works at: <https://scholar.uwindsor.ca/etd>

Recommended Citation

ROMASCHIN, ALEXANDER DIMITRI., "THE METABOLISM OF 3-DEOXY-3-FLUORO-D-GLUCOSE BY LOCUSTA MIGRATORIA." (1979). *Electronic Theses and Dissertations*. 4103.
<https://scholar.uwindsor.ca/etd/4103>

This online database contains the full-text of PhD dissertations and Masters' theses of University of Windsor students from 1954 forward. These documents are made available for personal study and research purposes only, in accordance with the Canadian Copyright Act and the Creative Commons license—CC BY-NC-ND (Attribution, Non-Commercial, No Derivative Works). Under this license, works must always be attributed to the copyright holder (original author), cannot be used for any commercial purposes, and may not be altered. Any other use would require the permission of the copyright holder. Students may inquire about withdrawing their dissertation and/or thesis from this database. For additional inquiries, please contact the repository administrator via email (scholarship@uwindsor.ca) or by telephone at 519-253-3000ext. 3208.



National Library of Canada

Cataloguing Branch
Canadian Theses Division

Ottawa, Canada
K1A 0N4

Bibliothèque nationale du Canada

Direction du catalogage
Division des thèses canadiennes

NOTICE

The quality of this microfiche is heavily dependent upon the quality of the original thesis submitted for microfilming. Every effort has been made to ensure the highest quality of reproduction possible.

If pages are missing, contact the university which granted the degree.

Some pages may have indistinct print especially if the original pages were typed with a poor typewriter ribbon or if the university sent us a poor photocopy.

Previously copyrighted materials (journal articles, published tests, etc.) are not filmed.

Reproduction in full or in part of this film is governed by the Canadian Copyright Act, R.S.C. 1970, c. C-30. Please read the authorization forms which accompany this thesis.

**THIS DISSERTATION
HAS BEEN MICROFILMED
EXACTLY AS RECEIVED**

AVIS

La qualité de cette microfiche dépend grandement de la qualité de la thèse soumise au microfilmage. Nous avons tout fait pour assurer une qualité supérieure de reproduction.

S'il manque des pages, veuillez communiquer avec l'université qui a conféré le grade.

La qualité d'impression de certaines pages peut laisser à désirer, surtout si les pages originales ont été dactylographiées à l'aide d'un ruban usé ou si l'université nous a fait parvenir une photocopie de mauvaise qualité.

Les documents qui font déjà l'objet d'un droit d'auteur (articles de revue, examens publiés, etc.) ne sont pas microfilmés.

La reproduction, même partielle, de ce microfilm est soumise à la Loi canadienne sur le droit d'auteur, SRC 1970, c. C-30. Veuillez prendre connaissance des formules d'autorisation qui accompagnent cette thèse.

**LA THÈSE A ÉTÉ
MICROFILMÉE TELLE QUE
NOUS L'AVONS REÇUE**

THE METABOLISM OF
3-DEOXY-3-FLUORO-D-GLUCOSE
BY LOCUSTA MIGRATORIA

by

Alexander Dimitri Romaschin.

A Dissertation
submitted to the Faculty of Graduate Studies
through the Department of
Chemistry in Partial Fulfillment
of the requirements for the Degree
of Doctor of Philosophy at
The University of Windsor

Windsor, Ontario, Canada

1978

©

Alexander Dimitri Romaschin
All Rights Reserved

1978

708191

TABLE OF CONTENTS

ABSTRACT.....		iii
DEDICATION.....		v
ACKNOWLEDGEMENTS.....		vi
LIST OF TABLES.....		vii
LIST OF FIGURES.....		viii
LIST OF APPENDICES.....		xi
LIST OF ABBREVIATIONS.....		xii
CHAPTER		
1	INTRODUCTION - PART I.....	1
11	MATERIALS AND METHODS.....	54
	Reagents	
	Equipment	
	Synthesis of 3FG and 3FGL	
	Locust Rearing Conditions	
	Injection Procedures and 3FGL Toxicity Study	
	Enzyme Isolation and Sorbitol Dehydrogenase and Aldose Reductase	
	Enzyme kinetics and Derivation	
	Reaction Scheme	
	Enzyme Recycling Scheme	
	Glyoxylate Colorimetric Assay	
111	RESULTS AND DISCUSSION.....	65
IV	INTRODUCTION - PART II.....	106
V	MATERIALS AND METHODS.....	111
	Reagents	
	Equipment	
	Glucose Isotope Dilution Study	
	Locust Extracellular Fluid Volume Measurements	
	Radiorespirometric Apparatus	
	Gas Chromatographic Determination	
	Liquid Scintillation Counting	
	Tritiated 3FG Preparation	

Assay of $^3\text{H}_2\text{O}$ from Locust Tissue Extracts
Isolation of Tritiated Phosphorylated Sugars
Separation of Phosphorylated Metabolites on
P.E.I. Cellulose Thin Layer Chromatographic
Plates
Procedure for Spraying P.E.I. Cellulose Plates
Preparation of Phosphorylated Metabolites
for Fourier Transform NMR
Fourier Transform NMR of Phosphorylated Material
Locust Tissue Fluoride Measurements

VI	RESULTS AND DISCUSSION.....	141
	APPENDIX 1.....	183
	APPENDIX II.....	189
	REFERENCES.....	190
	VITA AUCTORIS.....	199

ABSTRACT
THE METABOLISM OF
3-DEOXY-3-FLUORO-D-GLUCOSE
BY LOCUSTA MIGRATORIA

by

Alexander Dimitri Romaschin

The toxic effects of 3-deoxy-3-fluoro-D-glucose (3FG) in Locusta migratoria are investigated by a preliminary steady state kinetic characterization of the fat body enzymes aldose reductase and sorbitol dehydrogenase with respect to their native substrates and the fluoro-substrates 3FG and 3-deoxy-3-fluoro-D-glucitol (3FGL). These studies indicate that the aldose reductase and sorbitol dehydrogenase enzymes are respectively NADP^+ and NAD^+ dependent and catalyze the conversion of glucose to sorbitol and sorbitol to fructose. 3FG is shown to be a better substrate for the aldose reductase than glucose and 3FGL is shown to be a poorer substrate for sorbitol dehydrogenase than sorbitol. The latter is demonstrated by a K_m (app) of 0.5 M for 3FGL as compared to a K_m (app) of 0.07 M for sorbitol, both at 1 mM NAD^+ . The V_{\max} (app) for sorbitol is eight times greater than that of 3FGL. A similar effect is observed for both the native and fluoro-substrates using commercially prepared sorbitol dehydrogenase. These results are consistent with the unfavourable

intrinsic binding energy of the fluoro-substrate as predicted by the Circé effect proposed by W.P. Jencks. Apart from being a substrate, 3FGL is also shown to be a competitive inhibitor of sorbitol dehydrogenase. This kinetic duality is experimentally verified by adopting a ter-reactant kinetic scheme. The irreversible toxic effects of a 3FG metabolite are detected by radiorespirometric analysis of $^{14}\text{CO}_2$ expired from locusts injected with 3FG and 6- ^{14}C -D-glucose or 1- ^{14}C -acetate. The release of a high concentration of fluoride from a 3FG metabolite is also observed. It is proposed that 3FG is converted to 3-deoxy-3-fluoro-D-fructose (3FF) via aldose reductase and sorbitol dehydrogenase and subsequently phosphorylated. Chromatographic and NMR evidence for this conversion is cited. The extent of metabolism of a fluorinated-phosphorylated metabolite derived from 3FG is investigated by $^3\text{H}_2\text{O}$ production from D-[3- ^3H]-3FG. Evidence for the metabolism of 3FG as far as triose phosphate isomerase based on $^3\text{H}_2\text{O}$ yields is presented. A hypothetical scheme for concomitant defluorination and detritiation of D-[3- ^3H]-3FG is proposed. The irreversible toxic effect of 3FG is postulated to be via fluoride release from a 3FG metabolite resulting in the inhibition of enolase and possibly other Mg^{2+} dependent enzymes.

To the light of my life,
my wife, Maria

ACKNOWLEDGEMENTS

I would like to thank Drs. D.E. Schmidt, Jr., K.E. Taylor, W. Chefurka, J.E. Steele, A.H. Warner, R.J. Thibert, J. Dryden, D.J. McKenny, A.H. Khalil, S.J. Price and H. Sapiano for their help and advice during the course of this work.

To my supervisor, Professor Norman Fletcher Taylor, my sincerest appreciation for giving me the opportunity, freedom and guidance to expand my interest in biochemistry as well as in other areas of mutual concern.

To my family, my sincerest thanks for their support during this endeavour.

LIST OF TABLES

Number		Page
1.	3FGL Toxicity Study.....	66
2.	Recycling Reaction Progress.....	98
3.	Quench Correction Data.....	121
4.	Determination of Haemolymph Glucose Concentrations.....	142
5.	Locust Extracellular Fluid Volume Counting Data.....	143
6.	$^3\text{H}_2\text{O}$ Release from D-[^3H]-3FG and D-[^3H]-glucose.....	162
7.	Effects of 3FG and F^- on $^3\text{H}_2\text{O}$ Release from D-[^3H]-glucose.....	166
8.	Comparison of Tissue F^- levels in Control, F^- poisoned and 3FG poisoned locusts.....	170

LIST OF FIGURES

Figure		Page
1.	Four possible stereoisomers of fluorocitrate.....	5
2.	Condensation of F-acetyl CoA with oxaloacetic acid catalyzed by citrate synthase.....	8
3.	An early scheme proposed to account for the reversible and irreversible inhibition of aconitase by fluorocitrate.....	12
4.	Experimental system used by Kun in suspended liver mitochondria to first detect the inactivation of the citrate transport network....	17
5.	Citrate transport network in the mitoplast.....	21
6.	Transport scheme for the translocation of amino acids in intestinal epithelia.....	23
7.	Kinetic scheme for an affinity label acting at the enzyme active site.....	28
8.	Catalytic mechanism of 2-keto-3-deoxygluconate-6-phosphate aldolase (KdGtP).....	34
9a.	Suggested mechanism for thymidylate synthase reaction.....	38
9b.	Structure of the FdUMP · CH ₂ · FAH ₄ thymidylate synthase ternary complex.....	39
10.	Model studies with 5-trifluoromethyl-1-methyl-3-alkyl uracil.....	42
11.	Inactivation of thymidylate synthase by 5-trifluoromethyl-2'-deoxyuridylate.....	44
12.	Irreversible inactivation of pyridoxal phosphate dependent alanine racemase by D-fluoroalanine.....	48
13.	Proposed pathway for metabolism of 3FG.....	52

Figure		Page
14.	Graph of locust sorbitol dehydrogenase activity versus protein concentration.....	69
15a.	Kinetic data for locust sorbitol dehydrogenase illustrating competitive nature of 3FGL inhibition.....	72
15b.	Double reciprocal plot for locust sorbitol dehydrogenase with 3FGL as substrate.....	72
16.	Double reciprocal plot for sheep liver sorbitol dehydrogenase.....	74
17.	Locust sorbitol dehydrogenase double reciprocal plot in the thermodynamically favoured direction...	80
18.	Chromatogram of locust sorbitol dehydrogenase reaction mixture with 3-deoxy-3-fluoro-D-glucitol as substrate.....	83
19.	Locust aldose reductase double reciprocal plot with 3FG and NADPH as substrates.....	87
20.	Sheep liver sorbitol dehydrogenase double reciprocal plots at various concentrations of NAD^+ .	89
21.	Ordinate intercepts from Figure 20 plotted against the varying constant $1/\text{NAD}^+$	91
22.	Slopes from Figure 20 plotted versus $1/\text{NAD}^+$	93
23.	Enzyme recycling system used to attempt the synthesis of 3FF.....	96
24.	Glyoxylate assay graph.....	100
25.	^{19}F Fourier Transform NMR of 3FGL enzyme recycling system.....	103
26.	^{14}C quench correction curve for Nuclear Chicago Mark 11 scintillation spectrometer.....	116
27.	Glucose assay calibration graph using the modified Glucostat procedure.....	119

Figure	Page
28. Radiorespirometric apparatus.....	124
29. Calibration graph for gas chromatographic CO ₂ determinations.....	128
30. ¹⁴ C quench correction curve for Nuclear Chicago Unilux 11 scintillation spectrometer.....	130
31. Tritium quench correction curve for Nuclear Chicago Unilux 11 scintillation spectrometer.....	132
32. Semi-log plot of voltage potential versus fluoride ion concentration for potentiometric fluoride determinations.....	140
33. 1- ¹⁴ C-D-glucose radiorespirometric results.....	146
34. 6- ¹⁴ C-D-glucose radiorespirometric results.....	149
35a. 6- ¹⁴ C-D-glucose radiorespirometric results.....	151
35b. 6- ¹⁴ C-D-glucose radiorespirometric results.....	154
36. 6- ¹⁴ C-D-glucose radiorespirometric results.....	156
37. 1- ¹⁴ C-acetate radiorespirometric results.....	159
38. Stereochemistry of D-[3- ³ H]-glucose.....	164
39. Hypothetical inactivation mechanism of aldolase by a metabolite of 3FG.....	168
40. Sample chromatogram of locust phosphorylated metabolites on P.E.I. cellulose after injection of D-[3- ³ H]-3FG.....	175
41. ¹⁹ F Fourier Transform NMR of a phosphorylated fluoro-metabolite from locust after 3FG injection..	178
42. Proposed mechanism for concomitant detritiation and defluorination of pro-R- ³ H-monofluoro- hydroxyacetone phosphate by triose phosphate isomerase.....	182

LIST OF APPENDICES

Number		Page
1	Least Squares Method Mechanistic Aspects of Dehydrogenase Enzymes.....	183
11	Calculation of Standard Error in the Mean.....	189

LIST OF ABBREVIATIONS

ATP = adenosine triphosphate

KdGtP = 2-keto-3-deoxygluconate-6-phosphate

FdUMP = 5-fluoro-2'-deoxyuridylate

CF₃dUMP = 5-trifluoromethyl-2'-deoxyuridylate

3FG = 3-deoxy-3-fluoro-D-glucose

3FGL = 3-deoxy-3-fluoro-D-glucitol or sorbitol
(N.B. glucitol and sorbitol are identical)

3FF = 3-deoxy-3-fluoro-D-fructose

NAD⁺, NADH = oxidized and reduced nicotinamide adenine
dinucleotide respectively

NADP⁺, NADPH = oxidized and reduced nicotinamide adenine
dinucleotide phosphate respectively

enzyme·CH₂FAH₄·FdUMP = ternary complex of enzyme, 5,10-
methylenetetrahydrofolate and 5-
fluoro-2'-deoxyuridylate

PART 1 .

ENZYME STUDIES



INTRODUCTION

The purpose of this study has been to investigate the in vivo toxicity of 3-deoxy-3-fluoro-D-glucose (3FG) in Locusta migratoria. Prior to the consideration of this problem, it is proposed to briefly highlight the development of the story of fluoroacetate poisoning. Such an account is important in the context of this work since it represents the initial focal point of interest in the metabolism and toxicity of fluoro-analogues. This study has spanned three decades and although it is not yet complete, a basic understanding of fluoroacetate toxicity has been achieved. Most importantly, however, these studies illustrate the danger of applying in vitro biochemical results to the in vivo condition. The results also illustrate the potential of fluoroanalogues as biochemical probes.

Biochemical interest in monofluoroacetate was generated in 1943 when Marais demonstrated that it was the toxic component of the South African plant gifblaar or Dichapetalum cymosum (1). This plant was responsible for the death of many cattle in South Africa, as well as scattered incidents of human death. In 1947, C. Liebecq and R. Peters began to investigate the action of fluoroacetate in kidney homo-

genates (2)(3). They were able to substantiate the fact that fluoroacetate poisoning resulted in a marked citrate accumulation in virtually all tissues studied except for brain. The LD_{50} tissue level in rats was about $10^{-5}M$ and toxicity was manifested by the onset of convulsions which subsequently led to death. This toxicity was relatively slow to develop, requiring several hours. In 1953, Peters established that the toxic metabolite was in fact monofluorocitrate and not fluoroacetate (4). This was demonstrated by the isolation of the metabolite from kidney homogenates after pre-incubation with fluoroacetate and comparison with synthetic racemic fluorocitrate. Further evidence was based on the observation that racemic fluorocitrate inhibited respiration in brain homogenates, whereas fluoroacetate had no effect on respiration. This was due to the absence of acetate thiokinase in brain tissue. The preceding experiment was one of the first examples in which a carbon-fluorine compound was instrumental in drawing attention to tissue specific metabolism.

Peters referred to the conversion of fluoroacetate, (which was itself non-toxic) to the toxic metabolite fluorocitrate as a 'lethal synthesis'. Due to the acidic conditions used in Peters' isolation of fluorocitrate from the homogenates

a racemic mixture of the four isomers was obtained (Figure 1). Chemical synthesis of the same compound also gave such mixtures due to the lack of stereospecificity in the synthetic route employed.

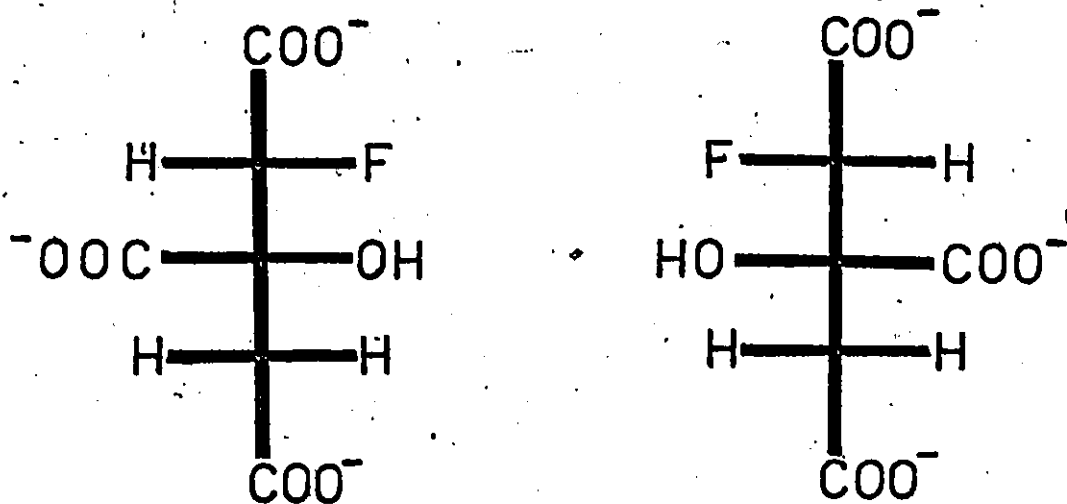
Early studies by Peters' group using a crude in vitro system (in which aconitase activity measurements were coupled to isocitrate dehydrogenase and NADH production) demonstrated that introduction of fluorocitrate into the system inhibited citrate stimulated NADH production (5). In such assays, 50% inhibition of aconitase was achieved with as little as 10^{-8} to 10^{-9} M racemic fluorocitrate. It was also shown that fluorocitrate was toxic at a lower dose than fluoroacetate when injected into pigeon, rat, and rabbit. In pigeon, as little as 11ug induced convulsions (6).

At this stage of the investigation (1953-54), it was evident that fluoroacetate was activated by a thiokinase to form fluoroacetyl-CoA and subsequently condensed with oxaloacetic acid via citrate synthase to form fluorocitrate. In 1955, Brady demonstrated that fluoroacetyl-CoA was considerably less stable than acetyl-CoA at the pH that the citrate synthase was most active (7). Saunders, who first synthesized both di and trifluoroacetic acids, found no toxic effect upon injection of either compound into

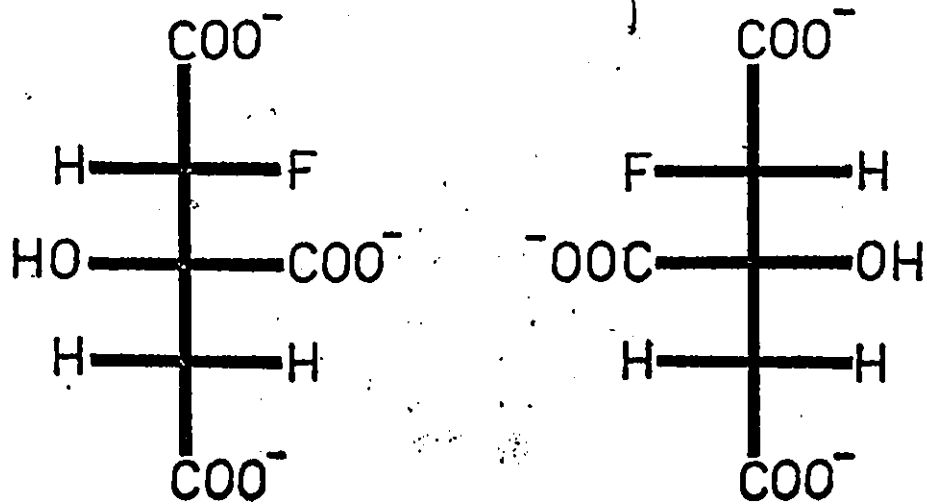
Figure 1

Four possible stereoisomers of fluorocitrate drawn as
Fischer projections.

Figure 1



erythro pair



threo pair

various mammalia (8). It was suggested that di or trifluoroacetic acids could no longer productively interact with either the thiokinase or citrate synthase enzymes. Kun later demonstrated that the K_m for fluoroacetyl-CoA was identical to that of acetyl-CoA but the V_{max} was $\frac{1}{300}$ th that of the native substrate (9). This could be partially rationalized by the adverse inductive effect of fluorine on the enolizability of fluoroacetate. Enolization is presumably a rate determining step in the formation of the enzyme catalyzed transition state (Figure 2).

One of the early problems concerning the effects of fluorocitrate on aconitase was the uncertainty with regard to the stereochemistry of the toxic isomer. Kun began to investigate this problem in 1961 and was able to show that enzymically synthesized fluorocitrate from fluoroacetyl-CoA and oxaloacetic acid was the toxic isomer (10)(11). All other isomers had no significant inhibitory effect on aconitase.

These tests were done on an impure mitochondrial aconitase preparation which was coupled to a Mn^{2+} or Mg^{2+} dependent isocitrate dehydrogenase assay. In these assays, fluorocitrate was shown to be a linearly competitive inhibitor of aconitase.

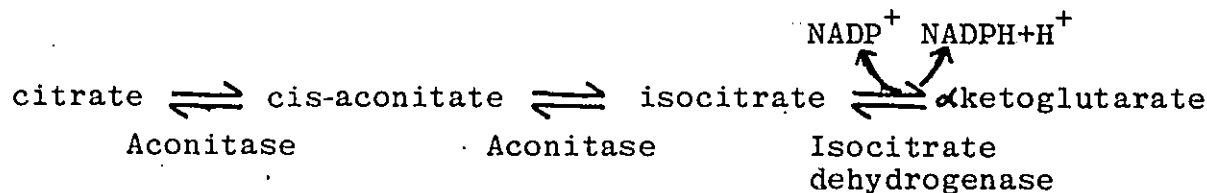
Figure 2

Condensation of F-acetyl CoA with oxaloacetic acid catalyzed
by citrate synthase.

In 1969-70, four significant advances were made. (a) Kun demonstrated that the toxic isomer of fluorocitrate belonged to the erythro pair of enantiomers which were separated from the diastereomeric threo pair of enantiomers by high voltage electrophoresis. The toxic isomer was shown to be (-) erythro-fluorocitric acid (or 1R : 2R 1-fluoro-2-hydroxy-1,2,3 propane tricarboxylic acid) by X-ray crystallographic analysis and comparison to the enzymically synthesized isomer (12)(13).

(b) Sir Rudolph Peters proposed that the toxic action of fluorocitrate was due to its inhibitory action on mitochondrial aconitase (14). There was evidence for the irreversible inactivation of mitochondrial aconitase by fluorocitrate under a variety of conditions (15).

(c) Guarriera-Bobyleva and Buffa found that after in vivo administration of toxic doses of fluorocitrate, only the metabolism of citrate was inhibited in whole mitochondria, whereas cisaconitate (which was also a substrate for aconitase) was oxidized normally (16). (d) Kun demonstrated that fluorocitrate did not inhibit NADPH formation when cisaconitate was the substrate (instead of citrate) in the NADP^+ dependent isocitrate dehydrogenase coupled system (12).



Furthermore, Kun demonstrated that fluorocitrate was also a competitive inhibitor of succinate dehydrogenase with a $K_{i(\text{app})}$ of 6×10^{-4} .

It is evident from the above discussion that a variety of anomalous phenomena were observed with regard to fluorocitrate toxicity. In particular, the lack of inhibition of *cis*-aconitate utilization in mitochondria and in vitro enzyme systems by fluorocitrate was particularly disturbing. This effect was inconsistent with the mechanism of aconitase proposed by Glusker (17). The situation was further complicated by the existence of two isoenzymes of aconitase, one mitochondrial, the other cytoplasmic.

In 1970, Carrel, Glusker and Kun proposed a mechanism for the reversible and irreversible inhibition of aconitase which was compatible with Glusker's mechanism (18). It was proposed that the competitive inhibitory action of fluorocitrate was due to a change in the chelation complex which 1R:2R fluorocitrate formed with Fe^{2+} in the active site, as compared to the complex formed with citrate. The non-competitive irreversible component was via alkylation of the enzyme with concomitant release of fluoride (Figure 3). Although Kun and co-workers were able to demonstrate fluoride release on pre-incubation with enzyme, Peters' group was unable to confirm this observation (19).

Figure 3

An early scheme proposed to account for the reversible and irreversible inhibition of aconitase by fluorocitrate.

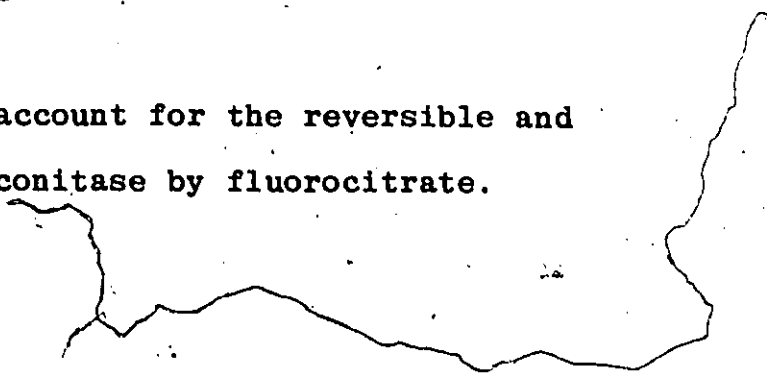
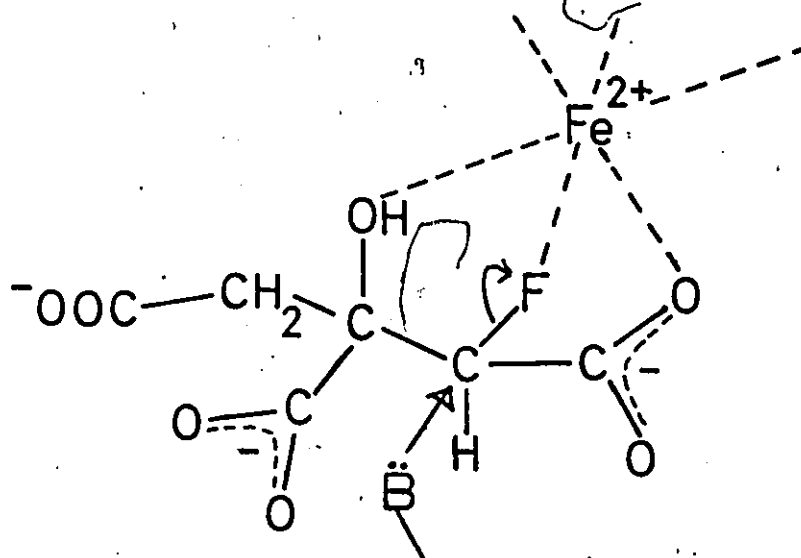
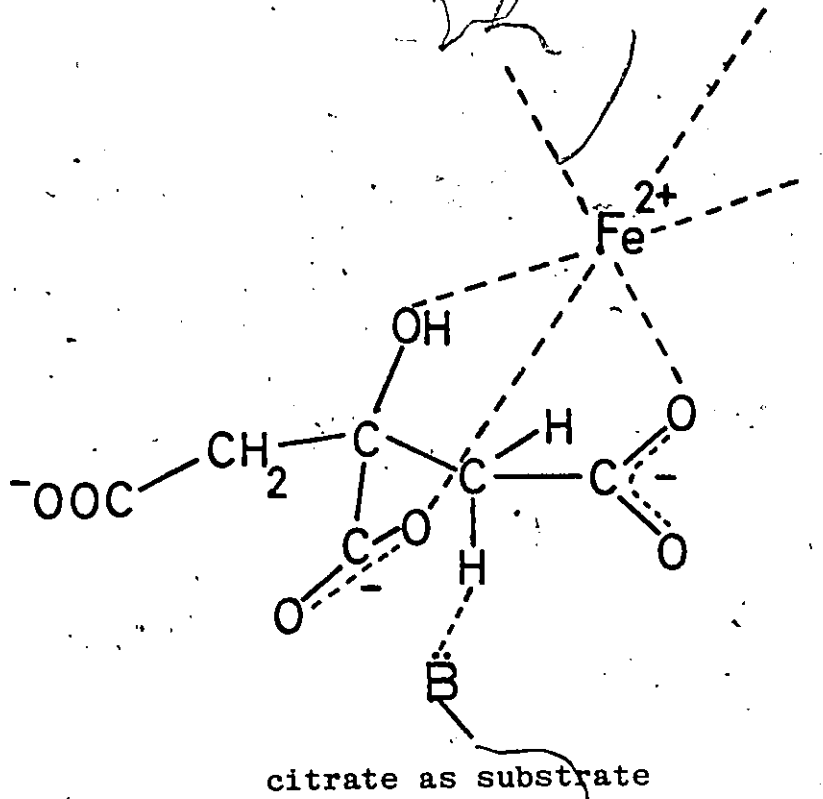


Figure 3



The enigmatic state of the aconitase problem during 1970-72 was aptly described by Kun (19):

"A molecular mechanism of fluorocitrate toxicity has to account for the irreversible cessation of cell function in certain specific cells of the nervous system, known to be the probable anatomical organ site of this poison (15). If inhibition of aconitase is the mode of action of fluorocitrate, irreversible inhibition of this enzyme should be demonstrated at submicromolar concentrations of the inhibitor because this range of concentration is most probably present in vivo (due to slow rates of fluorocitrate biosynthesis). Even if these requirements are met, there is some uncertainty why aconitase inhibition should prove fatal, when inhibitors of other citric acid cycle enzymes cause relatively small toxicity: eg. malonate is not a powerful poison, or as stated earlier, inhibition of malate dehydrogenase in vivo elicits no detectable toxic effects."

Eventually Kun was able to sort out the various anomalous results regarding the action of fluorocitrate on aconitase. Part of the problem was due to the artificiality of mitochondrial aconitase preparations. It was known for some time that aconitase interacted with the inner mitochondrial membrane. Attempts to purify the enzyme necessitated the disruption of this interaction. This resulted in a kinetic behavior which was not a reflection of the in vivo characteristics of this enzyme (19). As demonstrated by Kun in 1974

(20), various preparations of aconitase were susceptible to time dependent inactivation by divalent cations such as Mg^{2+} or Mn^{2+} , which were necessary constituents of the isocitrate dehydrogenase coupled assay. Unawareness of this complication often resulted in a variety of inhibitory patterns which mimicked competitive, non-competitive or mixed types of inhibition along with highly variable K_i values.

Isolation of an electrophoretically pure aconitase which was fully active for a short time without any artificial activators such as cysteine, Fe^{2+} , or ascorbate, revealed linear competitive inhibition for both the mitochondrial and cytoplasmic isozymes. These results did not explain the well known irreversible and highly potent toxic effects of (-) erythro-fluorocitrate. In fact, later work by Kun demonstrated that aconitase in mitochondria was active at concentrations of Mg^{2+} as high as 230mM; conditions which would have completely and irreversibly inactivated the purified in vitro enzyme preparation (21). Clearly the results with the improved in vitro preparation still did not stringently reproduce the physiological properties of this enzyme. This theme has been most poignantly expounded by E.A. Newsholme, particularly with regard to the regulatory

properties of allosteric enzymes (22). The dangers of extrapolating in vitro enzymology to physiological processes were painfully evident with regard to the properties of aconitase.

Experimental results pertaining to the irreversible inhibition of citrate-isocitrate exchange in isolated mitochondria by micromolar concentrations of fluorocitrate were the first indication of a biochemically significant event which was compatible with the etiology of fluoroacetate and fluorocitrate poisoning (23)(Figure 4).

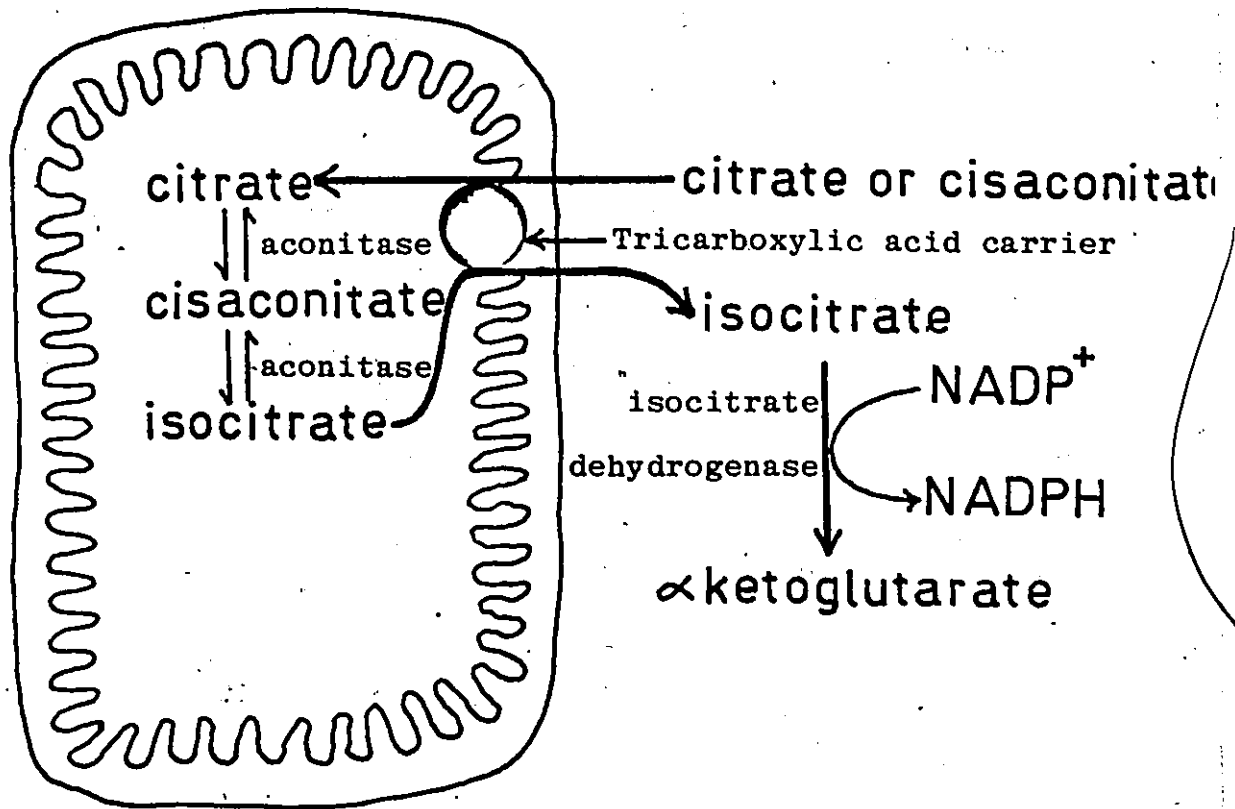
Irreversible inhibition of citrate-isocitrate exchange was achieved at fluorocitrate concentrations of 10^{-6} to 10^{-8} molar, when mitochondria were pre-incubated for two to eight minutes prior to the addition of citrate. It was suggested that fluorocitrate irreversibly inactivated the mitochondrial tricarboxylate transport system first elucidated by Chappel in 1968 (24). Although this proposal was later disputed by Chappel and his group (25) (on the basis of a failure to observe irreversible inhibition of citrate exchange in citrate pre-loaded mitochondria), the discrepancy was reconciled due to the stringent requirement for pre-incubation of mitochondria with fluorocitrate in the absence of high concentrations of citrate. In pre-loaded

Figure 4

Experimental system used by Kun in suspended liver mitochondria to first detect the inactivation of the citrate transport network.



Figure 4



After the addition of Triton X-100, the rate of isocitrate formation from cisaconitate was greatly accelerated, indicating that this reaction catalyzed by mitochondrial aconitase was limited by the rate of tricarboxylate carrier which was operative only in intact mitochondria. Fluorocitrate irreversibly inhibited citrate or cisaconitate dependent isocitrate efflux. This inhibition was relieved by disruption of the mitochondrial membrane by Triton X-100.

mitochondria, the citrate concentration was usually 3-4mM. Such an artificially high concentration of citrate invariably protected the tricarboxylate transporter from fluorocitrate concentrations in the range of 10^{-6} to 10^{-8} M. Further experiments by Kun have demonstrated that the rate of entry of oxidizable carboxylic acids into the mitoplast compartment of lysosome and microsome free mitochondria (as measured by incorporation of ^{32}P into ATP) was irreversibly inhibited by pre-incubation of mitochondria with 50 picomoles of (-) erythro-fluorocitrate per milligram of mitochondrial protein. Also, the efflux of radio-labelled citrate generated in the mitoplast compartment of mitochondria from U- ^{14}C -alanine and α -ketoglutarate was irreversibly inhibited by fluorocitrate (26). Furthermore, the formation of a stable covalent adduct, derived from radiolabelled fluorocitrate and mitochondrial membrane proteins was demonstrated. Fluorocitrate was shown to bind to two distinct protein bands extracted from liver mitoplasts. Fractionation of these proteins was achieved on Sephadex G-200, corresponding to molecular weights of 175,000 and 71,500. The binding process was shown to be enzyme catalyzed and activated by Mn^{2+} . Subsequent studies have uncovered an enzyme system extractable from mitoplast

membranes which catalyzed the formation of a 1:1 adduct of citrate and glutathione (27). This adduct was shown to be a thioester of glutathione. A hydrolase capable of degrading the adduct was also identified. Both enzymes were irreversibly inactivated by (-) erythro-fluorocitrate and formed covalent complexes with this toxin. A variety of specific enzyme systems which catalyzed the formation of glutathione-thioester adducts with succinate, malate, α -ketoglutarate, glutamate, pyruvate, isocitrate and glutamine have been identified in the inner mitochondrial membrane (27).

The coincidence of fluorocitrate inhibition of citrate transport in mitochondria with the inhibition of the soluble citrate-glutathione synthase and hydrolase systems tends to suggest that the synthase-hydrolase system may be an integral part of the mitochondrial citrate transport system. Various other pieces of evidence point in this direction (27).

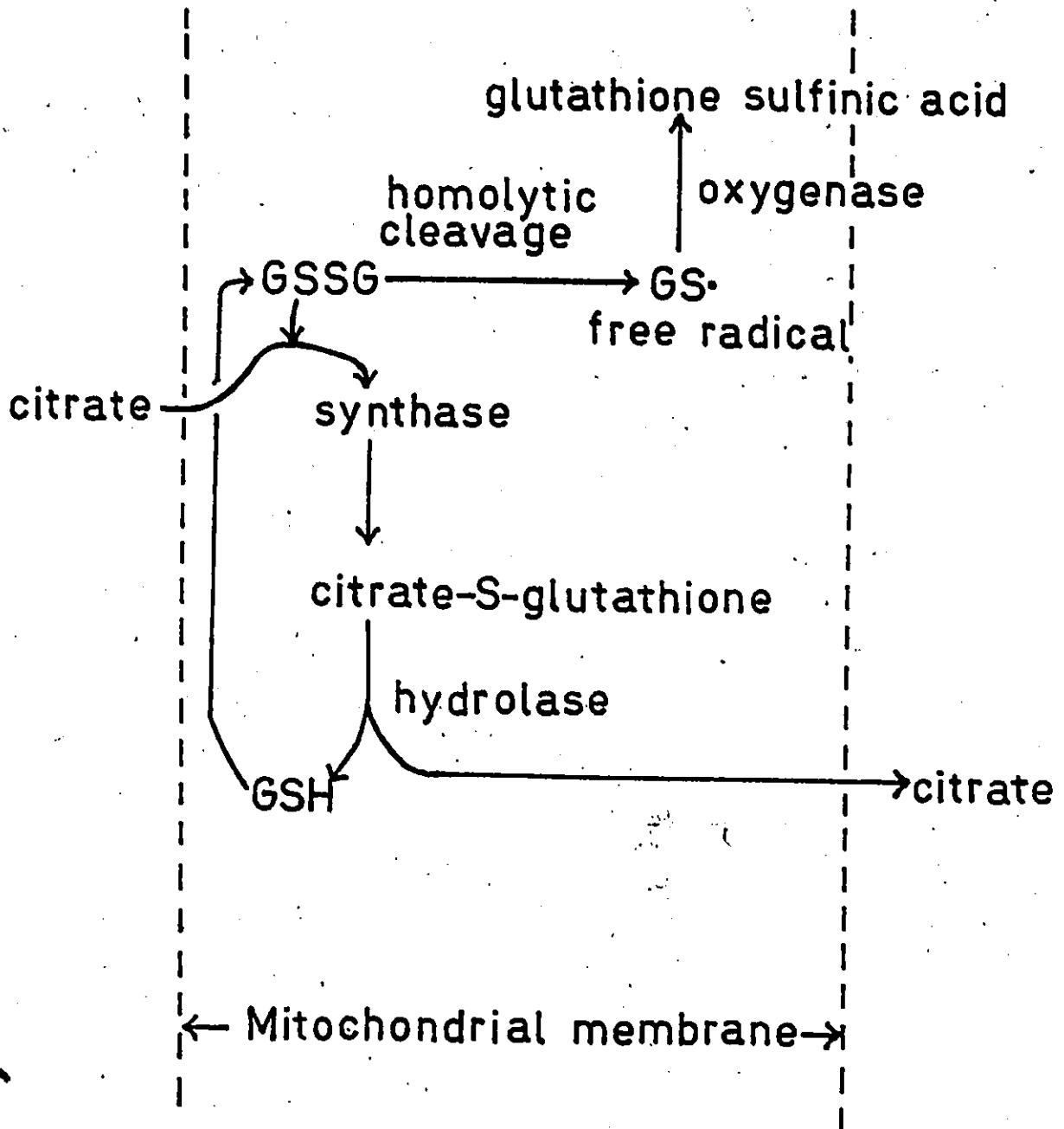
Figure 5 gives a brief outline of the proposed transport network.

It is evident, therefore, that there may be a ubiquitous mechanism in mitochondria requiring oxidized glutathione (GSSG) for the transport of various di and tricarboxylic metabolites. The function of glutathione in the transport of some amino acids has been elucidated by A. Meister (Figure 6). The

Figure 5

Citrate transport network in the mitoplast as proposed
by Kun.

Figure 5

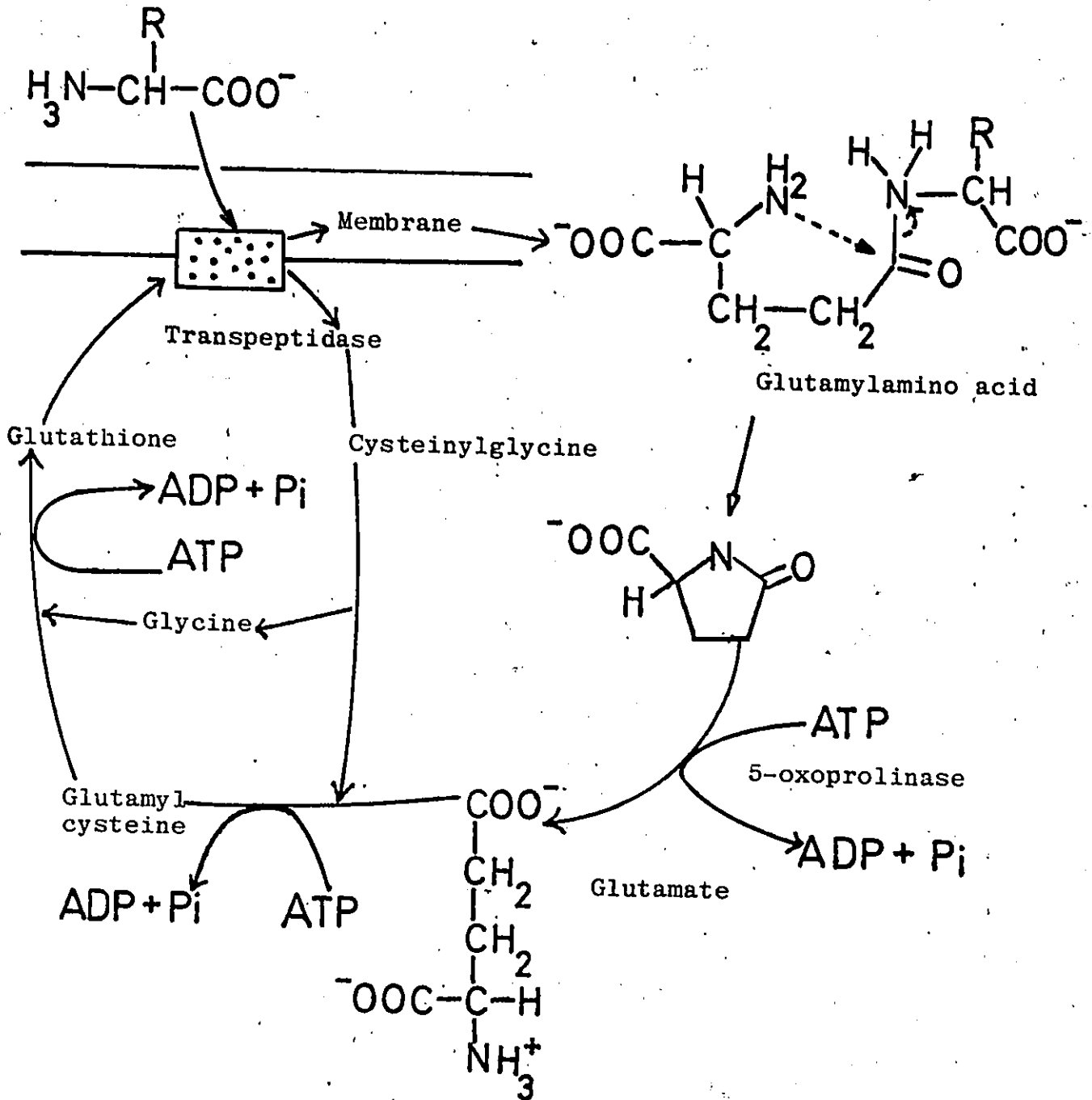


Thioester formation was prevented by the free radical trapping agent phenazine methosulfate.

Figure 6

Transport scheme for the translocation of amino acids in intestinal epithelia proposed by A. Meister.

Figure 6



importance of this peptide, which is present in virtually all cells at a concentration of $\sim 10\text{mM}$ has begun to emerge. Kun has suggested that the glutathione-carboxylic acid-thioester enzyme system may also serve as a regulator of Krebs cycle acids and thereby have profound effects on cellular metabolism.

During the past decade, there has been an increase in the design and use of fluoroanalogues as active site directed enzyme labelling agents (28)(29)(30). These reagents fall into two categories, those known as K_s affinity labels and those reagents known as k_{cat} inhibitors or suicide substrates (31).

The K_s affinity labels are substrate analogues with a chemically reactive functional group which is displaced by a catalytically active residue. One of the first examples of such a reagent was tosyl-L-phenylalanine-chloromethylketone (32). This reagent resembled substrates like tosyl-L-phenylalanine which had been used to study the kinetics of the enzyme chymotrypsin. This affinity reagent was later shown to modify histidine-57 at the active site and was one of the first examples of a highly reactive class of affinity labels known as α -haloketones. This class of affinity reagents has been shown to be more reactive in

alkylation reactions than the haloacetylated amines, both in model studies with good nucleophiles like thiols (33) and with relatively poor nucleophiles like carboxy anions at the active site of many enzymes (34)(35)(36)(37). Some early studies using bromopyruvate as an affinity label for the enzyme 2-keto-3-deoxygluconate-6-phosphate (KdGtP) aldolase were done by H.P. Meloche and his colleagues (38) (39)(40)(41)(42)(43). These studies exemplified the great potential of affinity labels as probes for catalytically important residues at the enzyme active site. One great advantage of these affinity labels was their susceptibility to sodium borotritide reduction upon alkylation. This was due to the retention of the keto group in the covalent adduct. If one used 1-¹⁴C labelled bromopyruvate, this allowed both ¹⁴C and ³H labelling of the covalent enzyme-affinity label complex. Double labelling ensured that the covalently modified residue could be isolated and readily tagged after protein hydrolysis. It was later discovered that ³H labelling was essential due to the loss of the 1-¹⁴C carboxyl moiety of pyruvate via decarboxylation during protein hydrolysis (43). Borohydride reduction of covalently incorporated ketones has become a widely practiced procedure. Not only does this reduction stabilize the protein-ligand

covalent adduct and other labile groups alpha to the carbonyl, but it also provides a facile means of quantifying reagent incorporation by measurement of the extent of radiolabelling.

When testing a putative affinity reagent, it is important to demonstrate that one is observing a bona fide active site process. This means that the binding of the agent to the active site brings catalytically active groups in a position favourable for their attack on the substrate reactive centre. The binding of a substrate mimicking affinity label by the enzyme will also enhance the reactivity of the label via entropic factors, induced fit, strain, stress, and distortion. In the scheme shown in Figure 7, this means that $\frac{k_{in}}{K_m}$ would be greatly increased for the enzyme catalyzed reaction as compared to the bimolecular inactivation rate constant for the collision of an α -halo ketone with a free nucleophile.

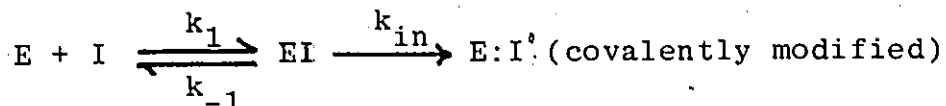
Vivid examples of the enhanced reactivity of an α -halo ketone have been given by Hartman (36)(33). The esterification of 20mM chloroacetol phosphate at 25°C, pH 8.1 by 1mM glutamic acid could not be demonstrated after 12 hours. Substitution of glutamic acid by the enzyme triose phosphate isomerase, however, resulted in the esterification of enzyme residue Glu-165 by chloroacetol phosphate with an apparent second order rate constant of

Figure 7

Kinetic schemes for a true affinity process and a
random bi-molecular collision.

Figure 7

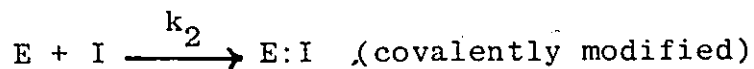
Kinetic scheme for an affinity label acting at the enzyme active site.



$$\text{Initial velocity } v_i = \frac{k_{in} (E_0)(I)}{K_m + (I)}, \quad K_m = \frac{k_2 + k_{-1}}{k_1}$$

If $k_2 \ll k_{-1}$, then $K_m = K_s$. K_s is a true dissociation constant. k_{in}/K_m is an apparent second order rate constant.

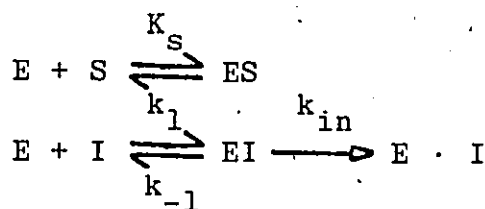
Kinetic scheme for a simple bi-molecular collision.



Initial velocity $v_i = k_2(E)(I)$ and k_2 is the second order rate constant.

$14 \times 10^3 \text{ M}^{-1} \text{ sec}^{-1}$ at 25°C , pH 7. The difference in reactivity was largely a function of entropic factors. Depending upon the relative gains and losses in internal rotation, the intramolecular reaction could be favoured entropically up to 190 J/deg/mol or $13\text{-}14 \text{ Kcal/mol}$ at 25°C . Such an entropic advantage could be visualized by imagining that the effective concentration of the attacking nucleophile was greatly increased in the vicinity of the substrate.

In order to demonstrate true affinity labelling, several criteria must be satisfied (41). (a) Inactivation must be first order with respect to remaining native enzyme. (b) A rate saturation effect must be observed with the affinity label. (c) The native substrate should protect against inactivation and be competitive with the affinity label. (d) In the absence of non specific labelling, the incorporation of label should be 1:1 per mole of catalytic subunit inactivated. The first three criteria may be tested by applying a steady-state kinetic rationale analagous to the Michaelis-Menten approach for competitive inhibition.



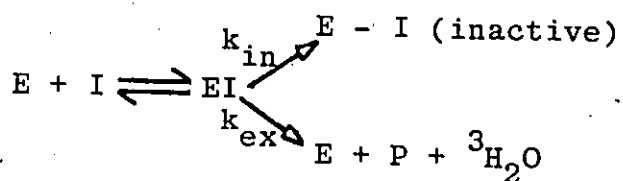
$$v_{in} = \frac{V_{in}}{1 + \frac{K_{in} (1 + (S)/K_S)}{(I)}}$$

If an agent acts as a true affinity label, the half time of enzyme inactivation \mathcal{T} , can be shown to be proportional to $1/v_{in}$ when $\mathcal{T} = \ln 2/k_{in}$. The minimum half time of inactivation at an infinite concentration of I is denoted T and T is proportional to $1/V_{in}$. For a true affinity process, a plot of \mathcal{T} versus $1/(I)$ should yield a straight line. The slope of the line is determined by K_{in} and the concentration of any competitive inhibitor, if present.

$$\mathcal{T} = \frac{T}{(I)} \left[K_{in} + \frac{K_{in} (S)}{K_S} \right] + T \quad (41)$$

Due to the close structural resemblance of bromopyruvate to the natural substrate pyruvate, Meloche was able to ascertain whether the affinity label did in fact alkylate the same group which was responsible for alpha proton abstraction in the native substrate. Initially, Meloche postulated that bromopyruvate formed a Schiff's base or imine complex with an essential amino group at the active

site, similar to the native substrate. He was able to demonstrate that 3-R,S-3-³H-bromo-pyruvate was a substrate for the isotope exchange reaction catalyzed by KdGtP aldolase. The enzyme was found to be stereospecific for the pro-R tritium. Isotopic exchange with the solvent occurred under conditions which resulted in 80% incorporation of label into an enzyme bound ester linkage. The kinetics of detritiation and inactivation were subsequently found to be consistent with a single mechanism occurring at the same site. This claim was substantiated by the demonstration of a constant ratio of inactivation : detritiation as a function of varying concentrations of affinity label. Furthermore, the half time of maximal inactivation was shown to be isotemporal with the half maximal rate of isotopic exchange at a fixed inhibitor concentration. This implied the following mechanism:

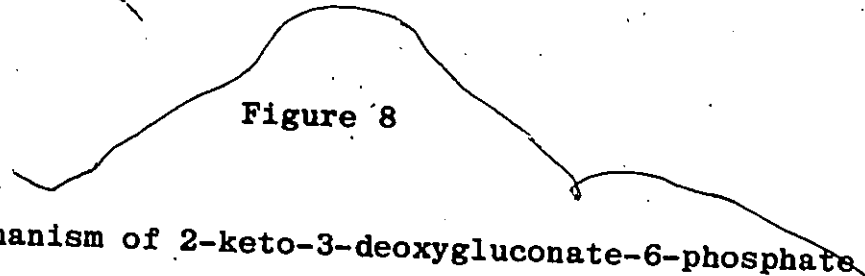


The ratio of exchange to alkylation (k_{ex}/k_{in}) was found to be 1:50 over a wide variation in (I). This dicotomy of action could be simply viewed as a probabilistic

event in which the probability of inactivation was fifty fold smaller than that of exchange. It also gave a relative measure of the two rate constants k_{in} : k_{ex} . The significance of these findings to the work presented in this dissertation will be elaborated in subsequent discussions. As a final note concerning the studies with KdGtP aldolase, it is important to add that borohydride reduction of the esterified inactivated enzyme in the absence of protein denaturant resulted in the cross-linking of an N-6 lysyl amino group to the carboxy keto-methyl group attached to a glutamic acid residue at the active site. This evidence substantiated the fact that the affinity label, like substrate, was also subject to the formation of an imino complex (Figure 8).

Haloacetol phosphates, including the fluoro analogue, have been tested as affinity labelling agents for several enzymes including aldolase, L-glycerophosphate dehydrogenase and triose phosphate isomerase (33)(44). Chloroacetol and bromoacetol phosphates did not inactivate aldolase or L-glycerophosphate dehydrogenase. Fluoroacetol phosphate was a substrate for L-glycerophosphate dehydrogenase but was a poor inactivator of triose phosphate isomerase when compared to the other haloacetol phosphates (44). This was primarily thought to be due to the poor leaving ability of fluoride,

Figure 8



Catalytic mechanism of 2-keto-3-deoxygluconate-6-phosphate aldolase (KdGtP) with the native substrates pyruvate and glyceraldehyde-3-phosphate.


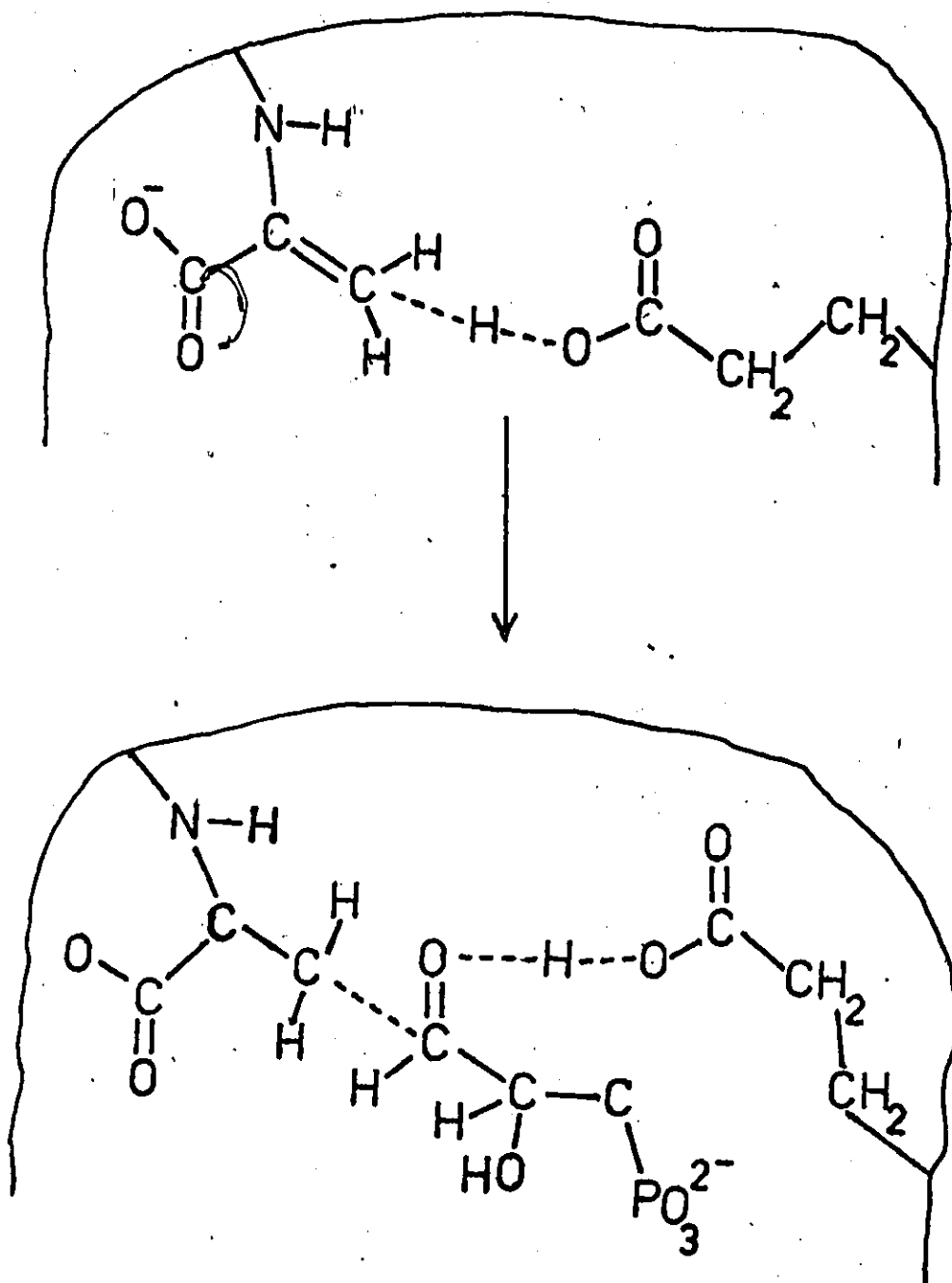


Figure 8



which is the most basic of the halides and hence the worst leaving group. This is the major reason that fluorine is seldom used as a leaving group in in vitro enzyme inactivation studies. This consideration is particularly important in the case of SN_2 reactions at 'soft' saturated electrophilic centres where leaving group polarizability is particularly important. However, this property can be used advantageously in vivo.

One of the problems of haloketone substituents other than fluorine is their susceptibility to non-specific nucleophilic attack. This deficiency was particularly evident in the case of bromopyruvate, which resulted in a high degree of alkylation of amino acid residues other than those at the active site of KdGtP aldolase. In addition, the stability of the haloketone in aqueous media was markedly affected by the nature of the halosubstituent. Such highly reactive labelling agents would therefore be very non-specific in the physiological milieu of the living cell. For this reason the relative stability of the carbon-fluorine bond could be used to invoke some greater measure of selectivity in vivo at the expense of reactivity. This is a particularly important consideration in the design of pharmacological agents. The strength of the carbon-fluorine bond does not, however, preclude its rupture when subjected to the

environment and forces at the enzyme active site (45).

An ingenious use of the fluoro substituent has been investigated by D. Santi in the reaction of 5-fluoro-2'-deoxyuridylate (FdUMP) with the enzyme thymidylate synthase from Lactobacillus casei (46)(47). In this case, a 5-fluoro substituent was used to activate the uracil ring to nucleophilic attack at the six position by a basic group on the enzyme. The result was the formation of a stable reversible covalent ternary adduct of enzyme·CH₂FAH₄·FdUMP (47). This complex was isolated and a hydrolytic peptide derivative was subjected to ¹⁹F NMR studies to obtain information regarding the stereochemistry of the native enzyme mechanism (48). The presence of fluorine at the five position eliminated the possibility of proton abstraction, thought to normally occur at this position in the native ternary complex (Figure 9).

Another interesting case documented by Santi involved the use of the 5-trifluoromethyl derivative of 2'-deoxyuridylate (CF₃dUMP) as an irreversible inactivator of the same enzyme (48). From model studies it was known that the CF₃ group of CF₃dUMP was susceptible to hydrolysis. This was a surprising finding since trifluoromethyl groups were known to be particularly stable under hydrolytic conditions.

Figure 9a

Suggested Mechanism for Thymidylate synthase Reaction

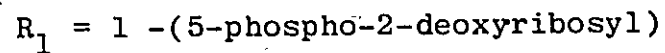


Figure 9b

Structure of the $\text{FdUMP} \cdot \text{CH}_2 \cdot \text{FAH}_4$ thymidylate synthase ternary complex, X represents a nucleophile of one of the enzyme amino acids.

Figure 9a

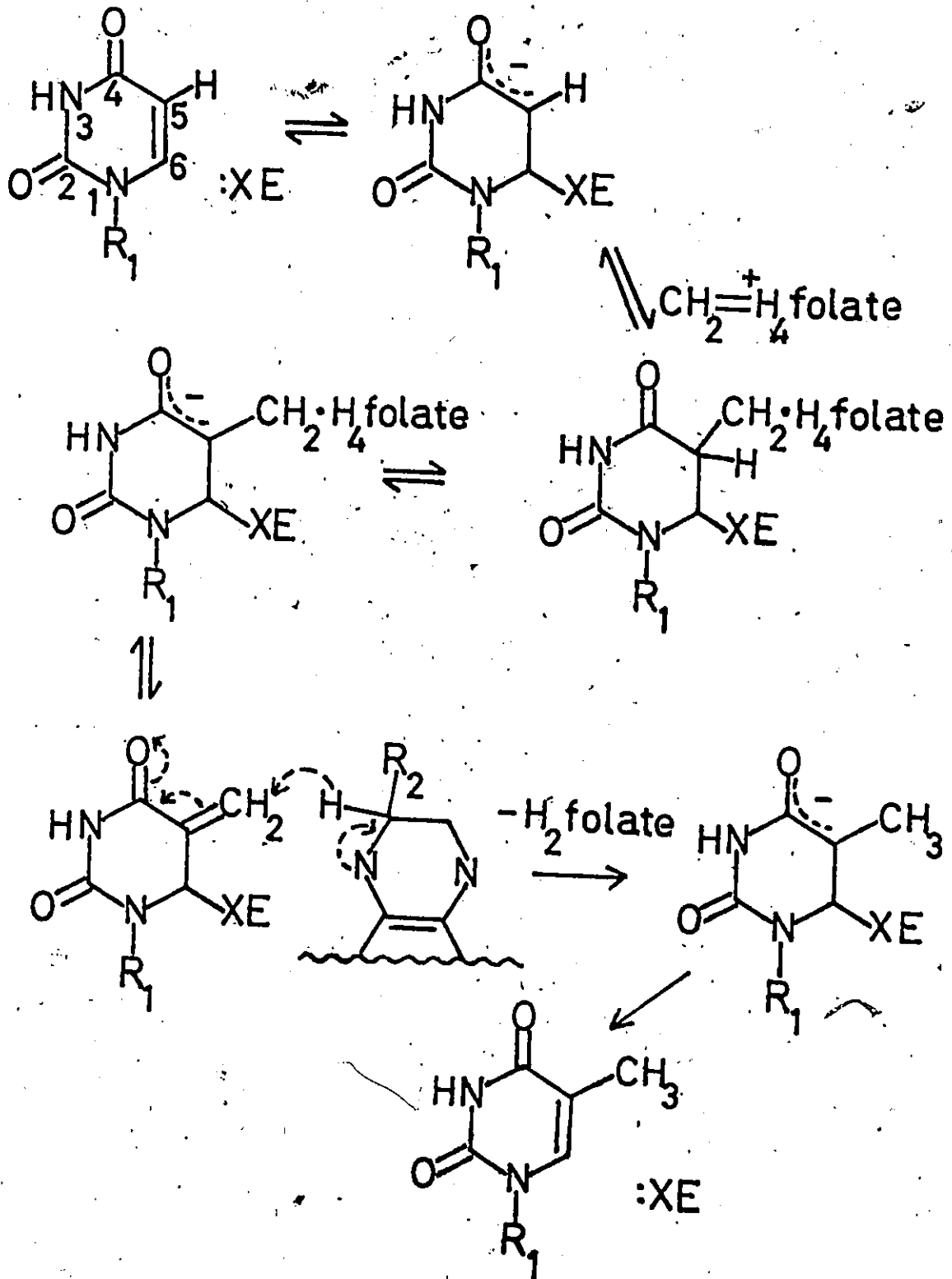
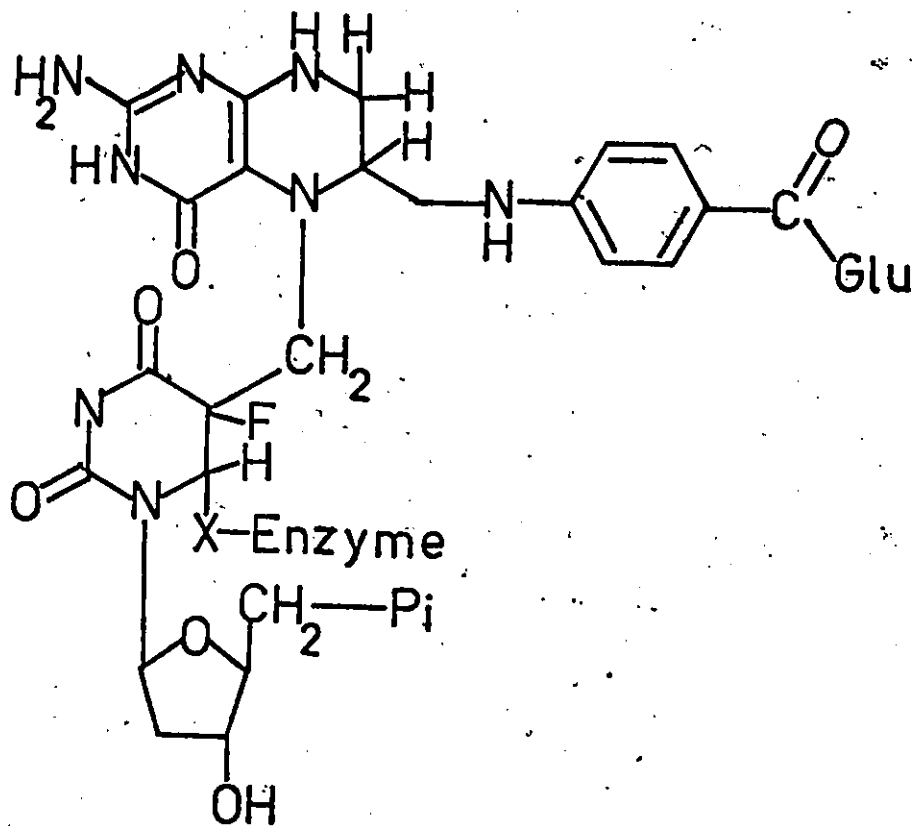


Figure 9b



Model studies revealed that 5-trifluoromethyl-1-methyl-3-alkyl uracil (A) was susceptible to nucleophilic attack at the six position with concomitant formation of a putative, highly reactive, exocyclic difluoromethylene intermediate (B) (Figure 10). On the basis of preliminary studies, it was proposed by Santi that CF_3dUMP irreversibility inhibited thymidylate synthase via a mechanism analogous to the hydrolysis of (A) (Figure 11).

Apart from providing valuable information regarding the general mechanism of folate enzymes and in particular thymidylate synthase, these fluorouracil analogues are currently in use as anti-tumour and anti-viral DNA agents.

From the preceding discussion it is evident that the reactivity of the carbon-fluorine bond may, under certain conditions, be greatly enhanced. The most subtle refinement regarding control over the chemical reactivity of substituent groups in enzyme catalyzed reactions has been achieved by the use of k_{cat} or suicide substrates. The salient features of suicide substrates and numerous examples of their potential have been reviewed (49)(50). In the context of this work it is important to outline a few unique features of this class of affinity agents.

As opposed to classical affinity reagents which depend

Figure 10

Model studies with 5-trifluoromethyl-1-methyl-3-alkyl
uracil (A); (B) = exocyclic difluoromethylene intermediate.

Figure 10

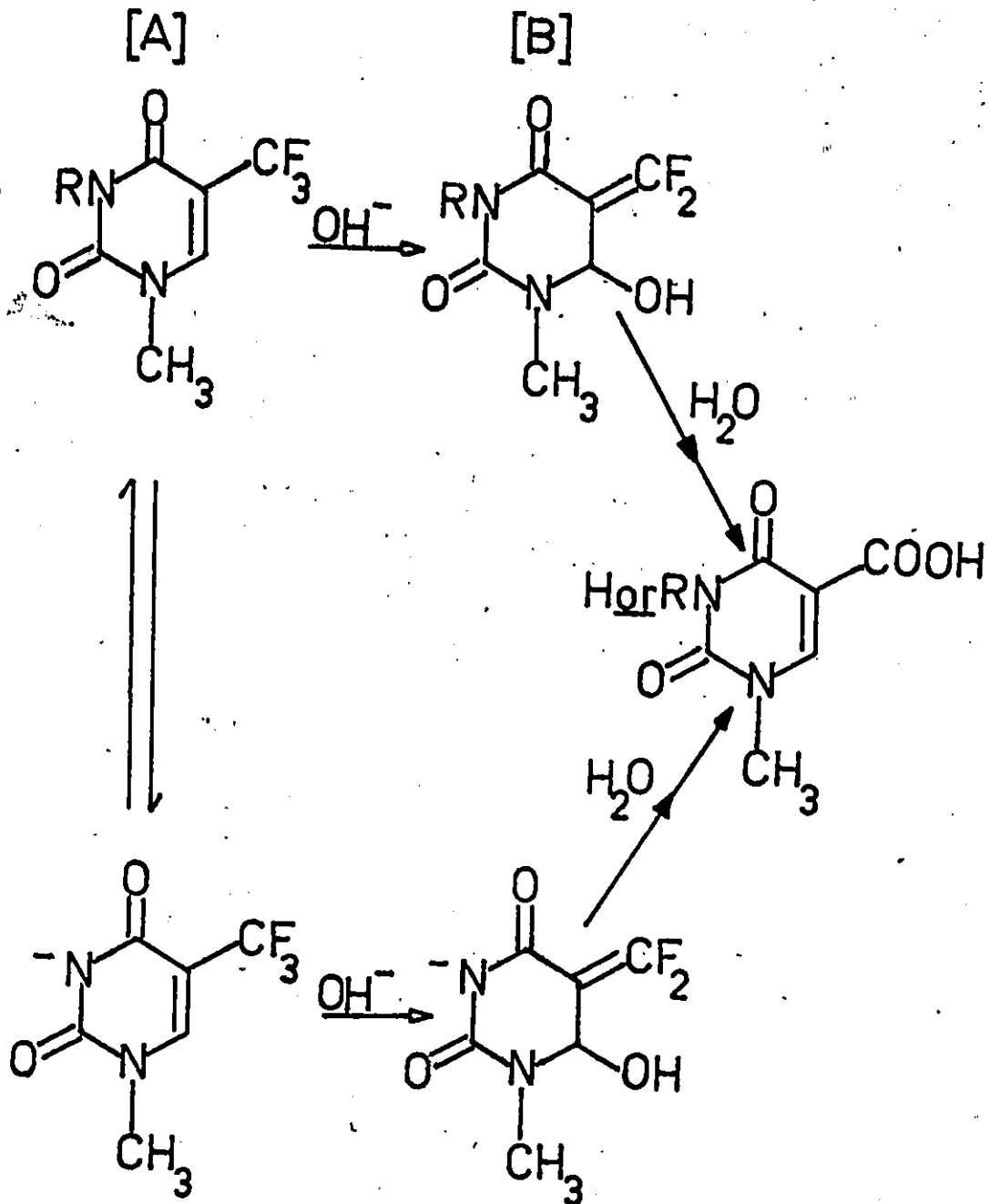


Figure 11

Inactivation of thymidylate synthase by 5-trifluoromethyl-
2'-deoxyuridylate (CF_3dUMP)

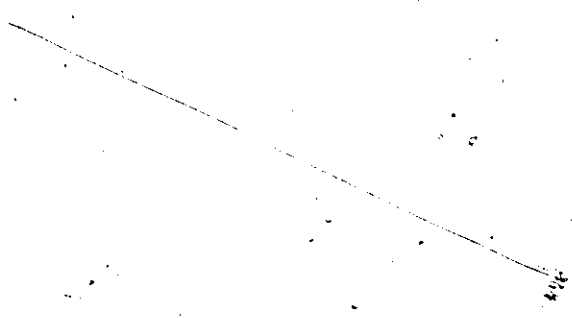
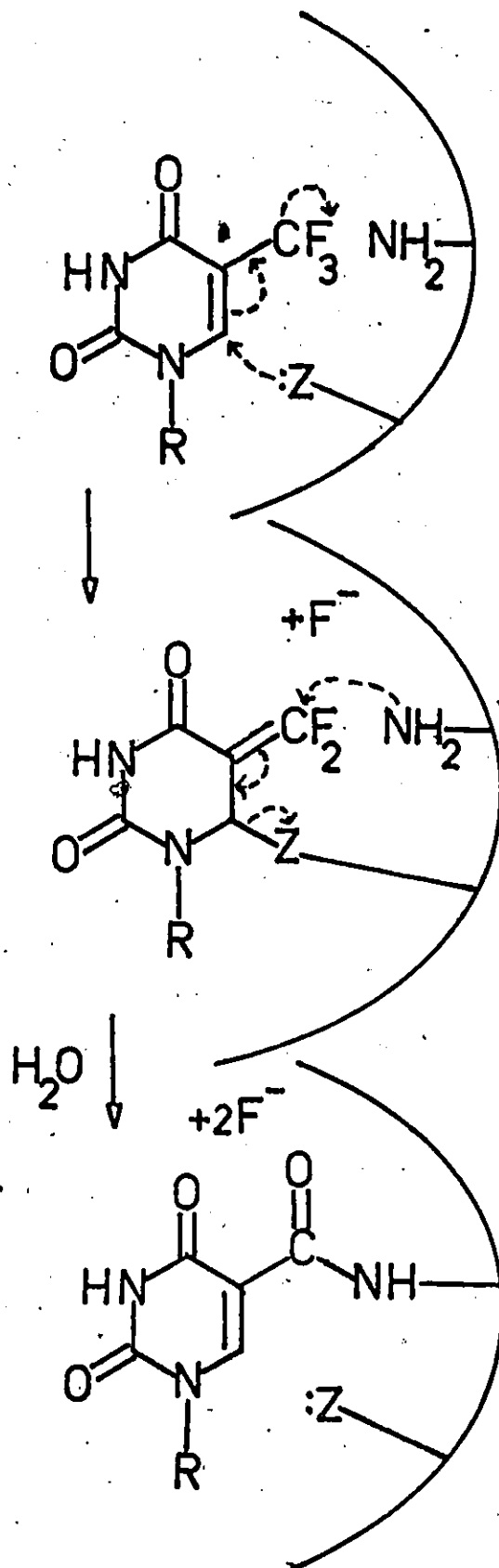
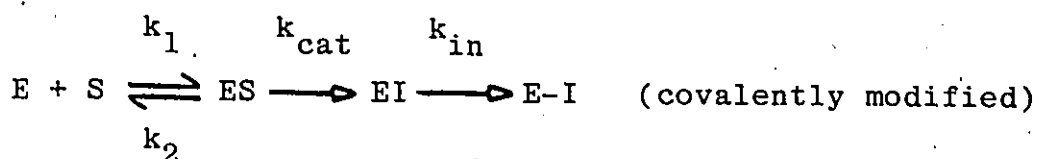


Figure 11



upon their binding affinity for the enzyme to determine specificity and effectiveness, suicide substrates rely upon prior catalytic activation by the enzyme in order to become chemically reactive. These substrates are themselves chemically unreactive and follow the general scheme outlined below:



The major advantage of these reagents is their specificity.

Suicide substrates are unreactive to foreign biomolecules.

"For this reason, they can be used with crude in vitro and in vivo systems without concern for competing non-specific reactions. Furthermore, since the chemically reactive inhibitor is generated at the active site, exceedingly reactive functionalities can be used that would not be possible with an affinity labelling agent. On a more pragmatic level, these reagents are, in general, more stable than affinity labelling agents because they are relatively chemically inert prior to enzyme activation" (49)

A wide variety of these reagents have been developed, utilizing different mechanisms of activation. General criteria for the design and evaluation of such reagents have been given by Rando (49). From a pharmacological point of view these are currently the ultimate in chemical

weaponry. Several elegant examples of suicide inhibitors utilizing the carbon-fluorine bond have been published (28) (29). The mechanism of inactivation of alanine racemase from E. coli by fluoroalanine as proposed by Walsh is particularly illustrative of the basic principles of k_{cat} inactivators (Figure 12). Both D-fluoroalanine and D-cycloserine have been used synergistically against infections in experimental animals (51). D-cycloserine is a naturally occurring suicide substrate (50). Alanine racemase is a particularly important target enzyme in bacteria because it is responsible for the production of D-alanine from L-alanine. D-alanine is an essential component of the peptidoglycan backbone of bacterial cell walls.

Previous studies with fluorocarbohydrates by Taylor have been primarily confined to enzyme specificity (52), microbial metabolism and transport (53)(54)(55) and carbohydrate transport (56)(57)(58). Although 3-deoxy-3-fluoro-D-glucose (3FG) displayed several physiological and biochemical effects in rats (59), it was not toxic even after massive intraperitoneal injections of 5 gram/kg. Some fluorinated compounds accumulated in the brain and testes, but the majority of the 3FG was rapidly excreted into the urine. It was considered to be of some interest, therefore,

Figure 12

Irreversible inactivation of pyridoxal phosphate dependent
alanine racemase by D-fluoroalanine.

to examine the effect of 3FG on an animal organism which had a greater degree of water retention than the rat and which required a smaller dose of 3FG to evoke a physiological response. It was found that 3FG was toxic to two closely related locust species, Schistocerca gregaria and Locusta migratoria, at an LD₅₀ dose of 4.8 mg/gm by injection or by oral administration (60)(61). A large portion of the injected dose was found to be rapidly excreted via the faeces and urine suggesting that the in vivo toxic cellular levels of this fluorosugar were considerably lower than those indicated by the LD₅₀. Toxicity was evidenced by a slow progressive loss of motor activity with death usually occurring between thirty hours and four days. These symptoms suggested the accumulation of a toxic metabolite reminiscent of the 'lethal synthesis' in fluoroacetate poisoning. This prompted a quantitative determination of neutral carbohydrates in the haemolymph, flight muscle and fat body of the locust following 3FG administration, using temperature programmed and isothermal gas chromatography of tissue extracts. Similar carbohydrate scans had been reported previously for locust flight muscle (62).

Gas chromatography of neutral tissue metabolites revealed that the injected 3FG was absent from all tissues

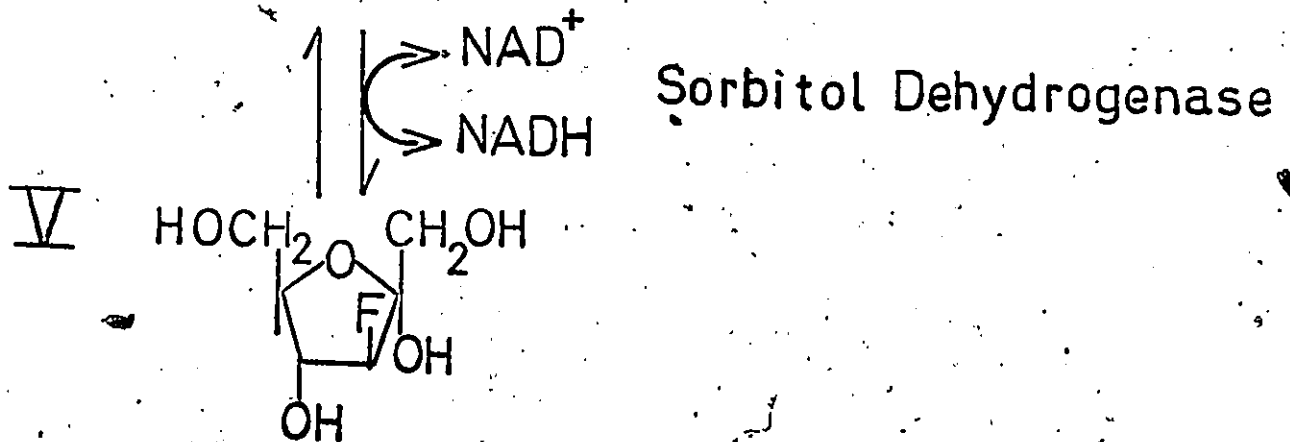
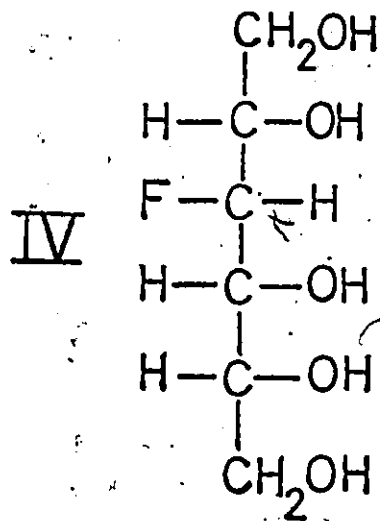
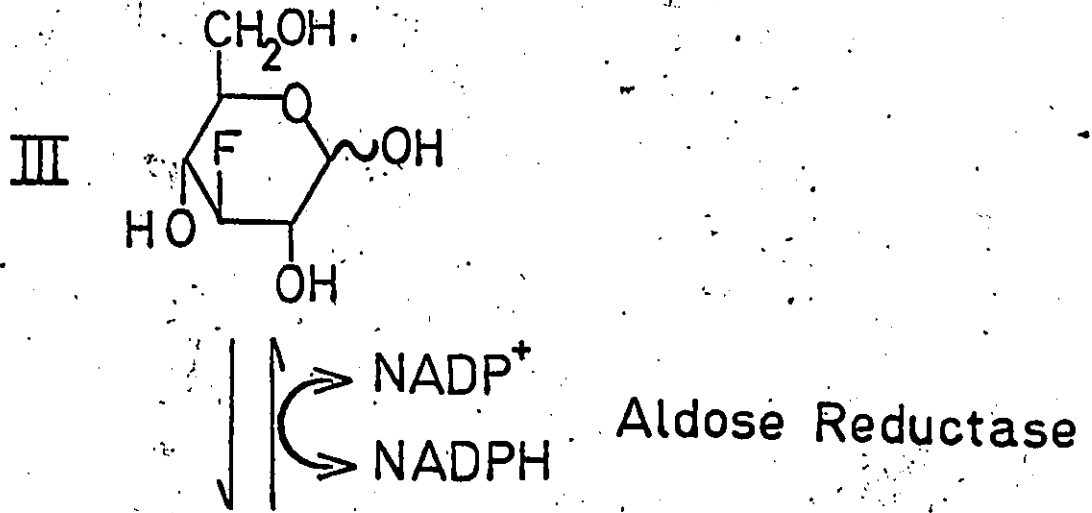
after one hour following injection. A new metabolite, however, appeared in both the fat body and haemolymph. This was identified as 3-deoxy-3-fluoro-D-glucitol (3FGL) by comparison to synthetically prepared material (60)(61). After insects were poisoned with a 10.8 mg dose of 3FG and twelve hours later haemolymph glucose levels were raised artificially by a 10.8 mg dose of glucose, the presence of 0.4-0.5 mg 3FGL per 100 mg of tissue and 0.3-0.6 mg of D-glucitol or sorbitol per 100 mg of tissue was detected. These results suggested that a pathway from glucose to fructose via sorbitol was active in these locust species and that 3FG was a substrate for aldose reductase (Figure 13). The fluoro-product of this reaction, 3FGL, seemed to block the subsequent conversion of sorbitol to fructose by inhibiting the enzyme sorbitol dehydrogenase. Also, a precursor-product relationship was evident between 3FG levels in the fat body and 3FGL levels in the haemolymph, suggesting that the fat body was the site of the conversion.

Sorbitol metabolism had been reported in the diapausing egg of Bombyx silkworm (63) and in the mosquito (64), but its presence and function in adult locusta had never been previously reported or discussed. No attempt has been made in this dissertation to review insect carbohydrate metabolism

Figure 13

Proposed pathway for metabolism of 3FG. (III) = 3FG,
(IV) = 3FGL, (V) = 3-deoxy-3-fluoro-D-fructose.

Figure 13



and regulation since many recent reviews have been directed toward this subject (65)(66)(67)(68)(69)(70).

Due to the proposed inhibitory action of 3FGL on sorbitol dehydrogenase and the proposed conversion of 3FG to 3FGL via aldose reductase, it was of considerable importance to isolate and study the properties of these enzymes in vitro. The presence of the glucose to fructose pathway in locusta could have provided an alternative route, whereby 3FG could enter glycolysis. Other studies had shown that 3FG was a very poor substrate for hexokinase from yeast (59)(71). The effects of 3FG on mammalian and insect hexokinase or glucokinase have yet to be investigated.

The objectives of Part 1 of this dissertation are:

- a) to locate and partially purify the enzymes involved in the metabolism of 3FG.
- b) to kinetically characterize the locust aldose reductase and sorbitol dehydrogenase with respect to the normal substrates as well as 3FG and 3FGL.

MATERIALS AND METHODS

Reagents

All reagents were of analytical grade or the highest purity commercially available, unless otherwise stated. All aqueous solutions were prepared using singly distilled de-ionized water. The following reagents were used: mercaptoethanol, dithioerythritol, Trizma base, Trizma HCl, NAD⁺, NADH, NADP⁺, NADPH, agarose immobilized NADP⁺ and NAD⁺, sorbitol dehydrogenase (L-iditol:NAD⁺ 5-oxidoreductase, sheep liver, EC 1.1.1.14), L-lactate dehydrogenase (EC 1.1.1.27) and glyoxylic acid were from Sigma (St. Louis, Missouri). D-sorbitol, D-glucose and D-fructose were from BDH (Toronto, Ontario). Dowex AG 50 WX12 (H⁺) and AG1-WX8 (formate) and an SDS polyacrylamide gel electrophoresis kit were from Biorad (Richmond, California). Sephadex G-25 and blue Dextran 2000 were from Pharmacia (Uppsala, Sweden). Silica gel and cellulose thin layer 0.2 mm chromatography plates were from Brinkmann and BDH (Toronto, Ontario).

Equipment

All pH measurements were performed on an analytical grade Metrohm model E-510 pH meter and ion potentiometer.

using a Fisher combination pH electrode. Centrifugation was performed on an IEC model B-60 ultra-centrifuge and an IEC model B-20A preparative centrifuge. Tissue homogenization was performed using a Polytron homogenizer with saw tooth generator or with a 100 ml Potter-Elvehjem homogenizer with a 0.013-0.020 cm clearance. All spectrophotometric measurements were done on a Beckman UV-VIS Acta VI spectrophotometer with a temperature controller.

Synthesis of 3-deoxy-3-fluoro-D-glucose (3FG) and 3-deoxy-3-fluoro-D-glucitol (3FGL)

Crystalline, twice recrystallized 3FG was prepared as previously reported (72). The purity of the material was checked by melting point, silica gel chromatography, ^{19}F NMR and IR. Thrice recrystallized 3FGL was synthesized as reported (60) and the purity was checked by silica gel chromatography, Rf 0.55, solvent isopropanol : ethyl acetate : water : acetic acid, 83:11:5:1 v/v and Rf 0.66, solvent ethanol : water : ammonium hydroxide, 80:16:4 v/v, ^{19}F NMR and IR. No reducing spots were obtained when the chromatograms were sprayed with the highly sensitive reagent aniline phthallate (73).

Locust Rearing Conditions

Locusts were reared under crowded conditions in a temperature and humidity controlled environment room, kept at 30° C and 30% humidity. Diet consisted of local field grass and store bought carrots with greens. Only healthy adult male locusta age 10-20 days were used throughout this study.

Injection Procedures and 3FGL Toxicity Study

Male adult locusta age 10-14 days were injected with various concentrations of 3FGL in a 30 μ l volume using a 50 μ l Hamilton syringe. All injections were into the haemocoel and were made using a 2 inch 24 gauge needle which was inserted to a fixed depth of 5 mm through the membranous septum at the base of the front thoracic leg. Any locust which was poorly injected as shown by haemolymph leakage was discarded from the study. Locusta were deprived of food for eight hours prior to injection. A similar toxicity study using a western Canadian grasshopper Melanoplus sanguinipes kindly conducted for us by Agriculture Canada, used abdominal injection of the same agent in a 25 μ l volume. In all cases distilled deionized sterile water was used to prepare injection solutions. Control locusta were injected with an

equal volume of water or water plus an equivalent amount of glucose. *Locusta* were observed for periods of up to 5 days for toxicity, during which time they were fed their normal diet.

Enzyme Isolation: Sorbitol Dehydrogenase and Aldose Reductase

A preparation of sorbitol dehydrogenase (EC 1.1.1.14) from insect fat body was carried out as follows. Adult *Locusta migratoria*, 10-14 days old, were stunned at -10°C for 10 minutes. Fat bodies were dissected out from 100 locusta and pooled to yield about 15 grams of tissue which was frozen in liquid nitrogen and stored at -10°C . This tissue was homogenized in a Potter-Elvehjem homogenizer with 10 volumes of ice-cold 0.05 M Tris buffer, pH 7.5, with 5 mM mercaptoethanol. The crude homogenate was filtered through cheesecloth and the filtrate centrifuged at $55,000 \times g$. The protein concentration of the supernatant was adjusted to 0.63 mg/ml using a nomograph of Warburg and Christian (121); the enzyme was precipitated between 40-80% saturation of ammonium sulfate and desalted with a Sephadex G-25 column. In most preparations the specific activity of sorbitol dehydrogenase was increased 4-10-fold over that of the crude homogenate. Polyacrylamide gel electrophoresis of the enzyme preparation revealed 10 distinct protein bands when performed on 7%

discontinuous gels. In the presence of dithioerythritol or mercaptoethanol the enzyme preparation maintained up to 50% activity over a 2 week period when frozen at -10°C .

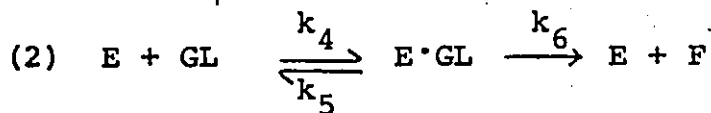
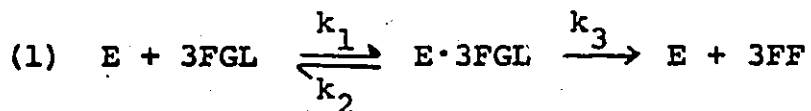
Aldose reductase (EC 1.1.1.21) was isolated from locust fat body by the following procedure. About 9.5 grams of fat body was homogenized in 50 ml of Tris buffer pH 7.5 with 5 mM mercaptoethanol at high speed for 10-15 seconds with a Polytron homogenizer. The resulting homogenate was filtered through cheesecloth and spun at $6,000 \times g$ for 30 minutes at 4°C . The enzyme active fraction was taken from the 40-100% ammonium sulfate cut. Desalting was performed as previously described. It was found that better yields of this enzyme were obtained using a Polytron homogenizer rather than the Potter-Elvehjem type. Aldose reductase and sorbitol dehydrogenase were assayed using 0.2 - 0.01 M glucose or sorbitol as substrates in the presence of 1.0 - 0.1 mM NAD^{+} or NADPH respectively, and observing the change in absorbance at 340 nm. Specific activity was expressed as micromoles NADH or micromoles NADPH per minute per milligram of protein unless otherwise stated. All assays were in 1.5 ml matched quartz cuvettes with a final volume of 1.0 ml at 25°C .

Enzyme Kinetics and Derivation

The kinetic parameters K_M (app), V_{Max} (app) and K_i were obtained using Lineweaver Burk double reciprocal plots. The best linear fit was determined by the method of least squares. The following method was used to derive an equation to explain the behavior of 3FGL as an inhibitor and substrate of sorbitol dehydrogenase in the presence of sorbitol.

Reaction Scheme

E = free enzyme, E·3FGL = enzyme - 3FGL complex,
 E·GL = enzyme - glucitol complex, GL = free glucitol,
 3FGL = free 3FGL, F = fructose, 3FF = 3-deoxy-3-fluoro-D-fructose. The concentration of NAD^+ was constant and neglected in this derivation.



Equation for Initial Velocity

$$(i) \quad \dot{x} = k_3 [E \cdot 3FGL] + k_6 [E \cdot GL]$$

Mass Conservation equation

$$(ii) \quad [E_t] = [E \cdot 3FGL] + [E \cdot GL] + [E]$$

Using the Steady State Approximation

$$(iii) \quad \frac{d[E \cdot 3FGL]}{dt} = 0 = k_1 [E][3FGL] - k_3 [E \cdot 3FGL] - k_2 [E \cdot 3FGL]$$

$$(iv) \quad \frac{d[E \cdot GL]}{dt} = 0 = k_4 [E][GL] - k_5 [E \cdot GL] - k_6 [E \cdot GL]$$

Rearranging equations (iii) and (iv) to solve for $[E \cdot 3FGL]$ and $[E \cdot GL]$

$$(v) \quad [E \cdot 3FGL] = \left(\frac{k_1}{k_3 + k_2} \right) [E][3FGL]$$

$$(vi) \quad [E \cdot GL] = \left(\frac{k_4}{k_5 + k_6} \right) [E][GL]$$

$$\text{let } \left(\frac{k_3 + k_2}{k_1} \right) = K_1 \text{ and } \left(\frac{k_5 + k_6}{k_4} \right) = K_2$$

Substituting equations (v) and (vi) into equation (i)

$$v = \frac{k_3 [E][3FGL]}{K_1} + \frac{k_6 [E][GL]}{K_2}$$

$$(vii) \quad v = \left(\frac{k_3}{K_1} [3FGL] + \frac{k_6}{K_2} [GL] \right) [E]$$

Substituting equations (v) and (vi) into equation (ii)

$$E_t = \left(\frac{[3FGL]}{K_1} + \frac{[GL]}{K_2} + 1 \right) [E]$$

or

$$(viii) [E] = \frac{[E_t]}{\left(\frac{[3FGL]}{K_1} + \frac{[GL]}{K_2} + 1\right)}$$

Substituting (viii) into (vii)

$$(ix) v = \frac{k_3 [E_t] [3FGL]}{[3FGL] + \frac{K_1 [GL]}{K_2} + K_1} + \frac{k_6 [E_t] [GL]}{[GL] + \frac{K_2 [3FGL]}{K_1} + K_2}$$

If we let $k_3 [E_t] = V_1$ and $k_6 [E_t] = V_2$ then

$$(x) v = \frac{V_1 [3FGL]}{[3FGL] + K_1 \left(\frac{[GL]}{K_2} + 1\right)} + \frac{V_2 [GL]}{[GL] + K_2 \left(\frac{[3FGL]}{K_1} + 1\right)}$$

The classical rate equation for substrate inhibition

is:

$$(xi) v = \frac{V_{\max} [S]}{K_m \left(1 + \frac{[I]}{K_i}\right) + [S]}$$

The verification for the use of equation (x) is illustrated in Figure 15a, in which a computer generated line using experimentally derived parameters substituted into equation (x) is compared to the line derived from direct experimental results.

Although it was not known at the time, a virtually

identical scheme was published by I.H. Segal in 1975 after the present scheme had been verified (74).

Kinetic data was linearized by least squares analysis. A sample calculation is given in Appendix 1.

Enzyme Recycling System

A recycling system utilizing sheep liver sorbitol dehydrogenase and lactate dehydrogenase was used in order to attempt the enzymic synthesis of 3-deoxy-3-fluoro-D-fructose.

System 1 - for native substrates, final volume 10 ml D-sorbitol 0.04 M, glyoxylate 0.2 M, NAD⁺ 1 mM, sorbitol dehydrogenase 0.5 mg protein, L-lactate dehydrogenase 2 mg M₄ isoenzyme, mercaptoethanol 5 mM, potassium phosphate buffer pH 7.35, 0.15 M.

System 2 - for fluorosubstrate, final volume 10 ml 3-FGL 0.1 M, glyoxylate 0.2 M, NAD⁺ 1 mM, sorbitol dehydrogenase 0.8 mg protein, lactate dehydrogenase 2 mg M₄ isozyme, mercaptoethanol 5 mM, potassium phosphate buffer pH 7.35, 0.15 M.

The following enzyme activities were used:
sorbitol dehydrogenase, 32 units/mg protein, at pH 7 and 25°C;
L-lactate dehydrogenase, 935 units/mg protein at 37°C and

pH 7.5. The progress of the recycling reaction was monitored by the disappearance of glyoxylate using the assay of McFadden and Howes (75). Thirty microlitre aliquots of the reaction mixture were withdrawn at 15 minute intervals and diluted 30 fold; 30 μ l of the resulting dilution was used in the assay system as described. All assays were done in triplicate. The non-ionic products were separated from the reaction mixture by the following procedure. The reaction mixture (approximately 10 ml) was loaded into a mixed resin column with a total volume of 15 ml containing Dowex AG-1 formate and Dowex AG-50 H⁺. The free sugars were eluted with 50 ml of distilled deionized water and then lyophilized. Fluoro-sugars were chromatographed on cellulose t.l.c. plates using the solvent system, ethyl acetate: pyridine : water, 120:50:40, and on silica gel using the solvent system ethanol : water : ammonium hydroxide, 80:16:4. Non fluoro-sugars were chromatographed on cellulose using the solvent ethyl acetate : pyridine : water, 50:50:45 and on Whatman #1 filter paper using the solvent phenol : water, 90:10.

Glyoxylate Colorimetric Assay (75)

To a 5.0 ml solution containing 0.025-0.3 μ mole

glyoxylate, 1.0 ml of 1 M oxalic acid buffer at pH 1 was added followed by 1.0 ml of 1% w/v phenylhydrazine hydrochloride. The solution was heated to boiling and cooled for 5 minutes. After chilling in an ice bath to approximately room temperature, 4.0 ml of concentrated HCl was added, followed by 1.0 ml of 5% w/v $K_3Fe(CN)_6$. After thorough mixing, the absorbancy was determined at 520 nm after a 7 minute incubation. Colour development was stable for about 1 hour at room temperature.

RESULTS AND DISCUSSION

A 3FGL toxicity study on male adult Locusta migratoria (Table 1) indicated that the approximate LD₅₀ for this compound was about the same as that of 3FG, namely about 4 mg/gm of locust. A similar study conducted at our request at the Agriculture Canada Institute (London, Ontario) using the western Canadian grasshopper Melanoplus sanguinipes also indicated an LD₅₀ of about 4 mg/gm of insect (76).

Preliminary experiments indicated that the activities of aldose reductase and sorbitol dehydrogenase were present only in fat body and that the enzymes were NADP⁺ and NAD⁺ dependent respectively. Attempts to extensively purify these enzymes using NADP⁺ and NAD⁺ affinity columns were not successful, presumably due to the weakening of enzyme binding as a result of the ligand spacer arm. It has been suggested that a dissociation constant less than 10⁻³ is prerequisite for success in affinity chromatography (77). Even though the enzyme preparations were not pure, their specificity permitted meaningful kinetic analysis in accordance with views expressed elsewhere (78)(79).

When using steady state kinetic analysis on impure enzyme preparations, it is important to establish the fact

Table I

3FGL Toxicity Study (Adult Male Locusta 10-14 days)

Dose 3FGL mg/gm tissue	Frequency of death	Approximate time till death
1	0% n=10	
2	30% n=10	4 days
3	40% n=10	3 days
4	50% n=10	3 days
8	70% n=10	1 day

Control locusts were injected with equivalent amounts of H₂O or D-sorbitol.

that one is working within the confines of the steady state approximation. With pure enzymes, a reasonable general rule is that the concentration of the most dilute substrate solution should exceed that of the enzyme at least 1000-fold. One may verify this assumption by plotting initial velocity against enzyme concentration for the most dilute substrate concentration to be used in the assays. An illustration of this is given in Figure 14. The linear portion of this plot obeys a pseudo first order rate law, ie

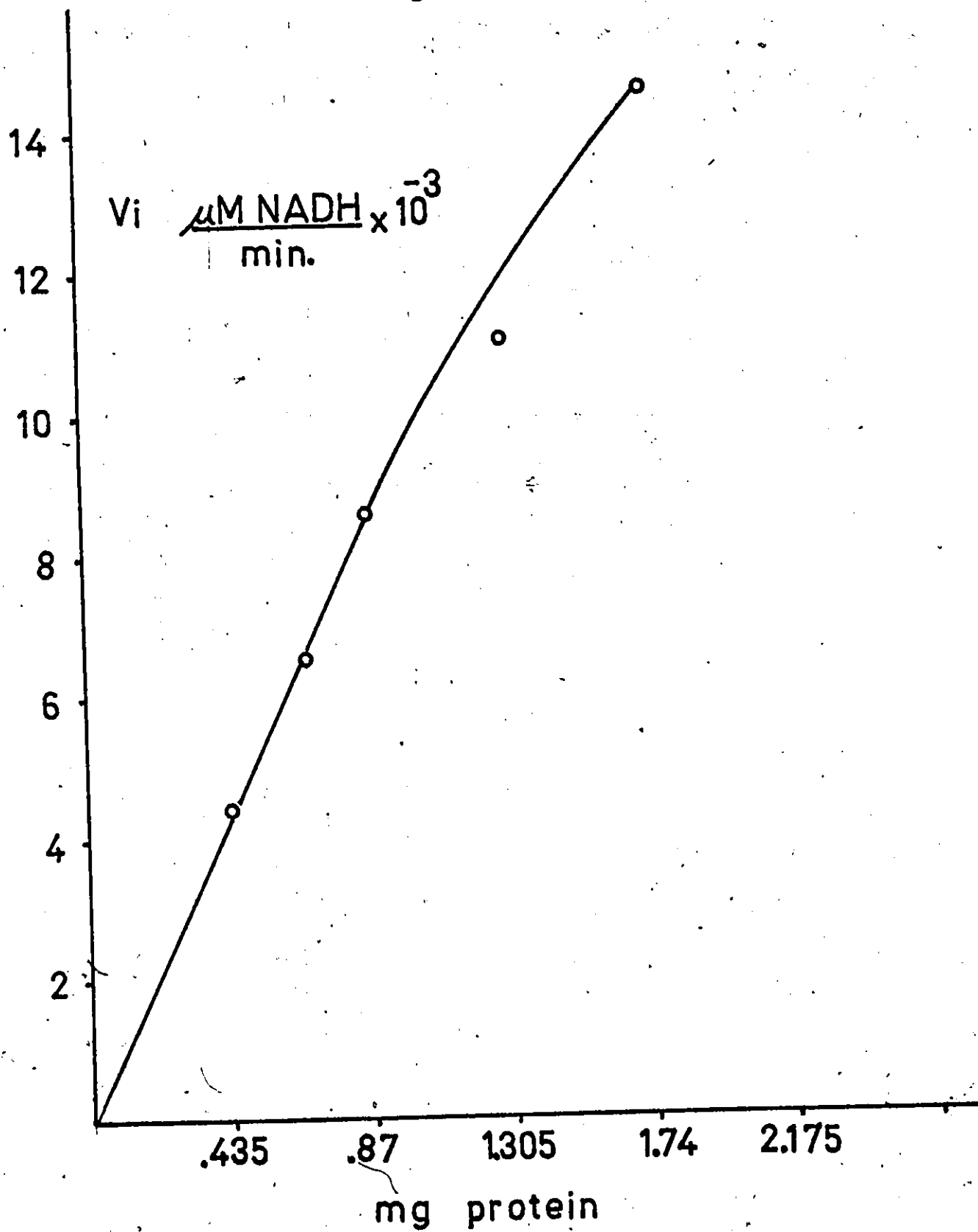
$$v_{\text{initial}} = k_{\text{obs}}(E), \quad \frac{k_{\text{obs}}}{(S)} = k_2 \quad (\text{second order rate constant})$$

This implies that the $(S) \gg (E)$, and for the duration of initial slope measurements (about 30 seconds), that $(S)_t = (S)_{t=0}$. For all steady state kinetics, a protein concentration which was well within the linear portion of such a plot was always chosen. Kinetic experiments were carried out at a variety of protein concentrations within the linear pseudo first order portion of initial velocity versus protein concentration plots and were shown to give consistent results. General treatments of this problem have been outlined by Cornish-Bowden (80) and, particularly Laidler (81). For a simple Michaelis-Menten type of mechanism Cornish-Bowden has shown

Figure 14

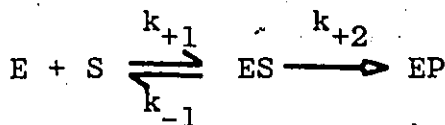
Graph of locust sorbitol dehydrogenase activity versus protein concentration, assay conditions 0.05 M Tris buffer pH 7.5, 5 mM mercaptoethanol, 25°C, 1 mM NAD⁺ and 0.01 M sorbitol.

Figure 14



that

$$v_i = \frac{V(S)(1 - \exp - (k_{+1}(S) + k_{-1} + k_{+2})t)}{K_m + (S)}$$



When t is sufficiently large,

$$v_i = \frac{V(S)}{K_m + (S)}$$

The K_m (app) for sorbitol in the presence of 1.0 mM NAD^+ and locust sorbitol dehydrogenase was 0.06 ± 0.015 M (Figure 15a). The relatively large uncertainty in the K_m (app) was due to the relatively small loss of enzyme activity during kinetic analysis which resulted in an increased point scatter for the double reciprocal plots. Any experiments in which the enzyme activity dropped greater than 10% during the duration of kinetic runs, were omitted from kinetic analysis. Such instability has been reported for other dehydrogenase enzymes (82). 3FGL was a competitive inhibitor (Figure 15a) with a

Figure 15a

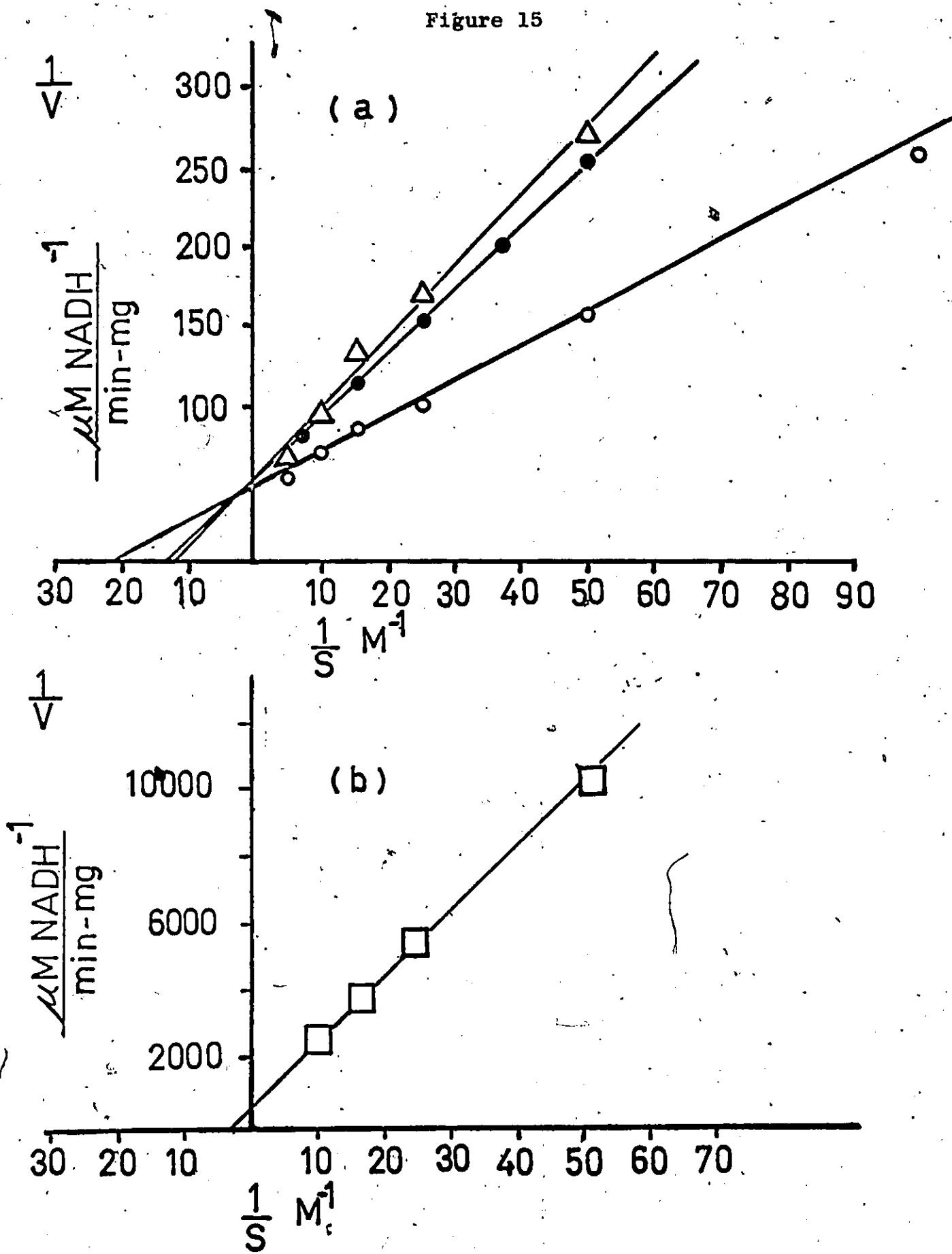
Kinetic data for locust sorbitol dehydrogenase illustrating the competitive nature of 3FGL inhibition. \circ sorbitol as substrate, Δ sorbitol in the presence of 0.1 M 3FGL,


● computer generated plot using experimentally determined kinetic constants substituted into equation (X). K_i (app) for 3FGL inhibition = 0.082 M. Temperature = 25°C, (NAD⁺) = 1 mM in all cases.

Figure 15b

Double reciprocal plot for locust sorbitol dehydrogenase with 3FGL as substrate \square . K_m (app) in the presence of 1 mM NAD⁺ is 0.5 M, temperature = 25°C.

Figure 15





K_i (app) of 0.082 M. It was shown that 3FGL was a substrate for the locust sorbitol dehydrogenase with a K_m (app) of 0.5 M at 1.0 mM NAD^+ (Figure 15b). The apparent V_{max} for sorbitol at this concentration of NAD^+ was $0.02 \mu M NADH \text{ min}^{-1} \text{ mg protein}^{-1}$. It had been reported previously that the K_m (app) for a sorbitol dehydrogenase from rabbit liver was 0.07 M (83). Kinetic data on commercial sheep liver sorbitol dehydrogenase gave a K_m (app) of 0.008 M and a V_{max} (app) of $0.01 \mu M NADH \text{ min}^{-1} \text{ ml}^{-1}$ for sorbitol (Figure 16). For the same enzyme 3FGL had a K_m (app) of 0.07 M and a V_{max} (app) of $0.0035 \mu M NADH \text{ min}^{-1} \text{ ml}^{-1}$ (Figure 16). It would appear, therefore, that the K_m (app) and V_{max} (app) parameters of 3FGL for both locust and sheep liver enzyme were in a similar direction. In both cases, 3FGL had about an eightfold lower K_m (app) and a considerably lower V_{max} (app) as compared to the native substrate. In the case of the locust enzyme, the V_{max} (app) of 3FGL was eight times lower, and in the commercial enzyme three times lower.

Initially, it was considered that 3FGL was acting as a classical competitive inhibitor (Figure 15a), but in view of the fact that 3FGL was also a substrate, a ter-reactant mechanism in the presence of 3FGL, sorbitol and NAD^+ was considered to operate. To account for this behavior and

Figure 16

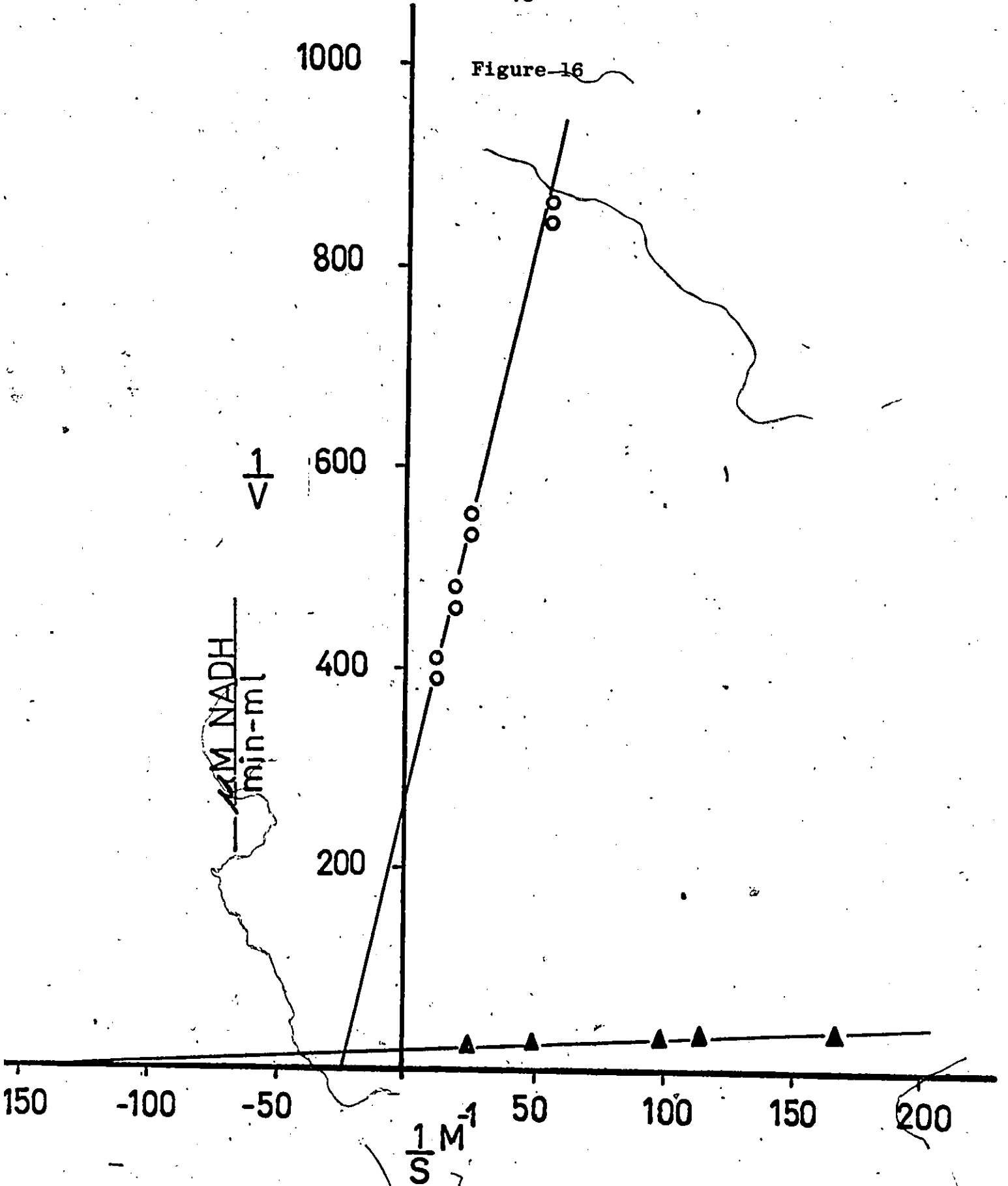
Double reciprocal plot for sheep liver sorbitol dehydrogenase.

▲ sorbitol as substrate in the presence of 1 mM NAD⁺.

K_m (app) = 0.008 M, temperature = 25°C, ○ 3FGL as substrate in the presence of 1 mM NAD⁺, temperature = 25°C.

K_m (app) = 0.07 M. Enzyme activity is expressed as $\frac{\mu\text{M NADH}}{\text{min} - \text{ml}}$ rather than $\frac{\mu\text{M NADH}}{\text{min} - \text{mg}}$ due to the inability to assaying minute amounts of protein using the spectrophotometric assay outlined in the Materials and Methods section.

Figure-16



rationalize the kinetic results obtained an alternative scheme was derived in which the concentration of NAD^+ was assumed to be constant and hence neglected (see Materials and Methods). This derivation yielded equation (x) instead of equation (xi) for the initial velocity.

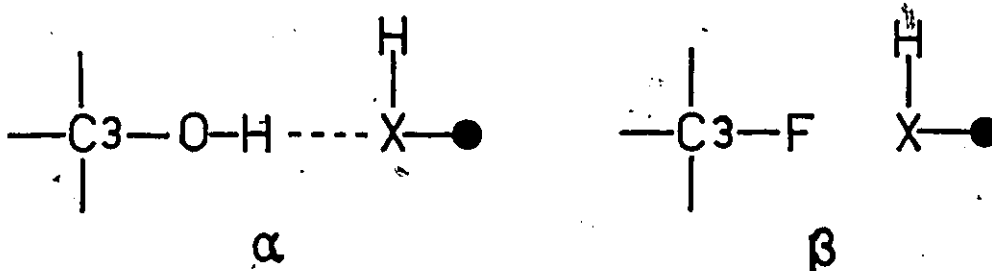
$$(x) \quad v_i = \frac{V_1(3\text{FGL})}{K_1(1+(G)/K_2) + (3\text{FGL})} + \frac{V_2(G)}{K_2(1+(3\text{FGL})/K_1) + (G)}$$

$$(xi) \quad v_i = \frac{V(S)}{K_m(1+(I)/K_i) + (S)}$$

The form of these two equations was similar, except that equation (x) involved two catalytic terms. Equation (x) also implied that, at a constant concentration of 3FGL , as the concentration of glucitol was decreased, the enzyme began to switch from oxidizing glucitol with a high V_{max} (app) to 3FGL with a lower V_{max} (app). This resulted in a kinetic pattern identical to classical competitive inhibition. The validity of this approach was established by using the experimentally determined values for V_1 ($2.5 \times 10^{-3} \mu\text{M NADH min}^{-1} \text{ mg}^{-1}$), V_2 ($2.0 \times 10^{-2} \mu\text{M NADH min}^{-1} \text{ mg}^{-1}$), K_1 (0.5 M) and K_2 (0.075 M) in equation (x) and generating a theoretically derived line which was almost superimposable

on the experimentally determined line for 3FGL inhibition (Figure 15a).

The higher K_m for 3FGL compared with sorbitol, for both the locust and sheep liver enzyme, suggests the possibility that stereospecific hydrogen bonding between the hydrogen of the hydroxyl group at $C_{(3)}$ of sorbitol (α) and a receptor group on the enzyme is necessary for maximum binding. The replacement of $-OH$ by F at $C_{(3)}$ (β) could eliminate or change the direction of hydrogen bonding between substrate and enzyme (88) and hence possibly affect the binding contribution at this position.



where \bullet = protein, X = electronegative element

It has been suggested by Jencks (87) that part of the total potentially available free energy of substrate binding is used for substrate destabilization through distortion, desolvation, electrostatic interactions, and the decrease

in entropy necessary to produce the reactive substrate conformation. If we assume that the V values reflect these catalytic parameters then a substrate which has fewer specific binding groups may be expected to have less intrinsic binding energy available for catalytic enhancement. This may, therefore, be an explanation for the lower V values observed for 3FGL than those found for sorbitol.

One must, however, concede that an argument such as the one presented above is somewhat speculative, and can only be offered as one possible explanation for the observed results. The basis of uncertainty resides in the realization that steady state kinetic parameters for bireactant enzymes do not reflect true dissociation constants or pure rate limiting kinetic constants in the case of V_{\max} values. This can be seen from the discussion in Appendix 1.

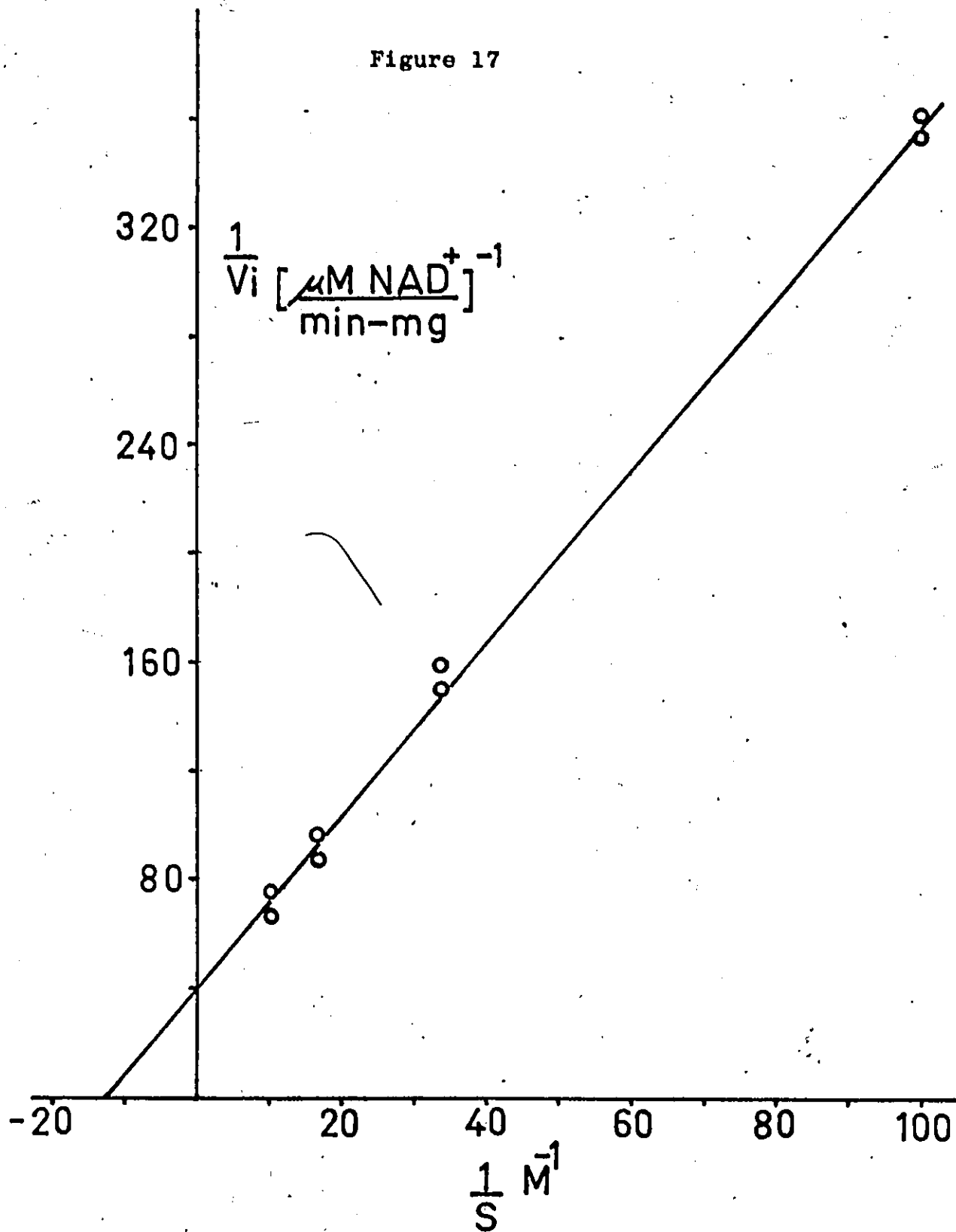
Attempts by Kun (19), Eisenthal and Harrison (88), and Fondy (89) to make some sense of the effect of fluoro-substitution on K_m and V_{\max} values in malate dehydrogenase, citrate synthase, L-glycerophosphate dehydrogenase have been confounded by the complexity and inappropriateness of these gross kinetic parameters in sorting out substituent effects.

Figure 17 shows a Lineweaver Burke plot of the locust sorbitol dehydrogenase in the thermodynamically preferred

Figure 17

Locust sorbitol dehydrogenase double reciprocal plot in the thermodynamically favoured direction (fructose \longrightarrow sorbitol). Assay conditions were 0.05 M Tris buffer pH 7.5, 5 mM dithioerythritol and NADH 0.1 mM, 25°C. Fructose was the varying substrate. K_m (app) \sim 0.08 M. V_{max} (app) \sim 0.025 $\frac{\mu\text{M NAD}^+}{\text{min} - \text{mg}}$.

Figure 17



direction at pH 7.5 (fructose \rightarrow sorbitol) at 0.1 mM NADH.

The K_m (app) for fructose was 0.08 M and the V_{max} (app) was $0.025 \mu\text{M NAD}^+ \text{ min}^{-1} \text{ mg}^{-1} \text{ protein}^{-1}$. The similarity of these kinetic constants to those determined in the sorbitol to fructose direction may have had a diagnostic feature.

"A general kinetic feature of dehydrogenases is that NADH usually binds more tightly than NAD^+ . The structural features responsible for this are not clear, although the charged nicotinamide ring is clearly more hydrophilic than the reduced form in NADH. The tight binding leads to the dissociation of the enzyme-NADH complexes being largely rate determining at saturating concentrations of reagents at physiological pH. Furthermore, although the equilibrium constant for the oxidation reaction in solution greatly favours NAD^+ and alcohol, the tighter binding of the NADH causes the equilibrium constant for the enzyme-bound reagents to be less unfavourable." (85)

This phenomenon may result in an equilibrium constant which is closer to unity in the case of locust sorbitol dehydrogenase than would be predicted by redox potentials alone.

A preliminary chromatogram of locust sorbitol dehydrogenase reaction products in the direction $3\text{FGL} \rightarrow \text{product}$ indicated the presence of a component with a different R_f value than either 3FG or 3FGL (Figure 18). Since this component ran faster than non-fluorosugars it was tentatively proposed to be 3-deoxy-3-fluoro-D-fructose (3FF).

Figure 18

Chromatogram of locust sorbitol dehydrogenase reaction mixture with 3-deoxy-3-fluoro-D-glucitol as substrate.

3FGL = 3-deoxy-3-fluoro-D-glucitol or sorbitol

3FG = 3-deoxy-3-fluoro-D-glucose

3FF = putative 3-deoxy-3-fluoro-D-fructose

U = unknown material (probably NAD^+)

G = D-glucose

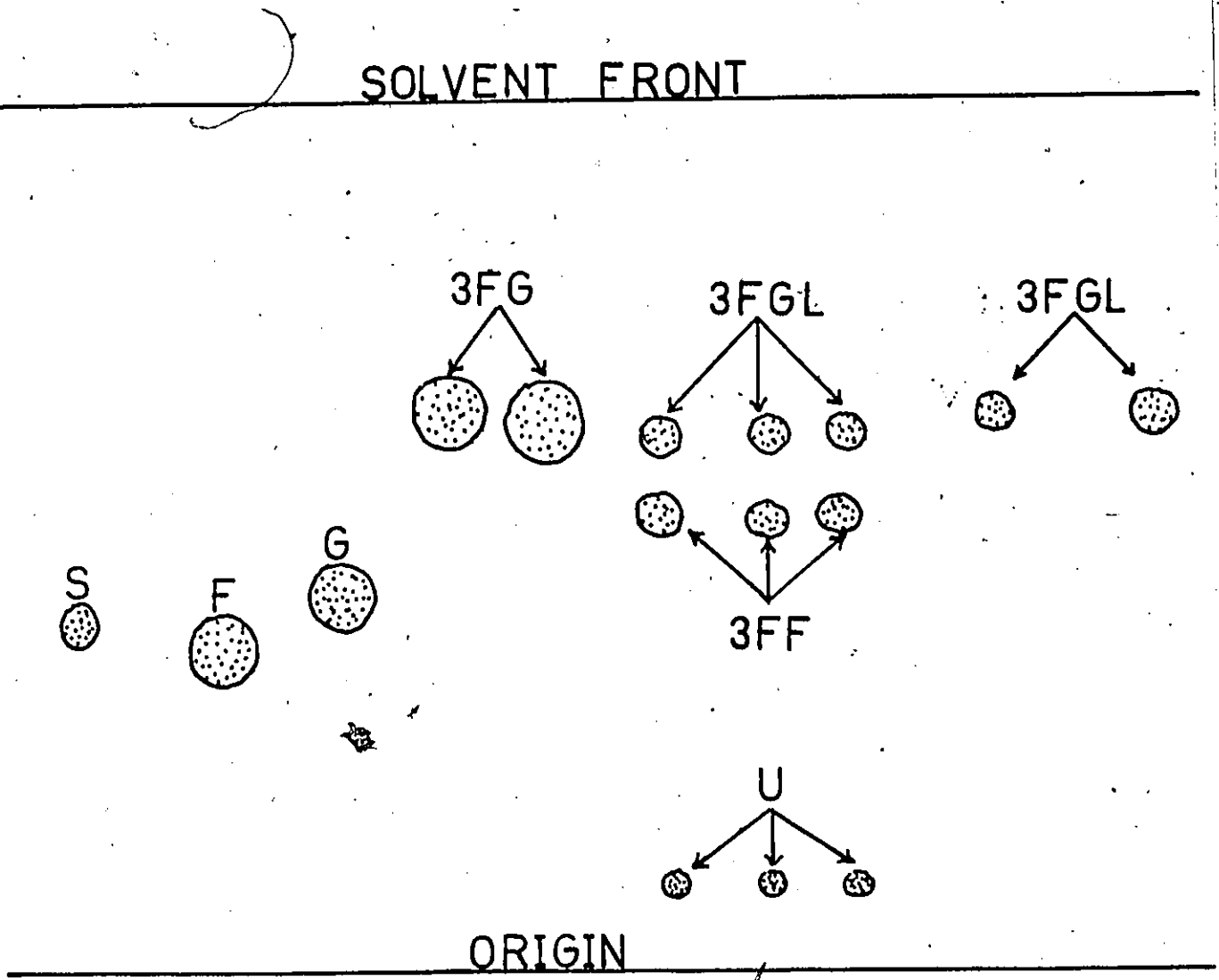
F = D-fructose

S = D-glucitol or sorbitol

The stationary phase was silica gel, the mobile phase was ethanol : H_2O : NH_4OH , 80:16:4.

Spots were visualized with ethanol : sulfuric acid spray, 50:50.

Figure 18



Attempts to obtain appreciable aldose reductase activity were fraught with difficulty. Out of six preparations, only one preparation contained sufficient activity to warrant preliminary kinetic studies. This preparation was obtained by using a Polytron homogenizer instead of the Potter Elvehjem type. The enzyme was found to be comparatively unstable at room temperature under the conditions of assay. Stable pure preparations of this enzyme have been prepared from liver (90).

Preliminary results did indicate, however, that at a NADPH concentration of 0.1 mM and a sugar concentration of 100 mM, 3FG gave initial velocities about 2.5 to 3 times greater than those obtained with an equi-molar concentration of glucose. This result was significant in light of the previous in vivo gas chromatographic studies which indicated that 3FG disappeared rapidly from locust tissues and was converted to 3FGL under conditions in which no traces of endogenous sorbitol could be found. The kinetic results with locust sorbitol dehydrogenase suggested that 3FGL was a much poorer substrate than sorbitol for this enzyme.

Therefore, it was possible to rationalize the in vivo results on the basis of in vitro studies. Accumulation of 3FGL in fat body and haemolymph was a consequence of the

fact that 3FG was converted to 3FGL faster than glucose was to sorbitol via aldose reductase, but at the next step, 3FGL was a poorer substrate for sorbitol dehydrogenase and therefore accumulated.

Preliminary in vitro results also indicated that the aldose reductase was operative in the direction of sorbitol to glucose, but at a much lower activity than the glucose to sorbitol conversion under identical cofactor and sugar concentrations. The only Michaelis-Menten plot obtained for aldose reductase in the direction of 3FG to 3FGL is given in Figure 19. The poor quality of this plot was due to enzyme stability problems and precluded the calculation of any precise kinetic parameters.

Figures 20, 21, 22 represent some kinetic studies which were done to further characterize the sheep liver sorbitol dehydrogenase with the intent of using it for synthetic purposes. The pattern in Figure 20 was indicative of the fact that the enzyme did not satisfy the substituted enzyme (ping-pong) mechanism but did obey the equation

$$v_1 = \frac{V_1(A)(B)}{K_{1a}K_b + K_b(A) + K_a(B) + (B)(A)} \quad (\text{Cleland})$$

Figure 19

Locust aldose reductase double reciprocal plot with 3FG and NADPH (0.2 mM) as substrates. 3FG was the varying substrate. Assay conditions, 0.05 M Tris buffer, pH 7.5, 5 mM dithioerythritol, 25°C.

Figure 19

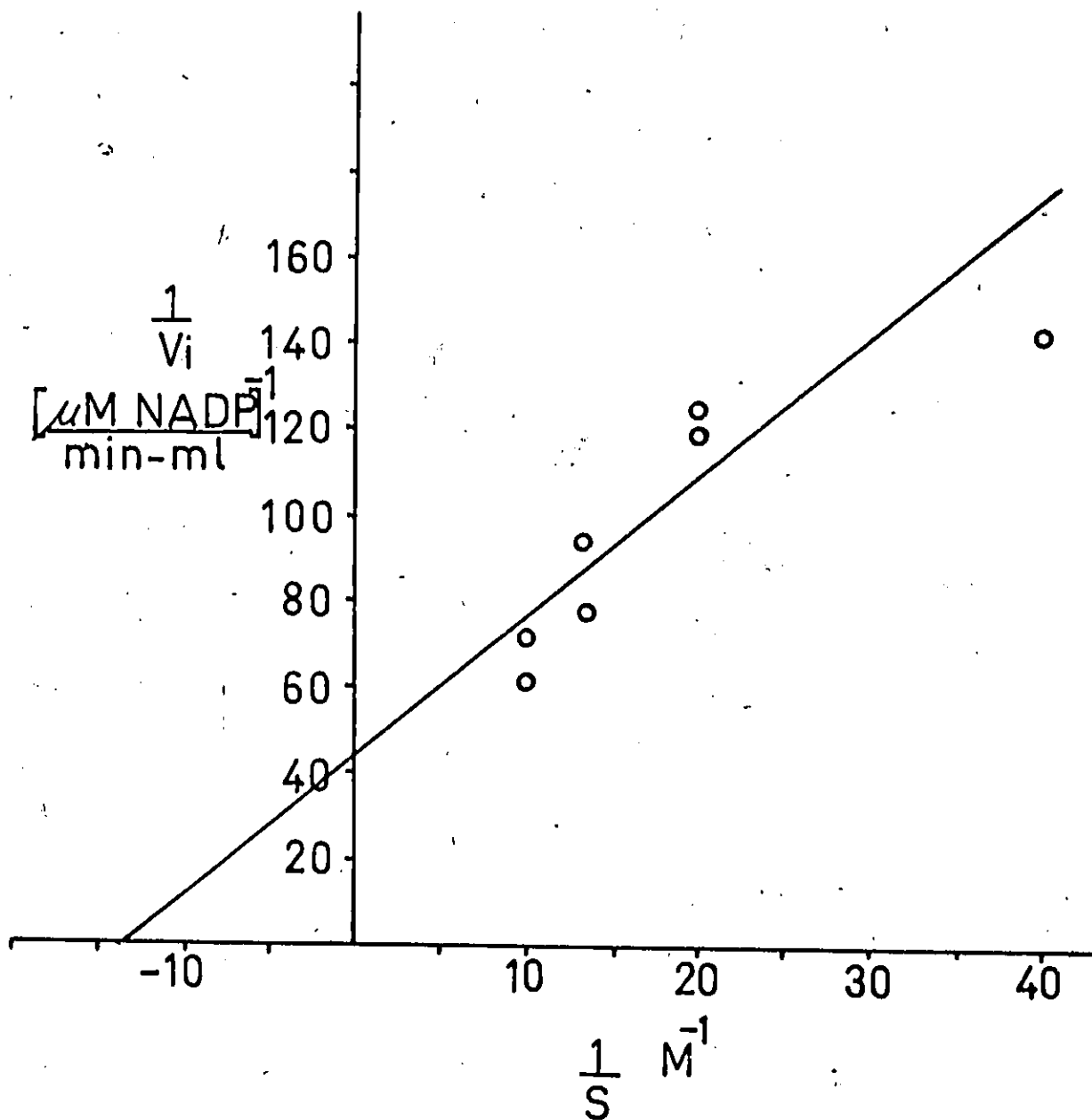


Figure 20

Sheep liver sorbitol dehydrogenase double reciprocal plots
at various concentrations of NAD^+ , pH 7.5, 0.05 M Tris buffer,
5 mM mercaptoethanol, sorbitol as the varying substrate.

○ - 0.2 mM NAD^+

△ - 0.5 mM NAD^+

● - 1.0 mM NAD^+

Figure 20

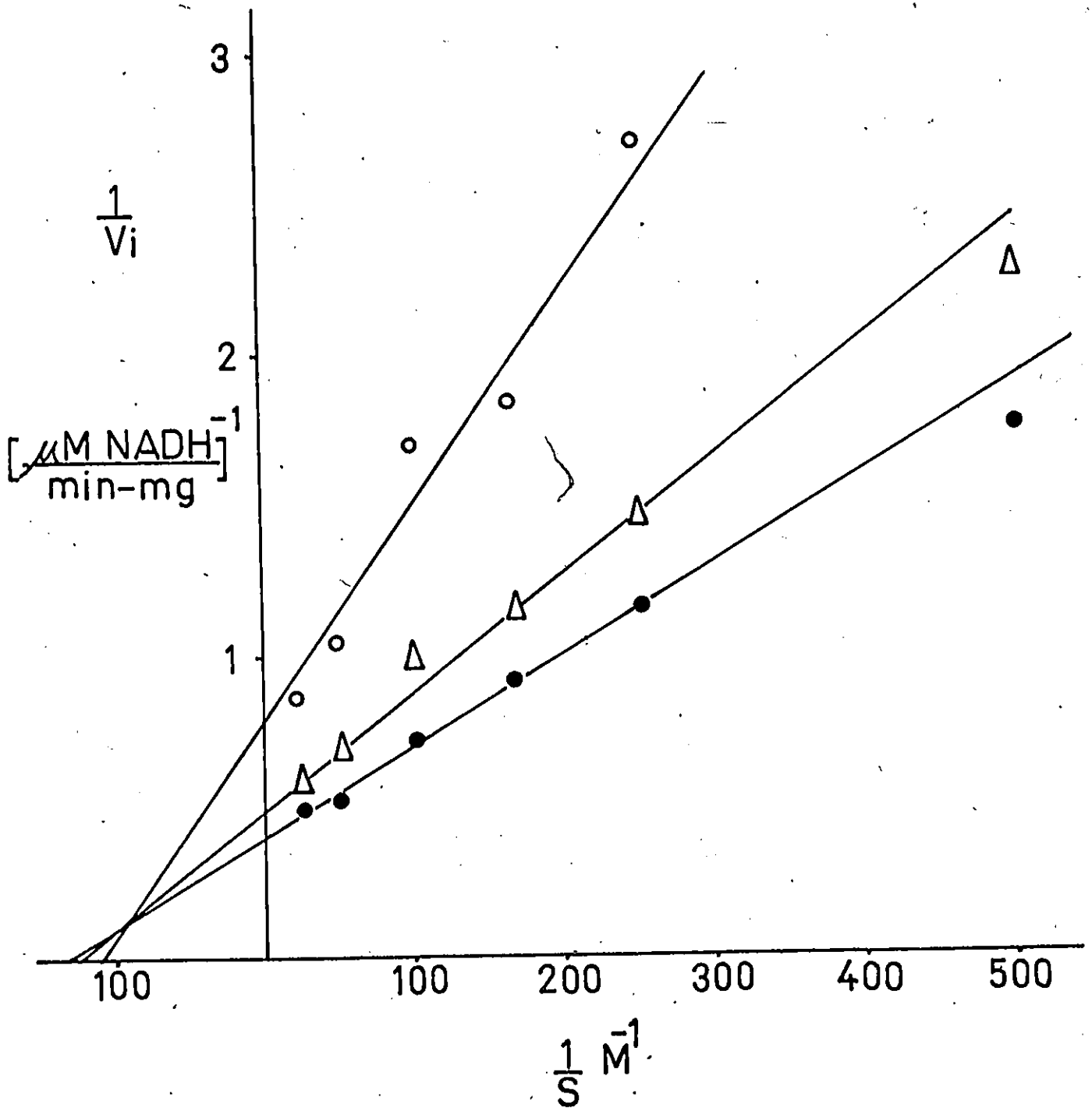


Figure 21

Ordinate intercepts from Figure 20 plotted against the varying constant $1/\text{NAD}^+$.

$$\text{Intercept from Figure 21} = 1/V_1 = 3 \times 10^5 \frac{\text{min} - \text{mg}}{\text{M NADH}}$$

$$\text{Slope from Figure 21} = K_a/V_1 = 1 \times 10^5 \frac{\text{min} - \text{mg} - \text{mM}}{\text{M NADH}}$$

$$K_a = 3.3 \times 10^{-4} \text{ M}$$

Figure 21

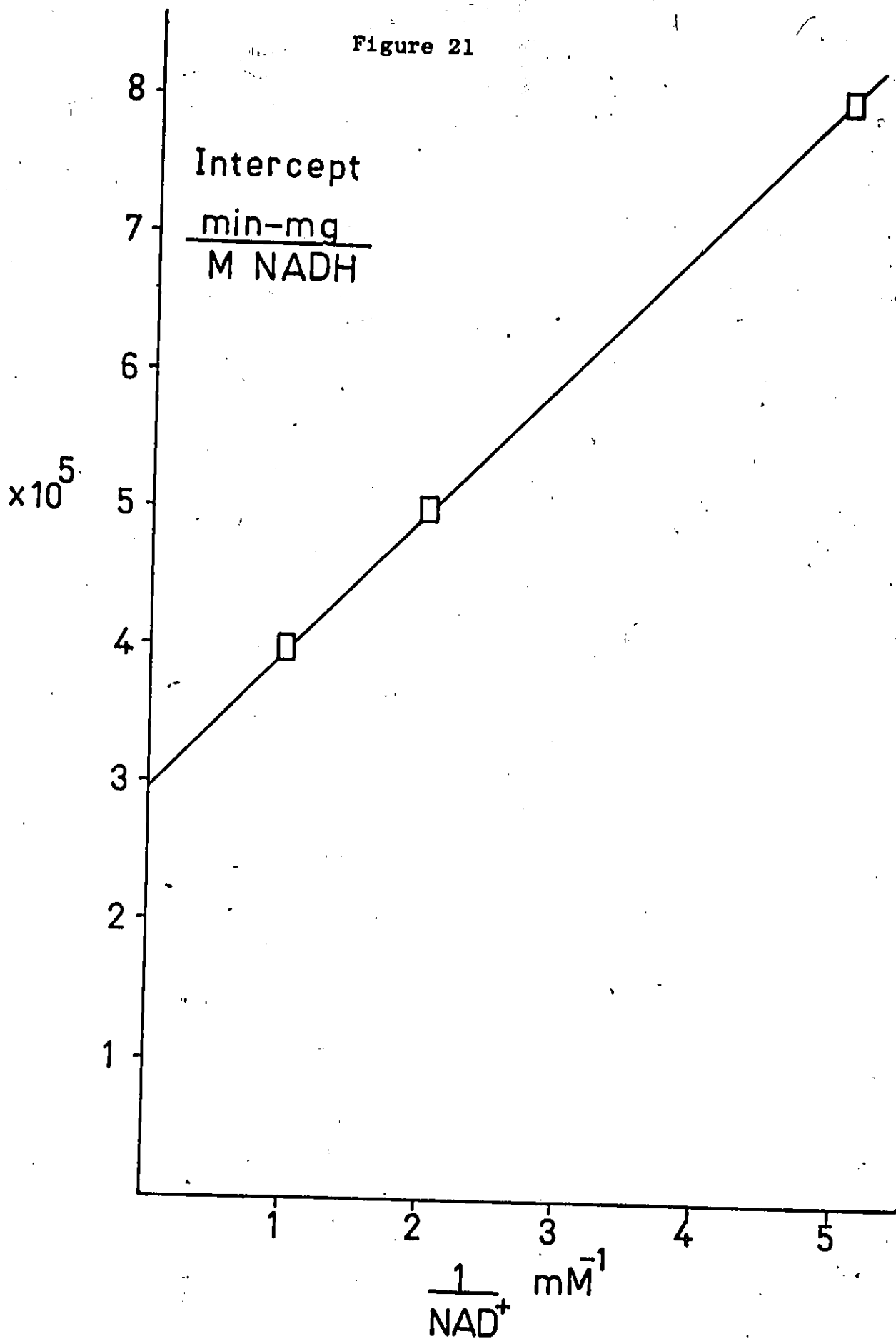


Figure 22

Slopes from Figure 20 plotted versus $1/\text{NAD}^+$

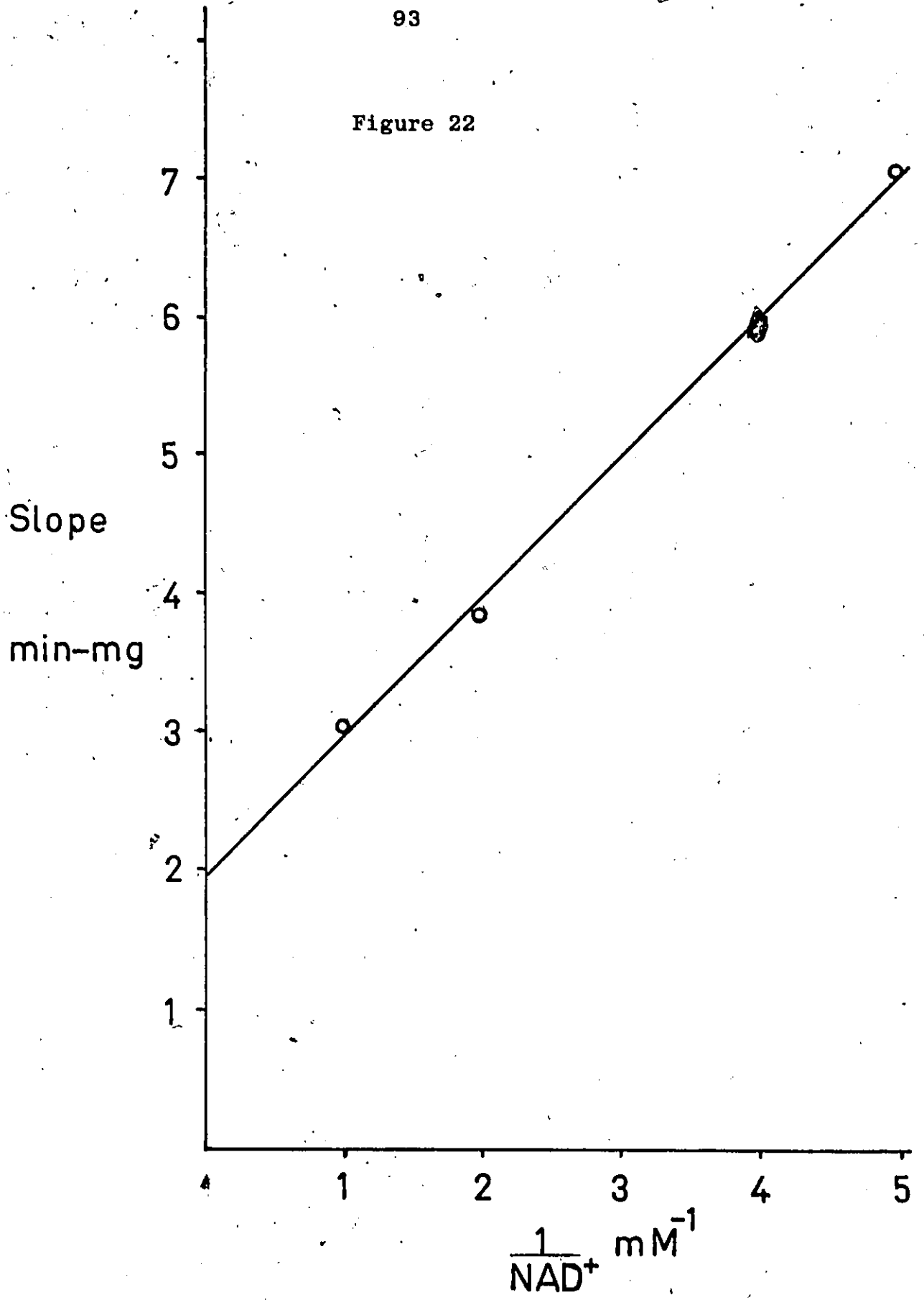
Ordinate intercept in Figure 22 = $K_b/W_1 = 1,950 \text{ min} - \text{mg}$.

Slope in Figure 22 = $K_{ia}K_b/V_1 = 1,010 \text{ min} - \text{mg} - \text{mM}$.

$$K_b = 6.5 \times 10^{-3} \text{ M}$$

$$K_{ia} = 5.18 \times 10^{-4} \text{ M}$$

Figure 22



Figures 21, 22 represent secondary replot functions used to calculate the parameters K_{ia} , K_b , K_a (78). These were calculated as $K_{ia} = 5.2 \times 10^{-4}$ M, $K_b = 6.5 \times 10^{-3}$ M, and $K_a = 3.3 \times 10^{-4}$ M. In an ordered mechanism, K_{ia} represented the true dissociation constant of the E.NAD⁺ complex. Since many of the most thoroughly studied dehydrogenases obeyed this mechanism, it gave a good preliminary indication of the tightness of NAD⁺ binding on the basis of steady state kinetics alone. This was useful information to have when attempting to design an enzyme recycling system.

From the in vitro kinetic results, it was not difficult to rationalize why 3FGL was not substantially more toxic than 3FG. This was likely due to the fact that the rate limiting step in the conversion of 3FG to 3FF was the sorbitol dehydrogenase step. One would therefore predict that 3FF would be considerably more toxic than 3FG or 3FGL.

Figure 23 illustrates the enzyme recycling system used to attempt the synthesis of 3FF. Enzyme recycling systems have been used synthetically for some time (since 1960's) due to their stringent stereospecificity. A thorough review of this subject has been written (91). One of the problems in the proposed system was the thermodynamic unfavourability of the sorbitol or 3FGL to fructose or 3FF

Figure 23

Enzyme recycling system used to attempt the synthesis of
3FF.

3FGL = 3-deoxy-3-fluoro-D-glucitol or sorbitol

3FF = 3-deoxy-3-fluoro-D-fructose

SDH = sheep liver sorbitol dehydrogenase

LDH = rabbit muscle L-lactate dehydrogenase


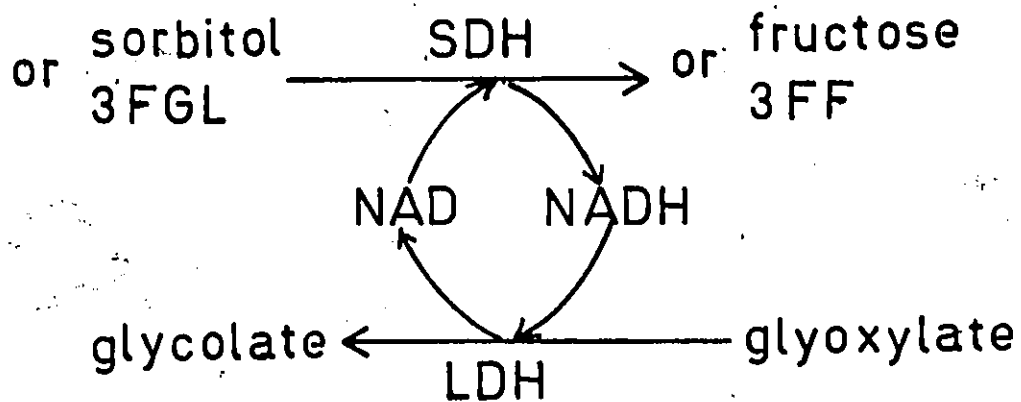


Figure 23



Standard Redox Couples expressed as midpoint potentials at pH 7 ($E^{\circ'}$).

NAD ⁺ /NADH	$E^{\circ'}$ = -0.320
Fructose/Sorbitol	$E^{\circ'}$ = -0.272
Pyruvate/Lactate	$E^{\circ'}$ = -0.185
Glyoxylate/Glycolate	$E^{\circ'}$ = -0.090

conversion. This was overcome by coupling the sorbitol dehydrogenase reaction to the L-lactate dehydrogenase catalyzed conversion of glyoxylate to glycolate which was thermodynamically favourable. Glyoxylate was chosen instead of pyruvate due to the known inhibitory abortive complex formed between pyruvate and NAD^+ as catalyzed by L-lactate dehydrogenase (92) and also due to the fact that the glyoxylate/glycolate redox couple was thermodynamically more favourable than the pyruvate/lactate couple. The reaction was further 'loaded' in the desired direction by using at least a 50-fold higher activity of L-lactate dehydrogenase and at least a two fold excess of glyoxylate. The reaction progress was monitored by assaying the decline in glyoxylate at 15 minute intervals over a period of two hours.

Preliminary experiments indicated that none of the reagents or products including fructose interfered with the assay. Figure 24 demonstrates the linearity of the assay over the span of glyoxylate concentrations monitored. Initially the recycling system was tested using the native substrate sorbitol (Table 2). It was found that about 90% conversion of sorbitol to fructose was achieved within 1 hour based upon the glyoxylate assay. The presence of fructose

Table 2

Recycling Reaction Progress

System 1 0.04 M sorbitol as substrate

Time in minutes	Absorbance of glyoxylate assay	Extent of reaction %	Approximate # of NAD ⁺ recycles
0	0.377 ± .007	0	0
15	0.350 ± .006	36 ± 8	14
30	0.343 ± .007	45 ± 9	18
60	0.303 ± .009	98 ± 12	39

System 2 0.1 M 3FGL as substrate

0	0.376 ± .006	0	0
30	0.374 ± .005	1 ± 3	1
60	0.372 ± .005	3 ± 3	3
90	0.339 ± .009	20 ± 5	20
120	0.350 ± .009	13 ± 5	13

± values given as S.E.M.

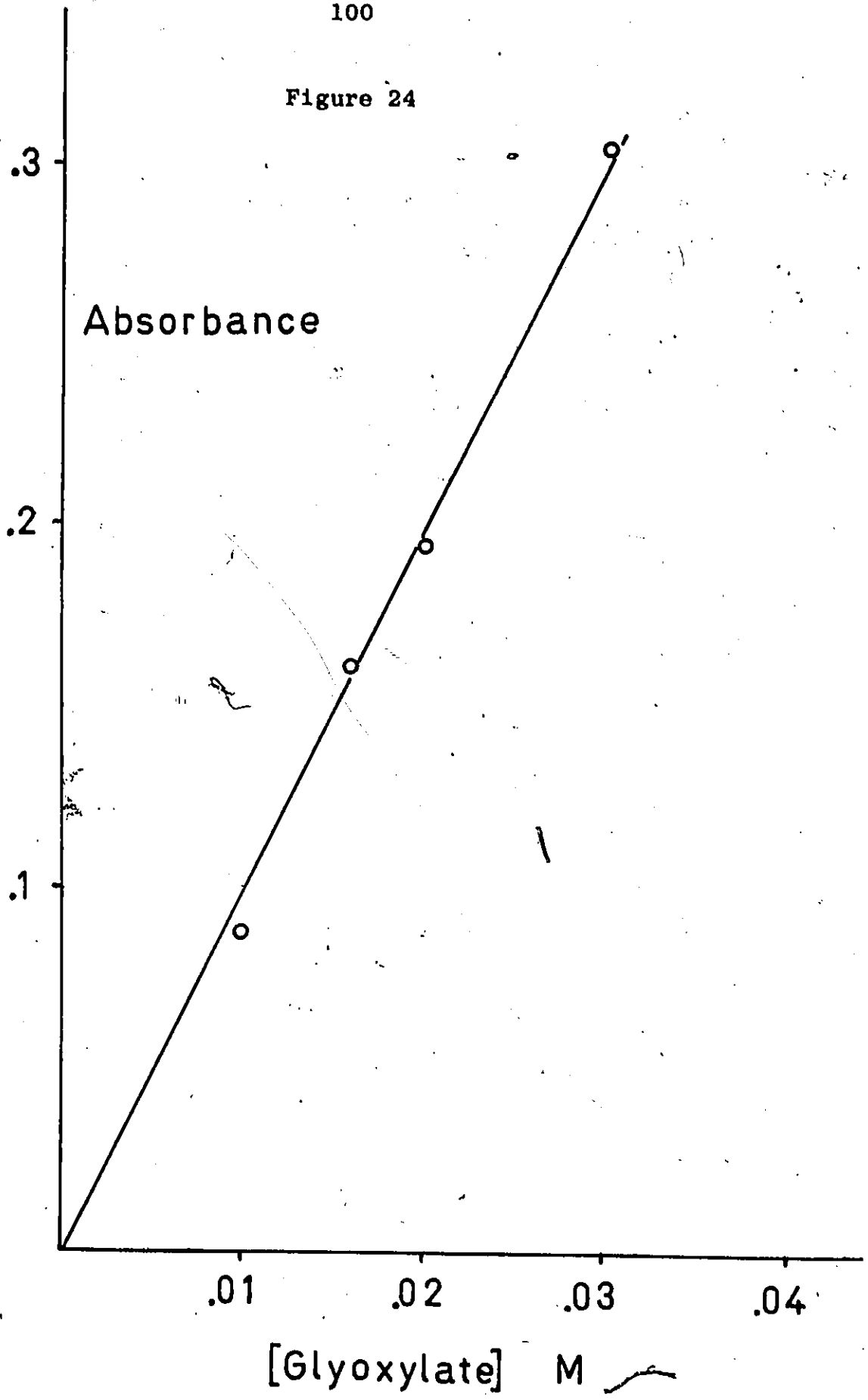
(All assays done in triplicate)

Figure 24

Glyoxylate Assay

30 μ l aliquots of the recycling reaction mixture were removed and diluted 30-fold prior to assay as described in Materials and Methods.

Figure 24



was confirmed by chromatography on cellulose plates, since a reducing component, which was not previously present was easily detectable with aniline-phthallate spray. With 3FGL as a substrate, glyoxylate analysis revealed an overall yield of about 10%. Subsequent analysis of products by ^{19}F -Fourier transform NMR revealed the presence of two fluorinated components in a ratio of about 25/1, suggesting a product yield of about 4% (Figure 25). No reducing component was detectable upon either paper, cellulose or silica gel t.l.c. plates, either before or after heating. Heating was attempted in order to regenerate any keto function from a putative hydrate. It is possible that insufficient product was present for t.l.c detection. It is evident, therefore, that the recycling reaction was not successful for synthetic purposes. Part of the problem may have been due to the fact that the enzymes were not stable for sufficiently long periods of time under the imposed conditions to drive the reaction towards completion.

After about 1 hour, enzyme precipitation was visible. The recycling reaction with sorbitol was fast enough to overcome this limitation but in the case of 3FGL, the reaction was much slower and could not reach completion due to time and temperature dependent enzyme denaturation.

Figure 25

 ^{19}F Fourier Transform NMR of 3FGL Enzyme Recycling System

A = 3FGL

B = putative 3FF

C = fluoride 1 M

D = trifluoro-acetic acid 1 M

Conditions used for scans A and B

sweep width = 41,666 Hz

offset = 31,000 Hz

O2 = 5700

AQ = .0492

FW = 50,000

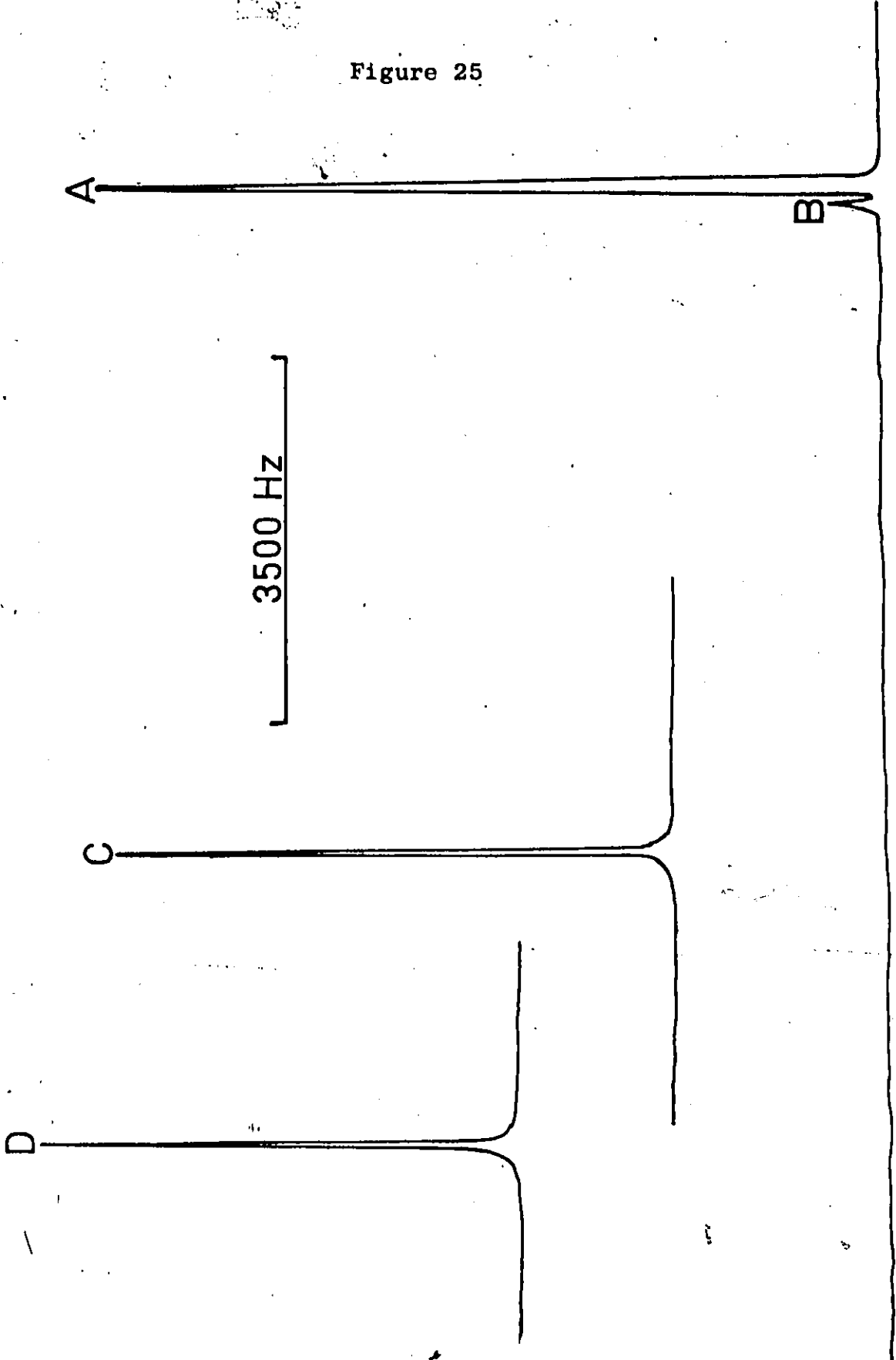
SI = 4

DW = 12

number of scans = 1,591

ratio of peak areas A/B = 15 : 0.6

Figure 25



One would expect that stabilization of these enzymes for long periods of time by immobilization or a more favourable reaction environment would lead to much higher yields of the desired product. Improved yields might also be obtained by using much higher concentrations of enzymes. This problem as well as other synthetic routes to 3FF are currently under investigation. Other dehydrogenase enzymes such as yeast alcohol dehydrogenase have been used successfully in recycling systems for periods in excess of 24 hours (91).

The NMR results did confirm the appearance of a fluorinated product which was in accord with the fact that no fluoride release was detectable for the duration of the recycling.

On the basis of the preceding results, it was not possible to rationalize the toxicity of 3FG, or 3FGL based upon the reversible competitive inhibition of sorbitol dehydrogenase. This was a similar dilemma to the one facing the investigators of fluoroacetate and fluorocitrate toxicity with regard to the competitive inhibition of mitochondrial aconitase by (-) erythro-fluorocitrate. Our problem was further compounded by the fact that we could not postulate a critical function for the glucose \rightarrow fructose pathway in fat body. This pathway is present in mammalian

testes for sperm dependent fructogenesis (92), and has been reported in adult rat hepatocytes (93). Subsequent investigations were directed towards locating a possible site of irreversible inhibition.

PART 11

RADIORESPIROMETRY AND ISOTOPE
TRACER STUDIES

INTRODUCTION

It was suspected that a phospholyated metabolite of 3FF was acting as a metabolic poison and inhibiting some energy deriving process. In order to test this hypothesis, a radiorespirometric procedure was used which measured the output of $^{14}\text{CO}_2$ from labelled substrates injected into locust. Using this procedure, it was possible to assess whether the injected poison affected the normal pattern of $^{14}\text{CO}_2$ evolution from a variety of labelled substrates such as 1- ^{14}C and 6- ^{14}C D-glucose and 1- ^{14}C acetate. A change in the pattern of $^{14}\text{CO}_2$ evolution from such labelled substrates upon administration of a poison was found to be diagnostic of a particular metabolic block. This type of approach has been used to demonstrate the presence of the pentose cycle (phosphogluconate pathway) in a variety of mammalian tissues, and in insects (94) (95)(96).

By using the radiorespirometric method, it was possible to assess the relative importance of glycolysis and pentose cycle activity in the carbohydrate metabolism of insects. This was possible using 1- ^{14}C and 6- ^{14}C labelled glucose and measuring the C_6/C_1 ratio. In Chefurka's studies (94) (97), C_6 was equal to the cumulative recovery of $^{14}\text{CO}_2$ from

6-¹⁴C-D-glucose over a time period t , and C_1 was equal to the cumulative recovery of ¹⁴CO₂ from 1-¹⁴C-D-glucose over a time period t . The rationale behind such a measurement was the following. If the glycolytic route was the sole pathway for the metabolism of glucose, the amount of ¹⁴CO₂ recovered from C-1 and C-6 should have been equivalent. If some of the glucose was metabolized via the pentose pathway, then C-1 of glucose would be oxidized more rapidly than C-6 via the 6-phosphogluconate dehydrogenase enzyme, of the oxidative portion of the pentose cycle.

Silva (95) had suggested a more elaborate quantitation of pentose cycle activity based on several assumptions. Both the C_6/C_1 ratio and the method suggested by Silva allowed assessment of pentose cycle activity and were sensitive to changes in the metabolic status of the insect, whether natural or induced.

The problem with quantitative measures of glucose utilization was that they relied upon inherent assumptions or conditions which required satisfaction in order that the results be quantitatively significant. Although the C_6/C_1 ratio was one of the most facile techniques for assessing oxidative glucose utilization, its quantitative use required corroboration with more tedious techniques such as the

measurement of 2-¹⁴C-glucose randomization into glycogen. It was decided that the C_6/C_1 ratio would be used to provide a qualitative measure of glucose catabolism, although like most radioisotopic quantitations, it suffered from some limitations. The most serious limitation was the possibility of preferential dilution of the labelled carbon atoms by endogenous substrate reserves after the label had dispersed to metabolites. To test whether such an effect occurred was both difficult and unnecessary in terms of the demands of our study. It was also necessary to be aware of the possible differences in transport and phosphorylation rates of the various labelled probes.

Chefurka demonstrated that C_6/C_1 ratios, taken at early intervals after injection of radiolabel, gave good estimates of oxidative glucose utilization. This was corroborated by more sophisticated procedures (94).

What was important in the context of our study was not a quantitative estimation of glucose utilization and the effect of 3FG on this, but rather a qualitative approach in which the emphasis was placed on whether 3FG affected oxidative glucose utilization and how such a possible effect may have been diagnostic of a specific metabolic block. This was attempted by comparing the metabolic effects of

known poisons such as fluoride and cyanide to those of 3FG. Using this approach, Chefurka demonstrated that many of the poisons which acted on the same metabolic pathways had similar effects (97). For example, in most cases when the glycolitic or TCA pathways were inhibited by a toxic agent, there was usually no increase in $^{14}\text{CO}_2$ derived from C-1 of glucose, but a depression was observed in $^{14}\text{CO}_2$ derived from the C-6 of glucose.

In cases where $^{14}\text{CO}_2$ from C-1 was depressed, the depression was less than that of C-6 and recovered more rapidly. If the toxic agent was an uncoupler like dinitrophenol, the rate of $^{14}\text{CO}_2$ recovery from C-1 or C-6 was accelerated to double or triple the normal rate. This was presumably due to ^{14}C mobilized from stored glycogen or trehalose derived from ^{14}C glucose.

It was important to ensure that all the injected labels affected the insects' metabolism to a minimal extent by acting only as tracers and not flooding the endogenous metabolite pool with any one specifically labelled metabolite. For this reason, tracers with the highest specific activity commercially available were used. A preliminary estimate of the locust extracellular glucose space was therefore undertaken before any radiorespirometric studies were attempted

in order to ensure that the concentrations of radiolabelled glucose used did not alter the normal metabolic pattern.

MATERIALS AND METHODS

Reagents

D-(3-³H)-glucose (12.4 mCi/mg), D-(1-¹⁴C)-glucose (21.5 μ Ci/mg), D-(6-¹⁴C)-glucose (16.1 μ Ci/mg), (1-¹⁴C)-sodium acetate (704 μ Ci/mg), (³H)-inulin (average molecular weight 5×10^3 g/mole, 139 μ Ci/mg), D-(U-¹⁴C)-glucose (217 μ Ci/mg), BBOT, OCS (Organic Scintillation Cocktail), NCS (tissue solublizer), scintillation grade toluene, CO₂ mMet (CO₂ trapping solution), borosilicate glass scintillation vials were purchased from Amersham (Toronto, Ontario). Aquasol (aqueous solublizer) was from New England Nuclear (Boston, Mass.). Gravimetric grade CO₂, 0.18% by mole fraction in air, high purity helium and medical breathing air were from Bull Welding Supply (Windsor, Ontario). Porapak Q (120 mesh) and molecular sieve 5A (50-60 mesh) gas chromatographic adsorbents were from Chromatographic Specialties (Brockville, Ontario). Ammonium tetraborate tetrahydrate, D-glucose-6-phosphate, D-fructose-6-phosphate, α -D-glucose-1-phosphate, D-fructose-1,6-diphosphate, phosphoenol pyruvate, ATP, glyceraldehyde-3-phosphate (diethylacetal), and 8-hydroxyquinoline were from Sigma (St. Louis, Missouri). Polyethylene imine (P.E.I.) cellulose and silica gel t.l.c. plates 20 x 20 cm were purchased from BDH (Toronto, Ontario). A Glucostat

reagent kit was from Worthington Enzymes (Freehold, New Jersey). Orion TISAB (total ionic strength adjusting buffer) and fluoride standards were from Fisher (Toronto, Ontario).

Equipment

CO₂, O₂ and N₂ measurements were made on a Hewlett Packard Model 2000 gas chromatograph equipped with a thermal conductivity detector. Gas separations were performed by injecting 1 cc samples through a $\frac{1}{8}$ inch OD x 12 inch Porapak Q column and a $\frac{1}{8}$ inch OD x 60 inch molecular sieve 5A column joined in series. Scintillation counting was performed on either a Nuclear Chicago Dsilux 11 or Mark 11 scintillation spectrometer equipped with a printout terminal. Freeze clamping tongs constructed of two aluminum plates 10 cm in diameter and 2 cm thick were used for tissue fixation (98). Gas flows were monitored using a calibrated rotameter 5-50 cc/min purchased from Union Carbide (Windsor, Ontario).

Glucose Isotope Dilution Study

Locust haemolymph (4 x 400 μ l) was pooled from 40 adult locusts (10-14 days after final ecdysis). Locusts were taken for bleeding 5 hours after feeding. The pooled haemolymph

was thoroughly mixed with 25 μ l of ^{14}C - uniformly labelled glucose solution with specific activity 217 $\mu\text{Ci}/\text{mg}$ in 1 ml of water. Duplicate 100 μ l aliquots of this mixture were removed and deproteinized with 400 μ l of absolute ethanol. Each resulting occult mixture was spun down in a micro-centrifuge, the supernatant removed and plated on 0.2 mm cellulose chromatography plates. The plates were developed for 4 hours in a mixture of ethyl acetate : pyridine : water, 120:50:40. Each plate was spotted with a glucose standard at each end of the sample band to aid the location of glucose in the sample after chromatography. Two plates were also run with 25 μ l each of ^{14}C -glucose from the ^{14}C -glucose vial purchased from Amersham in order to determine the bona fide specific activity and test for any radiolysis. These plates were also spotted with a glucose standard to aid the location of glucose in the sample after chromatography. After 4 hours of chromatography, the plates were dried and the portion of each plate which was spotted with a glucose standard was snipped out and sprayed with aniline hydrogen phthalate spray to visualize how far the glucose had moved.

The sprayed plates were developed in a 110°C oven for 10 minutes and glucose appeared as a brown spot against a pink background. These snipped out portions were compared

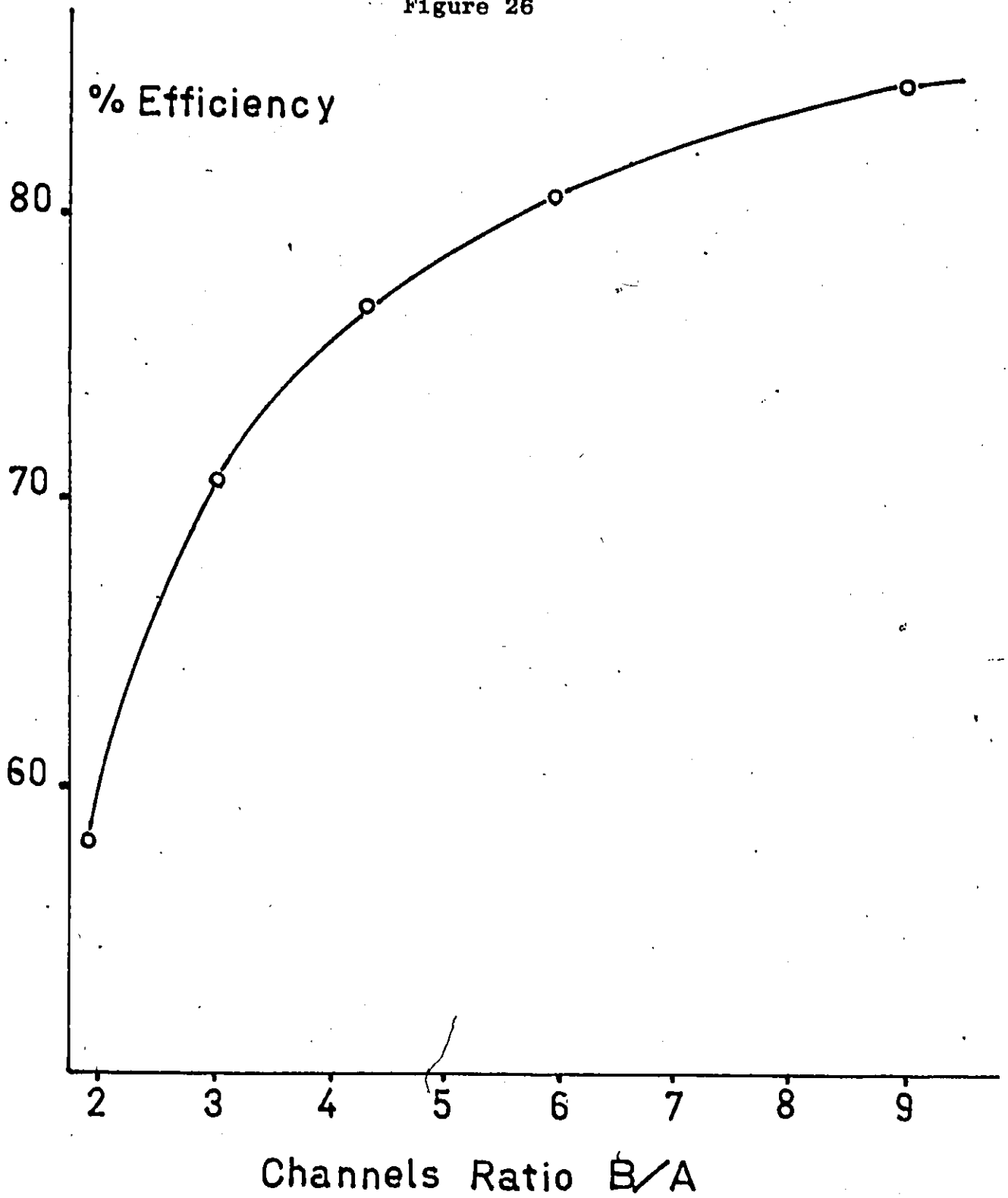
with their parent plates to determine how far glucose had migrated in the sample. The appropriate areas were scraped and thoroughly eluted with 2 mls of dry methanol. The methanol was separated from the cellulose by centrifugation and 0.5 mls of each sample were taken for counting while 0.2 mls from the same batch were taken for glucose assay. The samples for counting were mixed with 9.5 mls of scintillation cocktail. Sample counting efficiency was determined by the sample channels ratio method using a set of ^{14}C quenched standards from Nuclear Chicago (Figure 26).

Glucose concentration was determined using the glucose oxidase, peroxide, chromophore coupled reaction designed by Worthington enzymes (Glucostat). A semi-micro method of analysis was used with the following modifications (99). The sample (200 μl) in 100% methanol was mixed with 1.8 ml of distilled water, to this was added 2 mls of glucostat reagent reconstituted as in the semi-micro method according to the Worthington enzymes handbook (99). The reaction was allowed to proceed for 10 minutes and then terminated by the addition of 1 drop of 4N HCL. All samples and standards were run in duplicate. The following glucose standards were prepared and found to be linear when optical density was plotted versus concentration, 2 mg%, 5 mg%, 10 mg%, 15 mg%,

Figure 26

^{14}C quench correction curve for Nuclear Chicago Mark 11
scintillation spectrometer using the sample channels ratio
method.

Figure 26



20 mg%, 30 mg%, 50 mg%, and 100 mg% w/v. (Figure 27)

The haemolymph glucose concentration was calculated by isotope dilution analysis using the relationship

$$x = y \left[\frac{s_1}{s_2} - 1 \right] \quad (100)$$

where,

x = amount of glucose in 400 μ l of haemolymph

y = amount of glucose in 25 μ l of injected radiolabel

s_1 = specific activity of ^{14}C glucose before dilution

s_2 = specific activity of ^{14}C glucose after dilution

The following values for the above parameters were used:

$$y = 0.0322 \text{ mg}$$

$$s_1 = 134,400 \text{ dpm}/\mu\text{g}$$

$$s_2 = 1950 \text{ dpm}/\mu\text{g}, 2120 \text{ dpm}/\mu\text{g}, 2390 \text{ dpm}/\mu\text{g}, 2840 \text{ dpm}/\mu\text{g}$$

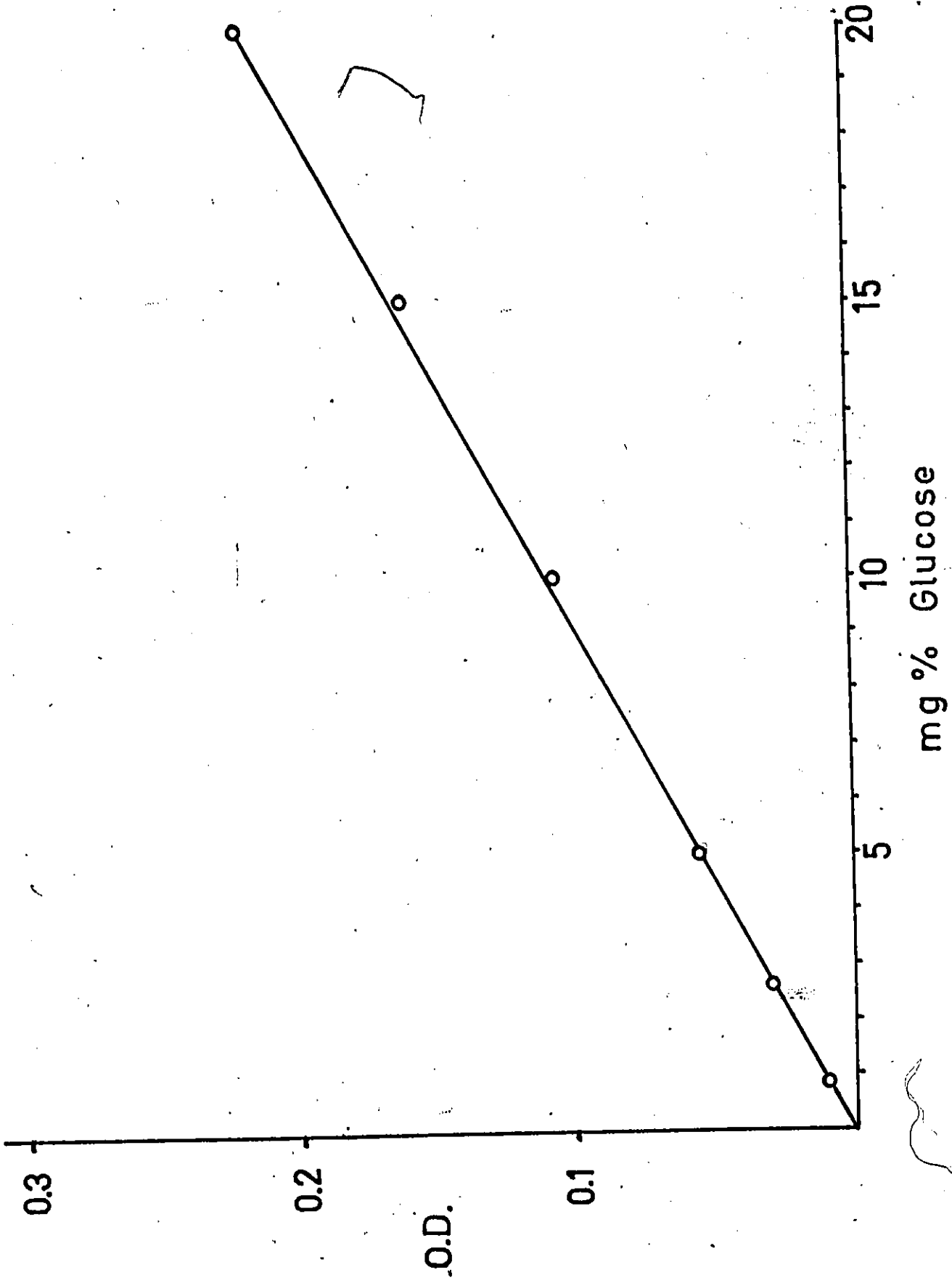
Locust Extracellular Fluid Volume Measurements

Tritiated inulin, (25 μ l) with an activity of 1.395×10^7 dpm/25 μ l, was injected intrathoracically via the membranous septum at the base of the first thoracic leg into five locusts. Haemolymph (25 μ l) was serially removed from each locust at 15 minute intervals after 1 hour of inulin randomization and mixed with 200 μ l of NCS solublizer. The locusts were encouraged to remain active during the initial

Figure 27

Glucose assay calibration graph using the modified Glucostat procedure.

Figure 27



1 hour randomization period to promote haemolymph flow. An aliquot of the solubilized mixture (100 μ l) was mixed with 10 mls of scintillation cocktail for counting.

The effect of haemolymph on sample counting efficiency was determined in the following manner. Duplicate samples of haemolymph (5, 10, 20, 25 μ l) were pipetted into 200 μ l of NCS and water was added to those haemolymph samples whose haemolymph volume was less than 25 μ l in order to adjust the final volume to 25 μ l. A second set of duplicate samples were prepared identically to the above procedure except that the NCS was spiked with a known activity of inulin (Table 3). All samples including those withdrawn from locusts were dark adapted for 8 hours and transferred in the dark into the scintillation counter. The samples were then counted continuously for 4 hours to make sure that a stable, non decaying count rate was achieved. This allowed a careful estimation of the sample counting efficiency.

The total extracellular fluid volume was calculated on the basis of the equation

$$v_t = \left[\frac{v_s}{x} \right] y - v_i$$

where,

y = total dpm injected in the volume v_i

Table 3

Quench Correction Data

Haemolymph samples without labelled inulin

Amount of Haemolymph	5	10	20	25
Amount of H ₂ O	20	15	5	0
CPM (background radiation and sample fluorescence)	23	25	118	155

Haemolymph samples with labelled inulin

Amount of Haemolymph	5	10	20	25
Amount of H ₂ O	20	15	5	0
Efficiency	50%	49%	48.7%	48.4%

x = counts recovered in 25 μ l after randomization

v_s = sample volume withdrawn after randomization (25 μ l)

v_t = total extracellular volume

Radiorespirometric Apparatus

The apparatus was assembled as outlined in Figure 28. Medical air was passed over the locusts at a flow rate of 17 cc/min as controlled by a rotameter. The flow rate was constantly checked using a soap bubble flow meter and stopwatch. This flow rate was maintained throughout all the experiments. Injected locusts were placed into a gas tight chamber C (Figure 28). Air samples were withdrawn from septum D every 10 minutes and CO_2 and O_2 levels were monitored by gas chromatography. Respired CO_2 was trapped in vessel E which contained 5 mls of CO_2 mMet. Preliminary investigations showed that 2 large adult locusts expired approximately 0.3-0.4 grams of CO_2 per hour while moderately active. The CO_2 mMet trapping solution had a CO_2 absorbing capacity of 0.25 gm/ml, so that 5 mls of the solution changed every 30 min. provided sufficient capacity to prevent saturation. Evaporation losses in this solution over a period of 30 min. due to gas flow were negligible, but were constantly monitored. Duplicate 1 ml samples of the trapping solution

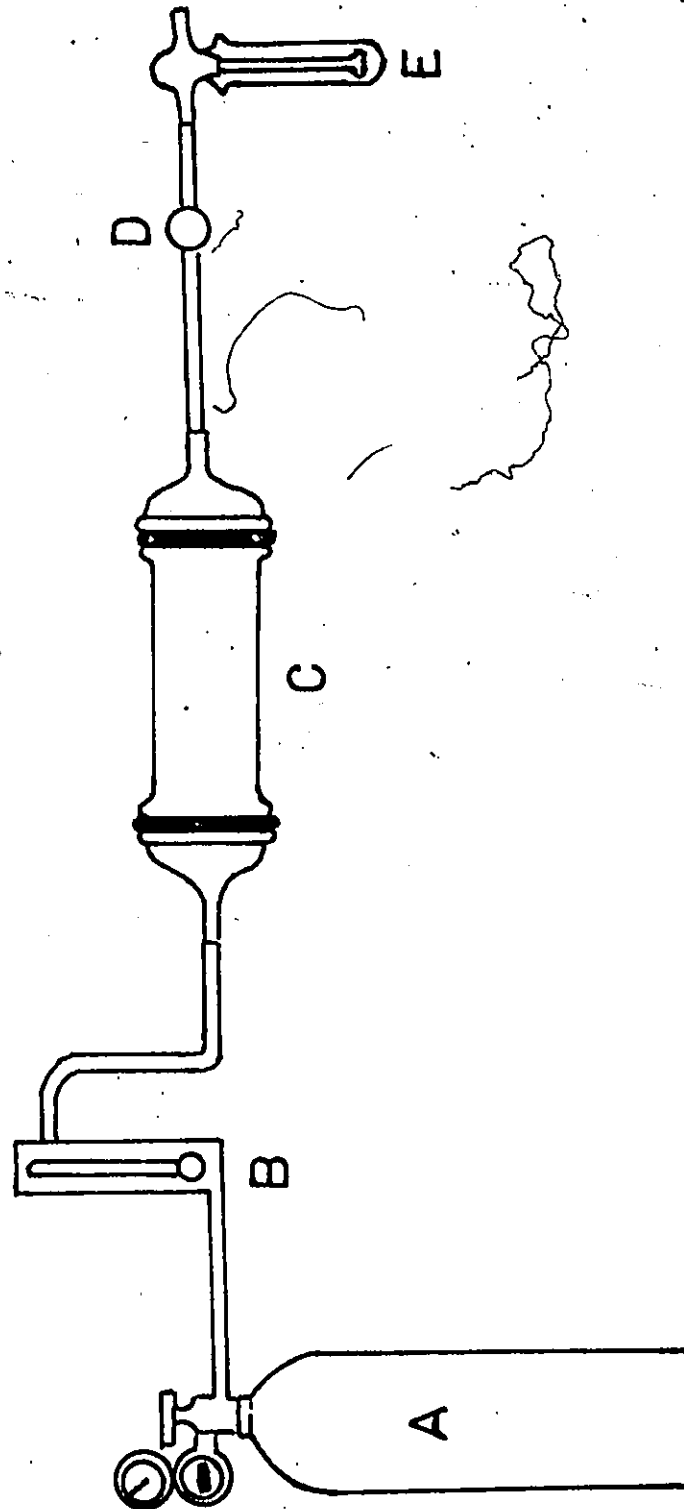
Figure 28

Radiorespirometric Apparatus

- A = compressed breathing air
- B = rotameter (flow meter)
- C = gas tight metabolic chamber
- D = septum for withdrawal of air samples
- E = gas trapping vial filled with 5 ml of CO₂ mMet

All joining tubing was $\frac{1}{8}$ inch I.D. heavy gauge 'tygon' vacuum tubing.

Figure 28



were transferred to 10 mls of OCS scintillation cocktail and counted. The dpm in each sample were divided by the average % CO₂ (mole fraction) to give a specific activity. Experimental results were expressed as \pm the standard error in the mean. A sample calculation has been provided in Appendix II.

Gas Chromatographic Determinations

1 cc gas samples in a gas tight Hamilton syringe with a 20 gauge needle were injected immediately into the Hewlett Packard Model 2000 GC run at a flow rate of 50 cc/min with high purity helium as carrier gas at a pressure of 75 psi. All columns were run at a temperature of 50°C and the bridge current was maintained at 250 mA. Both columns containing Porapak Q (120 mesh) and molecular Sieve 5A (50-60 mesh) were baked at 230°C for 12 hours prior to use. The columns were re-baked every week to remove adsorbed water and the columns were repacked every month. This ensured good recorder baselines and steady flow rates. GC septae were replaced every 25 injections. CO₂ standards were prepared in gas tight glass bulbs maintained at 0°C using a Teppler (mercury diffusion) gas manifold. This ensured that the CO₂ standards were at a higher pressure than atmospheric,

to prevent outside air contamination when samples were withdrawn by syringe. CO_2 levels were measured by peak heights against calibrated standards and were standardized internally against air O_2 peaks to correct for variations in injection volume. All calibrations were linear with respect to peak height (Figure 29).

Liquid Scintillation Counting

All counting was done to a statistical accuracy of 1% (100). Counting efficiency was determined either by the sample channels ratio or external standard channels ratio method (100). A quench correction curve for ^{14}C (Figure 30) and ^3H (Figure 31) was determined using quenched standards purchased from G.D. Searle (formerly Nuclear Chicago, Amersham-Searle). Attenuator and discriminator settings in each channel were determined as described in the Nuclear Chicago Unilux 11 operating manual.

Tritiated 3FG Preparation

D- $[\text{3-}^3\text{H}]$ -3FG was prepared synthetically by the procedure developed by Lopes and Taylor (101) with a specific activity of 17.1 mCi/mg. The crude product was purified by preparative chromatography on 40 x 20 cm cellulose plates 0.2 mm thick,



Figure 29

Calibration graph for gas chromatographic CO₂ determinations.

%CO₂ was by mole fraction in air.

Figure 29

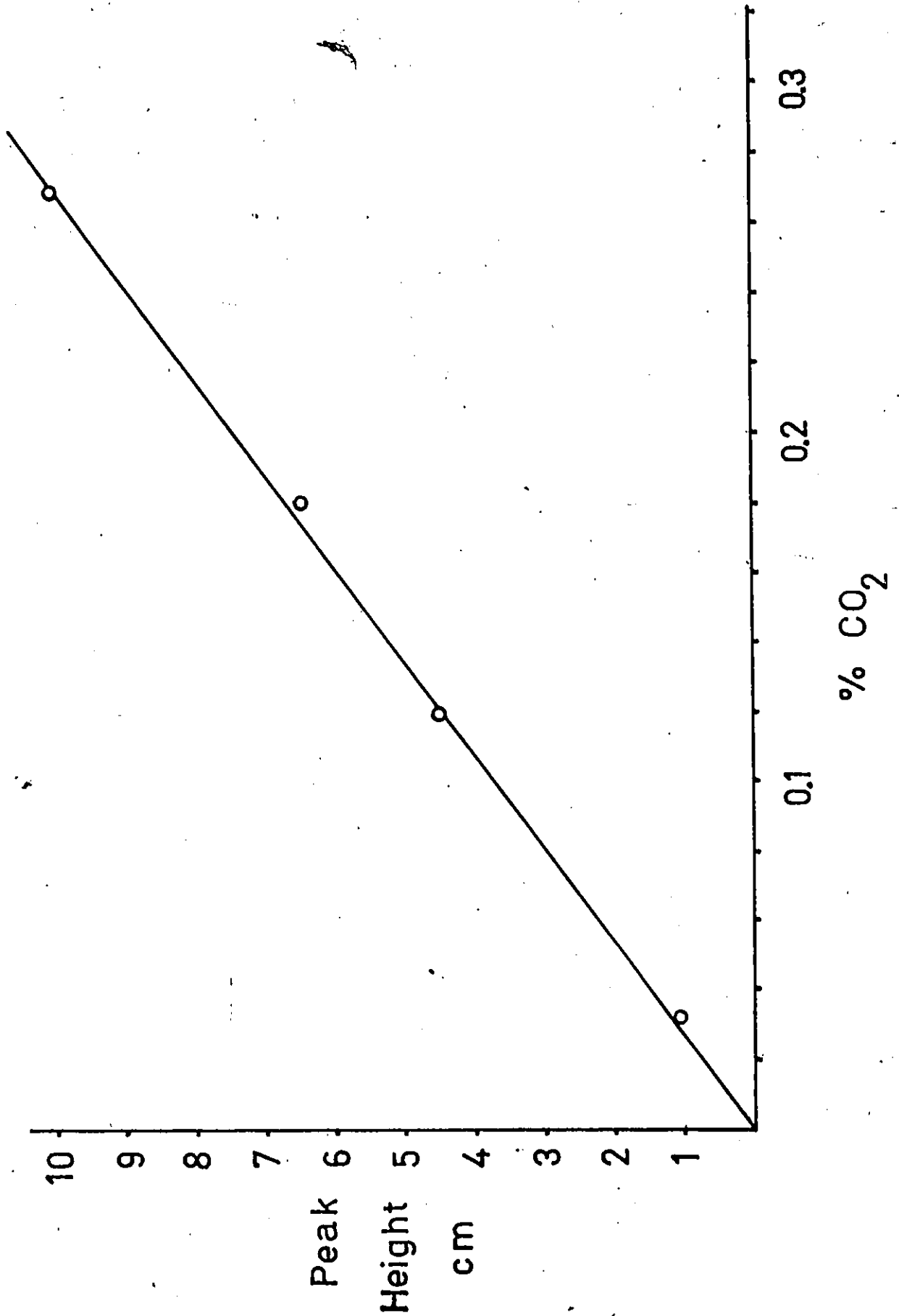


Figure 30

^{14}C quench correction curve for Nuclear Chicago Unilux 11 scintillation spectrometer using the sample channels ratio method.




Figure 30

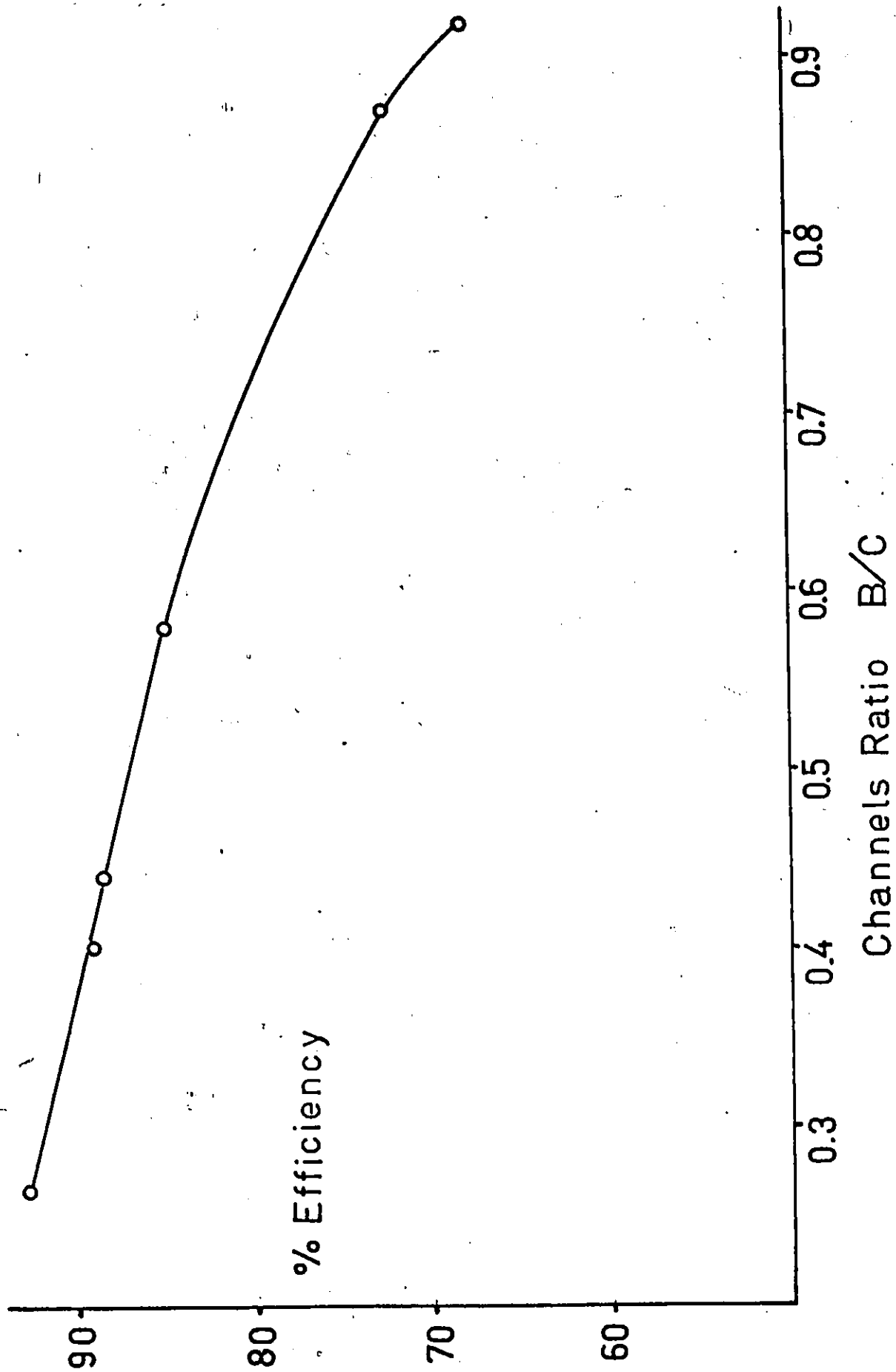
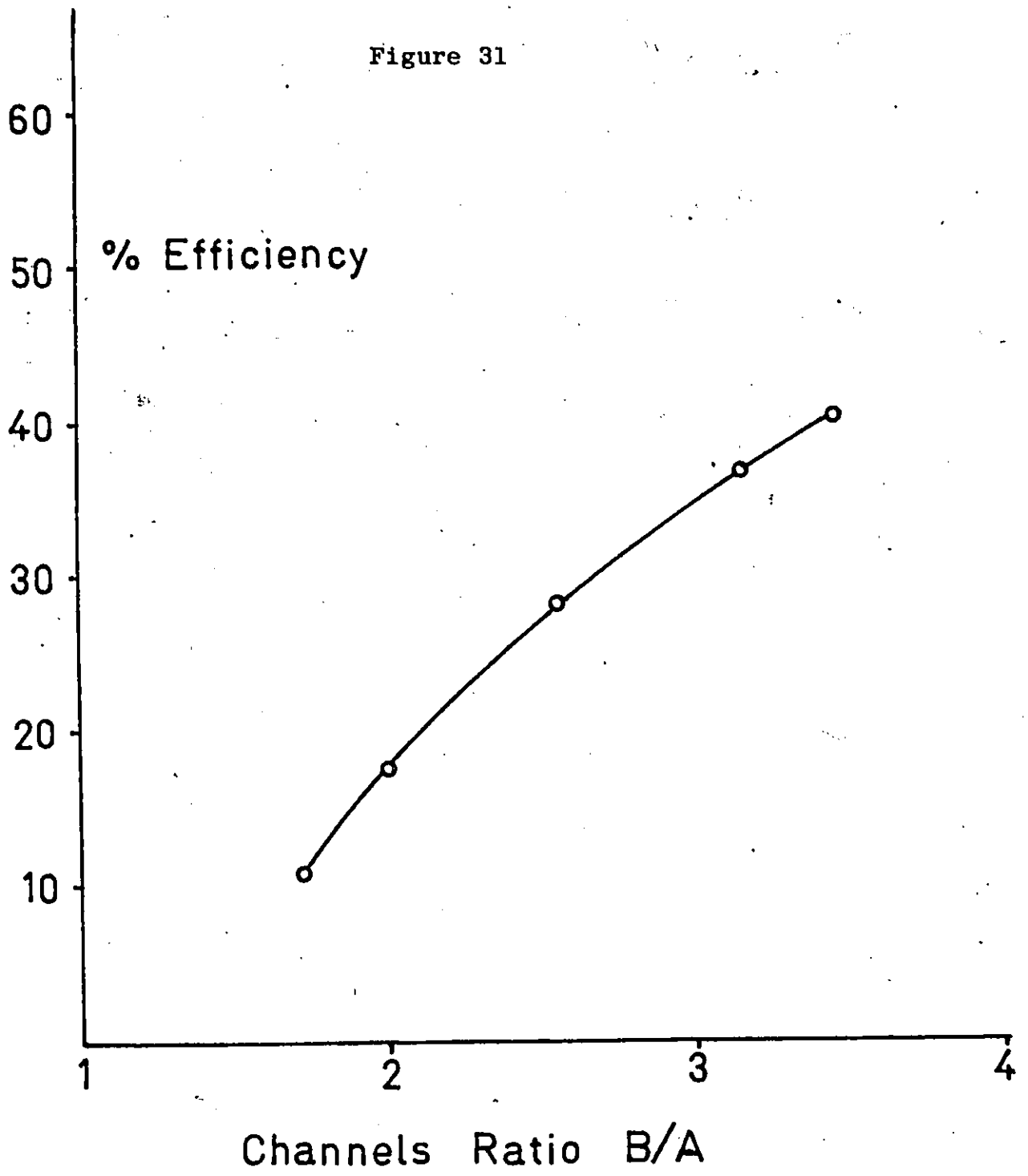


Figure 31

Tritium quench correction curve for Nuclear Chicago 11
scintillation spectrometer using the sample channels ratio
method.

Figure 31



using the solvent system ethyl acetate : butanol : ethanol : H_2O , 120:80:30:40, Rf 0.41 and recrystallized. 3FG spots were detected by fluorescence quenching. All solutions were prepared immediately prior to use.

Assay of 3H_2O from Locust Tissue Extracts

A simple micro-procedure for the assay of 3H_2O from locust tissues was used as described by Clark (102). Yellow plastic pipet tips (5.6 x 0.5 cm outside diameter) designed to fit Oxford brand automatic pipets were plugged at the small end using fine glass wool. Each pipet tip was filled with 0.4 g of wet Dowex AG 1 x 8 resin in the borate form. This was prepared by washing Dowex AG 1 x 8 (200-400) resin in the chloride form with 1 M potassium borate, pH 8.5-9, until the effluent was chloride free (about 30 volumes were required). A subsequent wash with water (10 volumes) was necessary to bring the pH down to 7.5. 100 microlitre samples of tritiated locust tissue extract were loaded onto each column. Tritiated water was washed through the columns by applying 3 x 0.4 ml aliquots of distilled water. The effluent was collected in scintillation vials and was dispersed with Aquasol. These mini-columns were found to retard glucose, sorbitol, 3FG, 3FGL, fructose as well as many other metabolites which have

been summarized (102). All $^3\text{H}_2\text{O}$ measurements were checked by differential lyophilization of samples (103); i.e., samples were counted before and after lyophilization. D-[^3H]-3FG and D-[^3H]-glucose injected locusts were prepared for $^3\text{H}_2\text{O}$ measurements by freeze clamping and subsequent powdering of tissue at liquid nitrogen temperatures with a mortar and pestle. The tissue powder was mixed with 4 mls of 7% w/v perchloric acid and homogenized at 4°C for 1.5 minutes at high speed in a Polytron Homogenizer. The homogenate was briefly warmed to ambient temperature and spun at 10,000 x g in an IEC centrifuge at 20°C for 20 minutes. The resulting supernatant was used for $^3\text{H}_2\text{O}$ determinations. 100 microlitre aliquots of supernatant were used for Dowex-borate estimation of $^3\text{H}_2\text{O}$, while 0.5 ml aliquots were used for differential lyophilization.

Isolation of Tritiated Phosphorylated Sugars

The adult locusts, previously starved for 8 hours, were each injected with 35×10^6 dpm of D-[^3H]-3FG in a volume of 20 μl . The locusts were killed 18 hours later by rapid freeze clamping at liquid N_2 temperature, powdered in a mortar and pestle at -190°C and homogenized in 5 volumes ice cold 7% w/v perchloric acid at high speed in a Polytron

homogenizer for 1 minute. The homogenate was immediately centrifuged at 10,000 x g for 15 minutes at 4°C and the supernatant neutralized with 2 M potassium hydroxide solution at 0°C. The resulting potassium perchlorate precipitate was removed by centrifugation at 10,000 x g for 15 minutes at 4°C.

The resulting neutralized supernatant was mixed with 2 drops of 1.6% w/v methylene blue. The resulting methylene blue-perchlorate complex was extracted off with 10 x 60 mls of chloroform (104). The chloroform extract was discarded and the aqueous phase was passed through a 25 ml column of Dowex AG 50 w x 12-H⁺ (200-400) mesh to remove interfering cations and any residual methylene blue. The Dowex AG 50 H⁺ extract was then concentrated to a final volume of 1.0 ml by lyophilization and stored at -20°C until ready for use. This fraction contained the tritiated phosphorylated metabolites which were subsequently chromatographed.

Separation of Phosphorylated Metabolites on P.E.I. Cellulose Thin Layer Chromatographic Plates

The method of separation was that of Newsholme, Conyers and Brand (105). P.E.I. cellulose thin layer chromatographic plates (0.1 mm) were stored dessicated at 4°C prior to use. Chromatographic plates stored longer than 2 months were

discarded. P.E.I. plates were prepared for chromatography in the following way: first they were pre-washed in 2 M hydrochloric acid followed by 8-hydroxyquinoline solution (15 g/2 litres). This was followed by several rinses of glass distilled deionized water. Samples and standards (0.002 M) were spotted (1 μ l) and the plates were again washed for 5 minutes with 95% methanol to remove any non-phosphorylated substances. The plates were dried and developed in 2 N formic acid : 0.5 M lithium chloride (106). Phosphorylated material was visualized by the method of Hanes and Isherwood (107). Chromatographic plates were prepared for scintillation counting by cutting into 1 cm² units, placing each square in 1 ml of 2 N formic acid : 0.5 M lithium chloride, 1:1, for one hour, and then mixing with 15 mls of aquasol scintillation cocktail.

Procedure for Spraying P.E.I. Cellulose Plates (107)

The spraying solution was prepared as follows: 5 ml of 60% w/w perchloric acid, 10 ml of 1 N HCl and 25 ml of 4% w/v ammonium molybdate were mixed together and diluted to a final volume of 100 ml with water. The chromatograms were then sprayed at a rate of 1 ml/100 cm². After drying the plates were heated for 7 minutes at 85°C. The plates were then placed in a rack and allowed to regain moisture

from the air for about 30 minutes. Afterwards, they were placed in an air tight jar containing dilute hydrogen sulfide gas for about 5 - 10 minutes. Phosphate esters appeared as brown spots on a faint buff background.

Preparation of Phosphorylated Metabolites for Fourier Transform NMR

The crude phosphorylated - tritiated metabolite extract (~1 ml) was loaded onto a 25 ml (1 cm x 8 cm) column of Dowex AG 1 x 8 borate (102). Tritiated water and glycogen were removed by washing with 16 mls of distilled deionized water. Non-phosphorylated sugars were removed by washing the column with 35 mls of 0.2 M ammonium tetraborate. Mono-phosphorylated metabolites and sugars were eluted with 50 mls of 0.35 M ammonium tetraborate (103). This fraction was repeatedly mixed with 10 x 100 mls of methanol and evaporated under reduced pressure to remove the volatile methyl borate. The pH was checked and adjusted to neutrality with 1 M hydrochloric acid and the sample was lyophilized to a final volume of ~1 ml and transferred to a NMR tube.

Fourier Transformed NMR of Phosphorylated Material

¹⁹F Fourier transformed spectra were obtained using a high power multinuclear probe on a Bruker 90 Mz Model XP 100

FT NMR. The magnetic field was homogenized on benzene and then switched to the ^{19}F resonant frequency (84.670 Hz). The 1 ml sample of phosphorylated metabolites was buffered with 0.1 M sodium phosphate buffer pH 7.35 and doped with trifluoro-acetic acid to a final concentration of 1 mM before placing in the sample compartment. Spectra were Fourier transformed after 75,000 scans. Standards of 0.1 M sodium fluoride and 0.1 M trifluoro-acetic acid were used to calibrate chemical shifts. Computer commands and scanning conditions are noted on individual spectra. Line broadening was used as indicated to improve signal to noise ratios.

Locust Tissue Fluoride Measurements

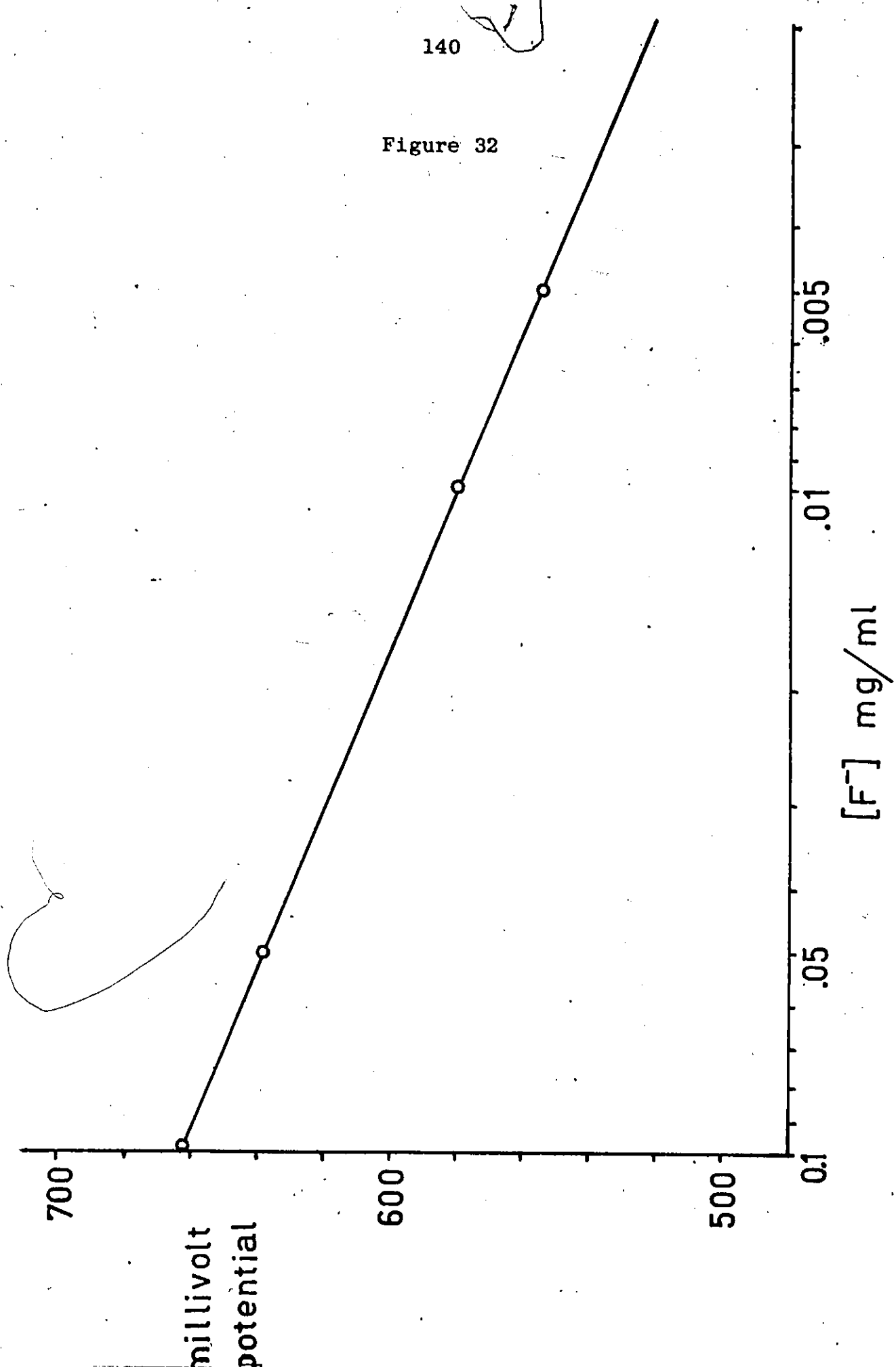
Groups of 3 poisoned or control injected locusts were frozen in liquid N_2 , powdered and homogenized in 4 mls of TISAB (orion) for 2 minutes at high speed in a Polytron homogenizer. The homogenate was spun at 10,000 x g for 30 minutes at 25°C and the supernatant removed for fluoride measurement. All beakers, volumetrics and containers used in this study were 'nalgene' plastic. All fluoride standards were prepared in TISAB and fluoride concentrations were determined from a semi-log plot of millivolt potential versus fluoride concentrations as shown in Figure 32.

Figure 32

Semi-log plot of voltage potential versus fluoride ion concentration for potentiometric fluoride determinations.

140

Figure 32



RESULTS AND DISCUSSION

Table 4 gives a summary of the results of the determination of haemolymph glucose levels. These ranged from 373 mg% to 547 mg% with a mean of 465 mg%. As shown in Figure 27, it was possible to measure haemolymph glucose concentrations as low as 1 mg% with reasonable accuracy using the modified assay procedure. Using the specific activity from Table 4, it was possible to calculate the haemolymph glucose concentration by isotope dilution analysis. Based on the measured values of s_2 , the glucose concentrations were calculated as shown in Table 4.

The data for the locust extracellular volume determination is given in Table 5. Since haemolymph contained flavoprotein, a strongly fluorescing agent, the samples were counted without prior exposure to light for eight hours. The counting procedure was repeated over a four hour interval to ensure that a stable count was achieved. This was done to check for any chemically induced fluorescence which was time dependent. All samples were counted immediately after complete solubilization in NCS had been achieved and were counted within 10 hours of haemolymph removal from locusts. A progressive colour darkening of the scintillation cocktail was noted upon standing longer

Table 4

Determination of Haemolymph Glucose Concentration

	Sample #					
	1	2	3	4	5	6
Cellulose elution volume	2 mls	2 mls	1 ml	2 mls	2 mls	2 mls
mls counted	0.5	0.5	0.2	0.5	0.5	0.5
DPM in sample x 10 ⁴	117	135	5.254	10.7	6.57	5.98
µg of glucose in cocktail	8.75	10	18.5	55	31	25
specific activity dpm/µg (average of 2 results)	133,700	135,100	2,840	1,950	2,120	2,390
glucose level mg% (average of 2 results)			373±30	547±35	500±37	440±35

± values given as S.E.M.

Samples 1 and 2 represent the ¹⁴C-glucose which was undiluted, samples 3 - 6 represent the ¹⁴C-glucose diluted with haemolymph.

Table 5

Locust Extracellular Fluid Volume Counting Data

	Locust #				
	1	2	3	4	5
Total counts from 25 μ l withdrawn (dpm)	379,800	697,000	520,000	646,000	488,300
Total extracellular fluid volume in μ l	893	475	645	514	690
Mass of locust in gms	1.5	1.0	1.03	1.35	1.75
Extracellular volume μ l/gm	595	475	630	380	395

than twenty-four hours with a resultant loss of counting efficiency. After standing for one week at 4°C, the samples were all deeply yellow coloured with a resultant 50% loss of counting efficiency.

The extracellular fluid volume was found to vary from 630-380 $\mu\text{l/gm}$ locust. The average value was 495 $\mu\text{l/gm}$. When combined with the average haemolymph glucose concentration, this gave an average extracellular glucose pool size of 2.3 mg glucose/gm locust. The range of values was 1.4 \rightarrow 3.47 mg glucose/gm locust.

As a result of these determinations, the following concentrations of radiolabelled glucose were used for radiorespirometric injections: 1- ^{14}C -D-glucose 0.0164 mg - 7.82×10^5 dpm/30 μl , and 6- ^{14}C -D-glucose 0.0233 mg - 8.3×10^5 dpm/30 μl . These amounts of glucose insured that no perturbation of in vivo glucose metabolism occurred.

The measurement of $^{14}\text{CO}_2$ specific activities allowed one to compensate for variations in locust size and activity. The pattern of $^{14}\text{CO}_2$ evolution from 1- ^{14}C of glucose is given in Figure 33. It can be seen that an 8 mg dose of 3FG caused only a slight depression in $^{14}\text{CO}_2$ levels from C-1. This decrease was about 10% of peak specific activities, as compared to a depression of about 20% due to the administration

Figure 33

1-¹⁴C-D-glucose Radiorespirometric Results

- Control; locusts were injected with 30 μ l H₂O 3 hours prior to injection with radiolabel, 3 trials.
- * 3FG poisoned, locusts were injected with 8 mg 3FG/30 μ l 3.5 hours prior to injection with radiolabel, 3 trials.
- △ F⁻ poisoned, locusts were injected with 12 μ g F⁻/30 μ l 1 hour prior to injection with radiolabel, 2 trials.

Experimental points were expressed as the means of several experiments. The ordinate represents specific activity of ¹⁴CO₂ respired expressed as dpm/% CO₂.

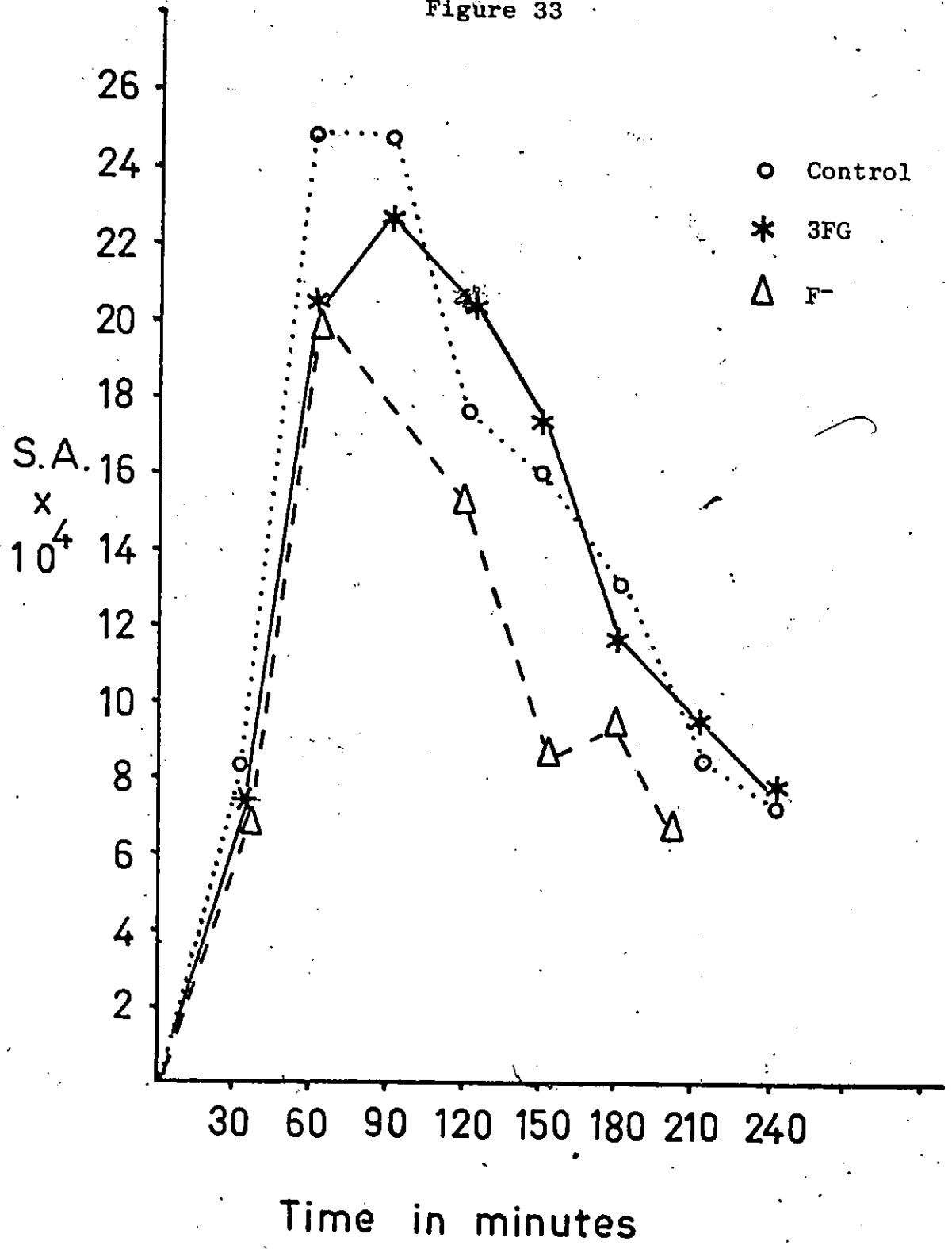
% CO₂ values were expressed as mole fraction % in air.

The standard error in the mean for each point are listed below. These were determined as shown in Appendix 11.

	Time (in minutes)							
	30	60	90	120	150	180	210	240
○	2.3	2.8	2.6	2.25	1.8	1.34	1.6	0.32
*	2.5	1.21	2.3	3.5	2.3	2.7	2.2	1.0
△	2.4	2.0	2.2	2.1	1.5	2.0	1.0	0.9

All values are $\times 10^4$

Figure 33



of 12 $\mu\text{g F}^-$ in 30 μl . Figure 34 displays the patterns of $^{14}\text{CO}_2$ evolution from 6- ^{14}C -glucose under a variety of conditions. It is important to note that the isotope dilution effect of an 8 mg dose of D-glucose was virtually abolished when the glucose was administered 4 hours prior to the radiolabel. This suggested that the 8 mg of glucose was metabolized within this period of time and could no longer dilute out the radiolabel. This is in direct contrast to the results obtained upon administration of an 8 mg dose of 3FG at various time intervals prior to the injection of the radiolabel (Figure 35a). The extent of 3FG inhibition remained constant at about 50% at peak specific activity but the onset of inhibition was faster when the 3FG was administered at a shorter time interval between 3FG injection and radiolabel injection. These results suggested that 3FG was not exerting its inhibitory effect due to isotope dilution or by competing with the radiolabel for tissue uptake. The observed results implied that 3FG had established a bona fide metabolic block in glucose degradative metabolism. This idea was also supported by previous observations which demonstrated that 3FG was rapidly removed from haemolymph and could not be detected in haemolymph or other tissues 1 hour after injection. For this reason, it was unlikely that sufficient 3FG remained

Figure 34

6-¹⁴C-D-glucose Radiorespirometric Results

* Control, locusts injected with 30 μ l H₂O 1 or 3 hours prior to radiolabel (3 trials).

○ Glucose 4 hr., locusts injected with 8 mg/30 μ l of glucose 4 hours prior to radiolabel (2 trials).

△ Glucose 2 hr., locusts injected with 8 mg/30 μ l of glucose 2 hours prior to radiolabel (2 trials).

● Glucose $\frac{1}{2}$ hr., locusts injected with 8 mg/30 μ l of glucose $\frac{1}{2}$ hour prior to radiolabel (2 trials).

Ordinate represents the specific activity of respired ¹⁴CO₂ as dpm/% CO₂.

	S.E.M. values for time interval (in min.)									
	30	60	90	120	150	180	210	240	270	300
*	2.2	2.3	2.2	2.2	1.9	1.7	1.5	1.0	1.1	1.1
○	2.5	2.1	2.3	2.3	2.0	1.2	1.5	1.1	1.0	0.9
△	2.5	2.6	2.6	2.0	1.5	1.3	1.6	1.4	1.2	1.2
●	0.5	0.4	0.5	0.6	0.9	0.3	0.6	0.9	1.0	1.2

All values were $\times 10^4$

Figure 34

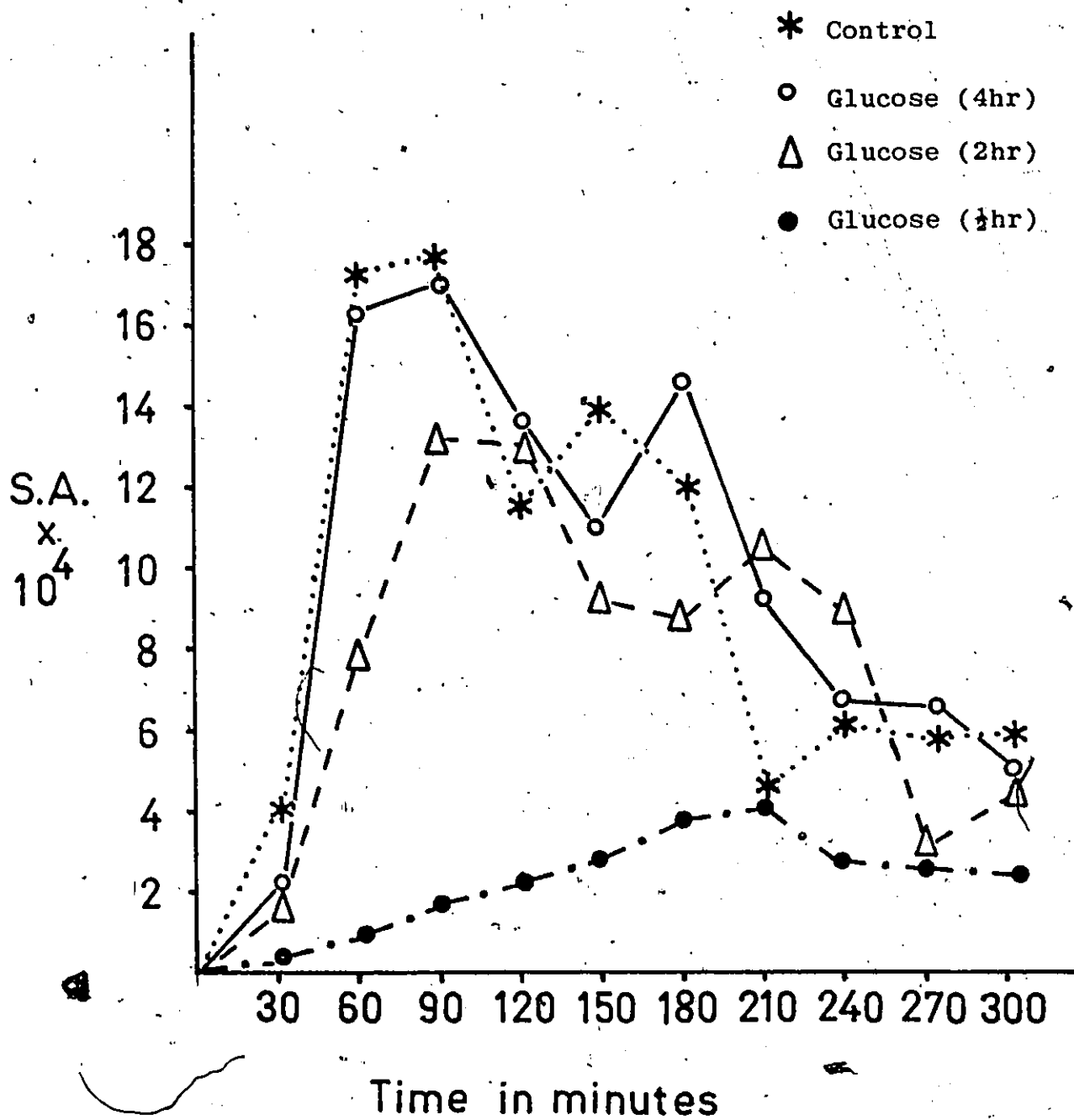


Figure 35a

 $6\text{-}^{14}\text{C}$ -D-glucose Radiorespirometric Results

○ Control, locusts injected with 30 μl H_2O 1 or 3 hours prior to radiolabel (3 trials).

* 3FG 4 hr., locusts injected with 8 mg/30 μl of 3FG 4 hours prior to radiolabel (2 trials).

△ 3FG 2 hr., locusts injected with 8 mg/30 μl of 3FG 2 hours prior to radiolabel (2 trials).

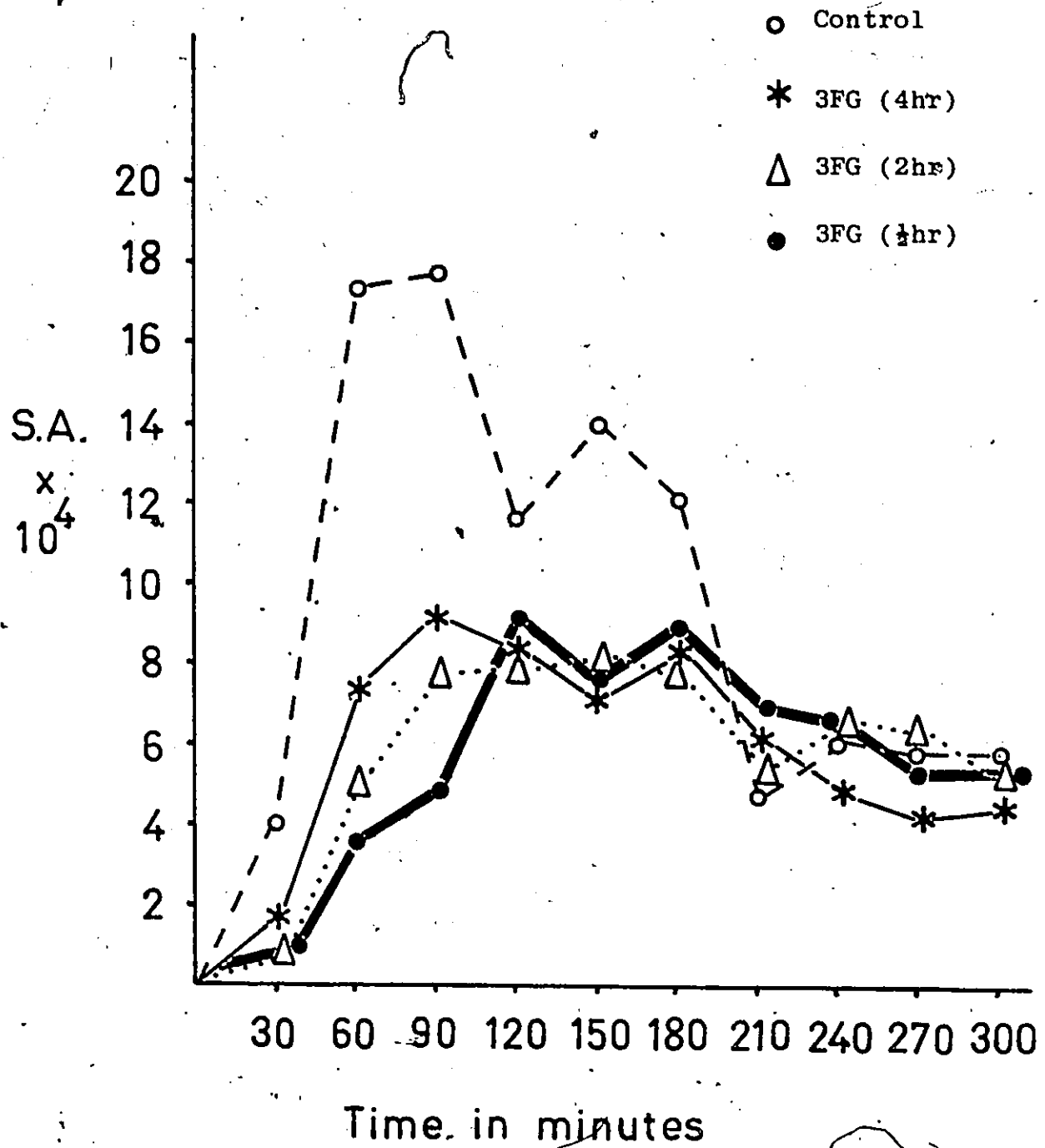
● 3FG $\frac{1}{2}$ hr., locusts injected with 8 mg/30 μl of 3FG $\frac{1}{2}$ hour prior to radiolabel (2 trials).

Ordinate represents the specific activity of respired $^{14}\text{CO}_2$ as dpm/% CO_2 .

	S.E.M. values for time interval (in min.)									
	30	60	90	120	150	180	210	240	270	300
○	2.2	2.3	2.2	2.2	1.9	1.7	1.5	1.0	1.1	1.1
*	0.9	1.2	1.3	0.8	0.7	1.0	1.6	1.4	1.3	1.4
△	0.8	1.1	1.3	1.0	1.0	1.1	1.3	0.9	1.0	1.0
●	0.6	1.1	1.5	0.9	0.8	0.8	1.3	1.2	1.4	1.2

All values were $\times 10^4$

Figure 35a



in the extracellular fluid compartment to exert an isotope dilution effect 1 hour after injection.

Although small doses of cyanide elicited a potent inhibitory effect on $^{14}\text{CO}_2$ release from C-6 of glucose (Figure 35b), the remarkable ability of locusts to detoxify cyanide levels as high as $45 \mu\text{g}/30 \mu\text{l}$ as had been previously reported by Chefurka (97) was also observed. One surprising finding, however, was the sensitivity of locusts to small levels of fluoride (Figure 36). A $12 \mu\text{g}/30 \mu\text{l}$ dose of fluoride resulted in about 40% inhibition of $^{14}\text{CO}_2$ release from C-6 of glucose. This was about the same level of inhibition as was achieved by a $17 \mu\text{g}/30 \mu\text{l}$ dose of cyanide. Chefurka previously reported about 40% inhibition of C-6 dependent $^{14}\text{CO}_2$ evolution by $400 \mu\text{g}$ of fluoride in the cockroach Periplaneta americana (97). To our knowledge this sensitivity by locusts to fluoride had not been previously reported.

Since 3FG solutions contained small amounts of fluoride (always less than 0.008 mg/ml) we injected locusts with $0.5 \mu\text{g F}^-/30 \mu\text{l}$ (equivalent to a 3FG fluoride concentration of 0.016 mg/ml) and found that this level of fluoride had no measurable effect on $^{14}\text{CO}_2$ yields from either C-6 or C-1 labelled glucose. Figure 36 also showed that $^{14}\text{CO}_2$ yields decreased as a function of 12 hour pre-injection of locusts

Figure 35b

6-¹⁴C-glucose Radiorespirometric Results

○ Control as in Figure 35a

* CN⁻ poisoned, locusts poisoned with 17 μg/30 μl of CN⁻
1 hour prior to injection of radiolabel (2 trials)

Ordinate represents the specific activity of respired ¹⁴CO₂
as dpm/% CO₂.

	S.E.M. values for time intervals (in min.)									
	30	60	90	120	150	180	210	240	270	300
○	2.2	2.3	2.2	2.2	1.9	1.7	1.5	1.0	1.1	1.1
*	0.8	1.0	1.5	2.3	2.2	2.5	1.0	1.0	1.3	0.8

All values were x 10⁴.

Figure 35b

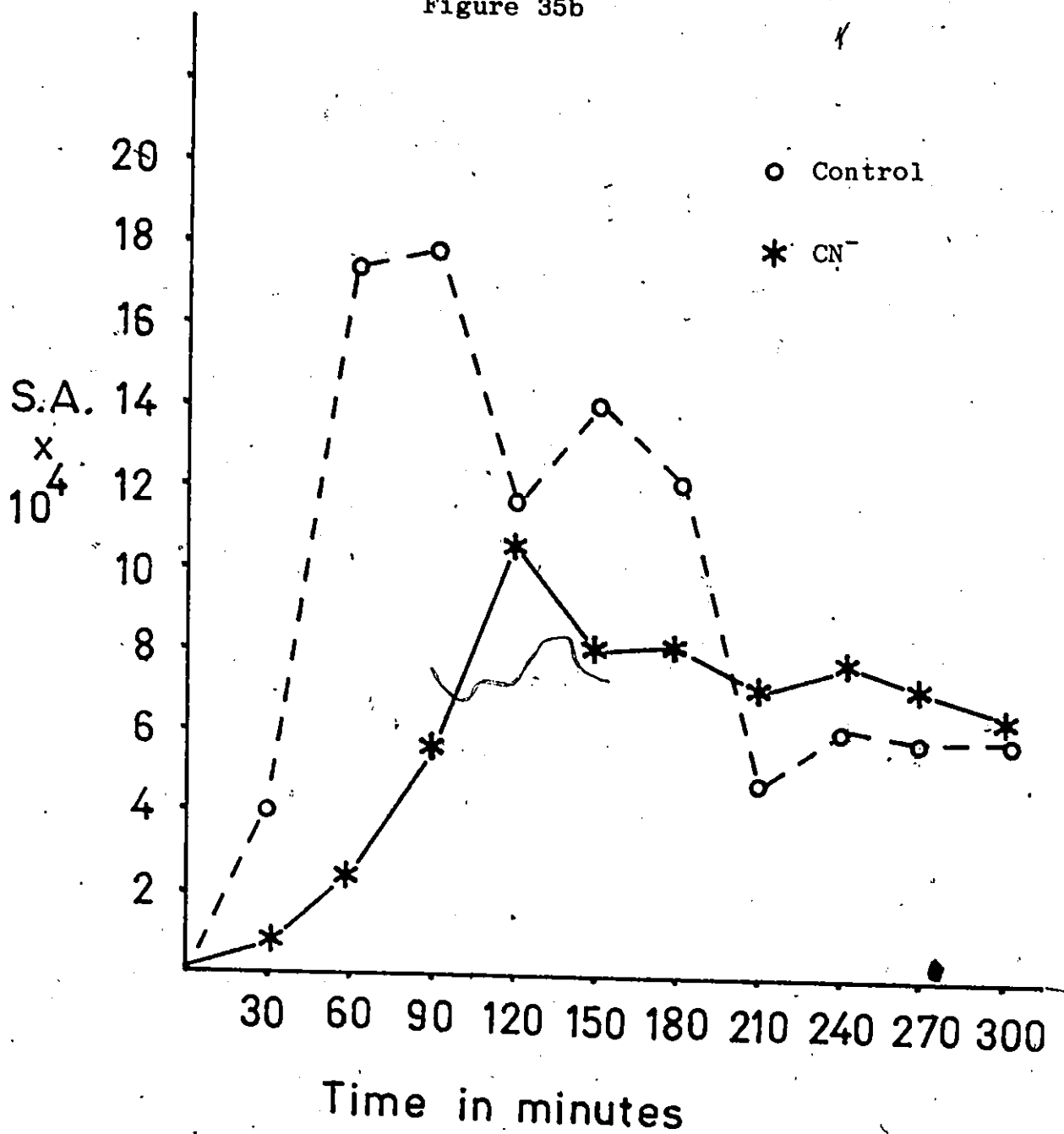


Figure 36

6-¹⁴C-D-glucose Radiorespirometric Results

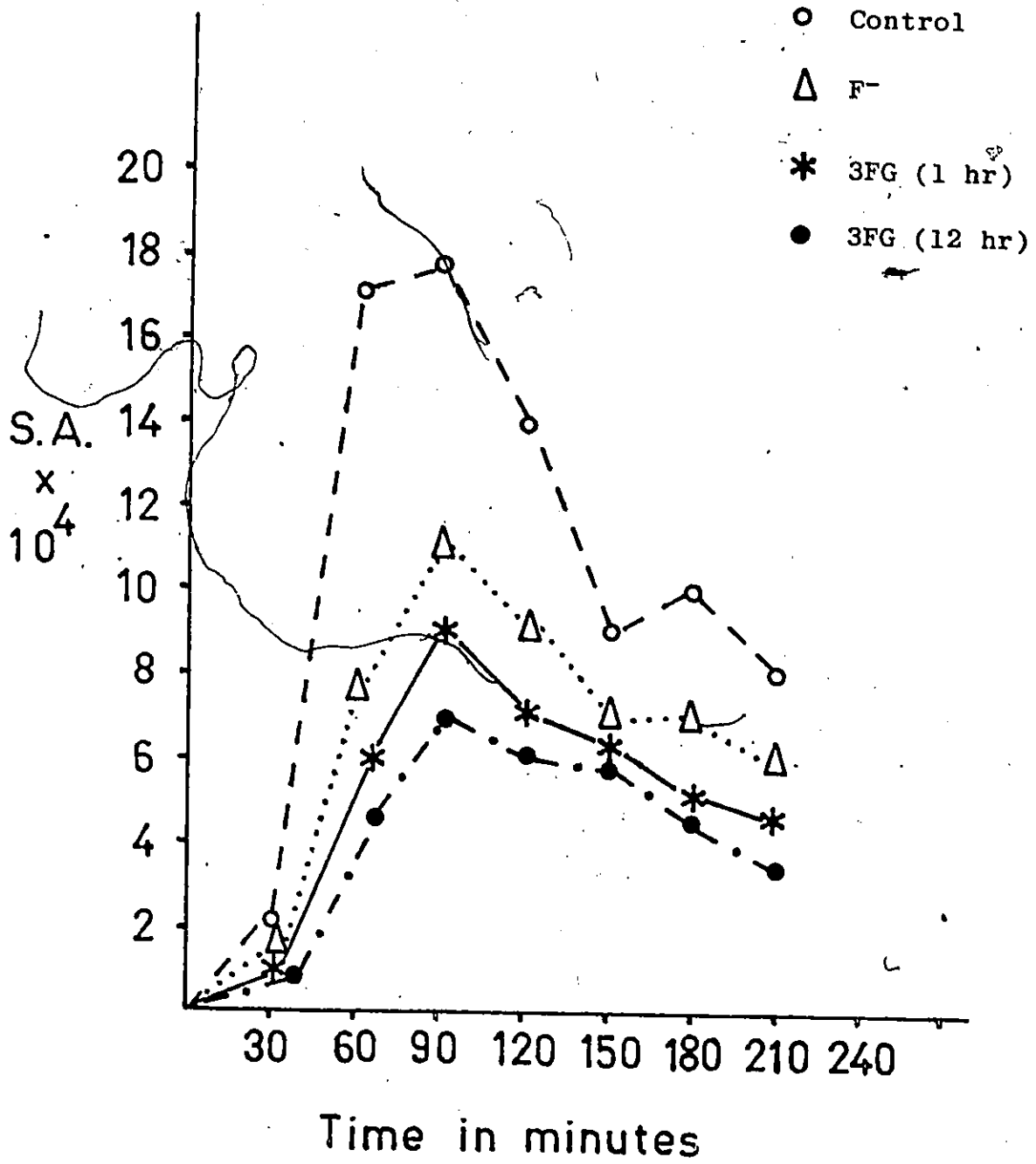
- Control, locusts injected with 30 μ l H₂O 1 hour prior to radiolabel (2 trials)..
- △ F- poisoned, 12 μ g/30 μ l, injected 1 hour prior to radiolabel (2 trials)
- * 3FG poisoned, 8 mg/30 μ l, injected 1 hour prior to radiolabel (2 trials)
- 3FG poisoned, 8 mg/30 μ l, injected 12 hours prior to radiolabel (2 trials)

Ordinate represents the specific activity of respired ¹⁴CO₂ as dpm/% CO₂.

	S.E.M. values for time intervals in minutes						
	30	60	90	120	150	180	210
○	2.0	2.5	2.4	2.0	1.5	1.2	1.0
△	2.5	2.6	2.3	2.2	1.9	1.5	1.2
*	2.5	2.2	2.0	2.0	1.6	1.0	1.1
●	2.1	2.1	2.0	2.1	1.4	1.0	1.0

All values were $\times 10^4$

Figure 36



with 3FG prior to radiolabel injection, as compared to locusts pre-injected with 3FG only 1 hour prior to radiolabel injection. This suggested that the metabolic block induced by 3FG intensified with prolonged exposure.

The above results suggested that 3FG was exerting an inhibitory effect somewhere within the glycolytic or TCA pathways rather than the pentose or phosphogluconate pathway. It was also evident that the phosphogluconate pathway did make some contribution to the overall oxidative glucose degradation since the C_6/C_1 ratio at peak specific activities (90 min) was about 0.7.

In order to further narrow the location of 3FG inhibition, we attempted to measure the effects of this agent as well as others on $^{14}CO_2$ evolution from 1- ^{14}C acetate. Locusts were injected with 2.63×10^{-4} mg acetate/30 μ l with an activity of 4.1×10^5 dpm. As indicated in Figure 37, both an 8 mg dose of 3FG and a 12 μ g dose of fluoride resulted in an increase in the specific activity of $^{14}CO_2$. On the other hand, an 8 mg dose of glucose and a 12 μ g dose of cyanide both resulted in a decrease in the specific activity of $^{14}CO_2$ evolved. These results could be rationalized on the basis on the following argument. An increase in the specific activity of $^{14}CO_2$ derived from 1- ^{14}C acetate could result

Figure 37

1-¹⁴C-acetate Radiorespirometric Results

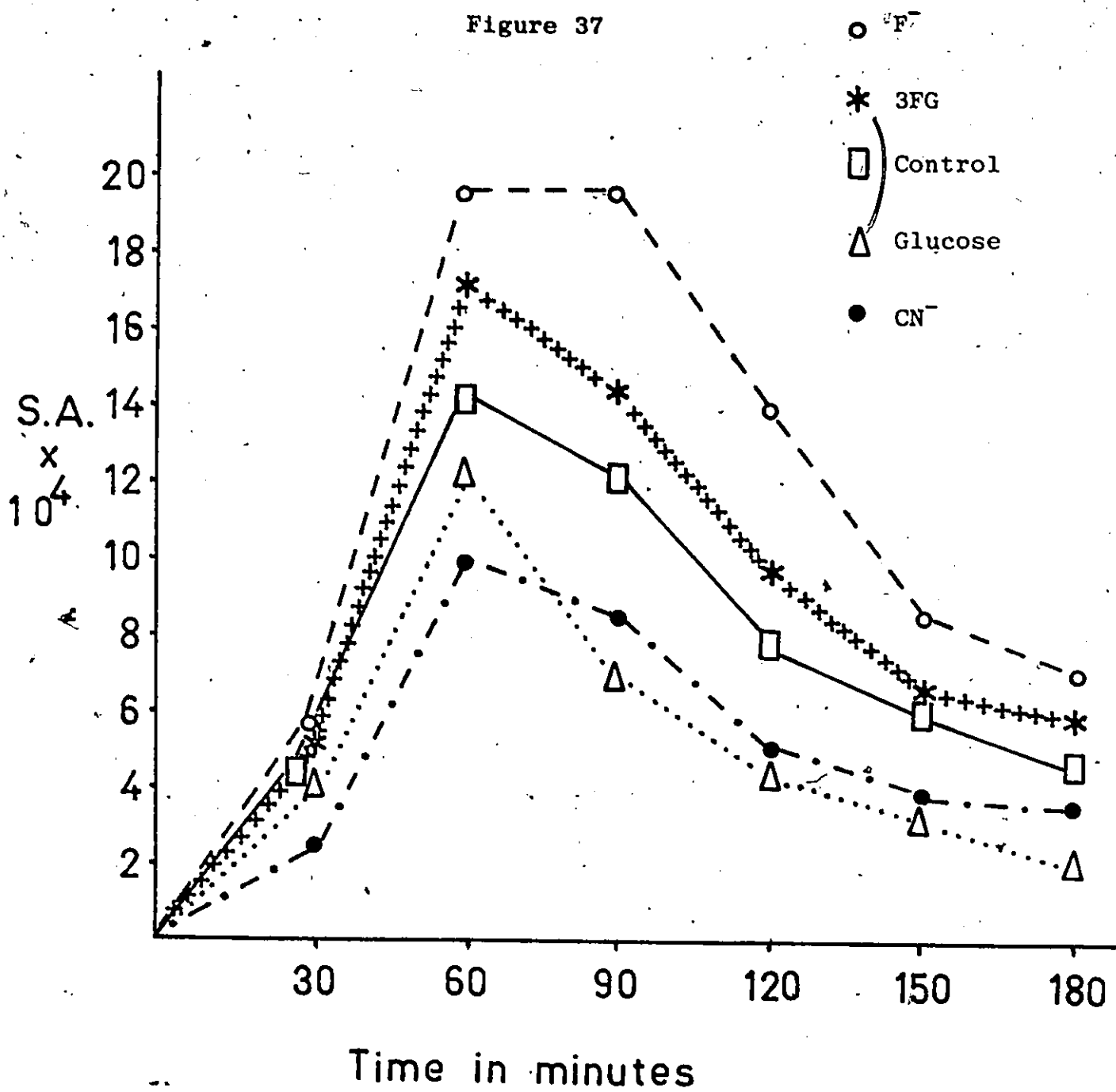
- F⁻ poisoned, locusts were injected with 12 μg/30 μl of F⁻ 1 hour prior to radiolabel (2 trials)
- * 3FG poisoned, locusts were injected with 8 mg/30 μl of 3FG 1 hour prior to radiolabel (3 trials)
- Control, locusts were injected with 30 μl of H₂O 1 hour prior to radiolabel (4 trials)
- Δ Glucose 8 mg, locusts were injected with 8 mg/30 μl of glucose 1 hour prior to radiolabel (3 trials)
- CN⁻ poisoned, locusts were injected with 12 μg/30 μl of CN⁻ 1 hour prior to radiolabel (3 trials)

Ordinate represents the specific activity of respired ¹⁴CO₂ as dpm/% CO₂.

	S.E.M. values for time intervals (in min)					
	30	60	90	120	150	180
○	2.3	2.6	3.0	3.0	1.5	1.6
*	2.6	3.1	2.7	2.0	1.0	1.2
□	2.0	2.5	2.5	2.0	1.5	1.0
Δ	1.0	1.9	2.0	2.0	2.0	2.1
●	1.0	2.5	2.2	2.0	1.5	1.6

All values were x 10⁴

Figure 37



as a consequence of the inhibition of glucose or glycogen conversion to acetyl-CoA via glycolysis or by an inhibition of fat mobilization. This would result in the decrease of the endogenous acetate or acetyl-CoA pool size and hence increase the specific activity of the radiolabel. Conversely, an increase in the acetyl-CoA endogenous pool or a block in the TCA cycle or electron transport chain would decrease the specific activity of $^{14}\text{CO}_2$ derived from C-1 acetate. It is presumed that the former effect applied in the case of 3FG and fluoride and the latter effect in the case of glucose and cyanide. Therefore it was likely that 3FG was exerting its inhibitory effect on a particular metabolic conversion in the glycolytic sequence.

It is important to emphasize that all studies discussed thus far involved only adult male locusts 10-16 days after final ecdysis. Locust age was found to be critical in terms of reproductability of radiorespirometric results. Young adult locusts displayed a degradative glucose metabolism which was substantially lower in terms of $^{14}\text{CO}_2$ yields from C-6 of glucose.

The availability of synthetic D-[3- ^3H]-3FG was fortuitous in view of the fact that the stereospecific exchange of the tritium from the C-3 position of D-[3- ^3H]-glucose with

solvent water had been used as a measure of the rate of fructose-6-phosphate phosphorylation and for estimation of substrate recycling via fructose-1-6-diphosphatase and phosphofructokinase (108). We had hoped to use the yield of $^3\text{H}_2\text{O}$ from D-[^3H]-3FG as a measure of the relative rate or extent of 3FG metabolism when compared to identical experiments using D-[^3H]-glucose.

Rose has shown that the pro-R C-3 tritium of dihydroxyacetone phosphate derived from the 3 position of glucose was exchanged with solvent water (109)(110)(111). The extent of this exchange is known to be large due to the pKa of the catalytic group at the active site of triose phosphate isomerase (112). Figure 38 depicts the stereochemistry of the ^3H -(C3) position. It was assumed that if appreciable tritium loss occurred from D-[^3H]-3FG that this was a good indication that 3FG was metabolized at least as far as triose phosphate isomerase. Table 6 summarizes the results of $^3\text{H}_2\text{O}$ release from D-[^3H]-glucose and 3FG.

The cold sugars were included in the injection solution to help 'wash' out the label into $^3\text{H}_2\text{O}$. This was particularly important in the case of 3FG due to its poor ability to act as a substrate for sorbitol dehydrogenase as discussed in the previous chapter. Control experiments indicated that neither

Table 6

 $^3\text{H}_2\text{O}$ Release from D-[^3H]-3FG and D-[^3H]-glucose

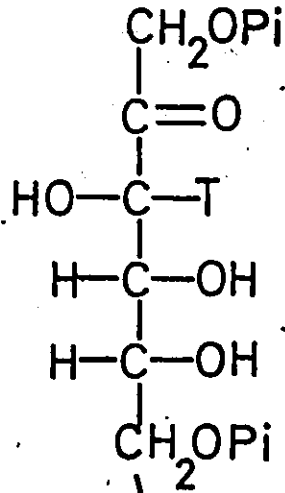
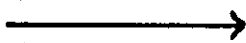
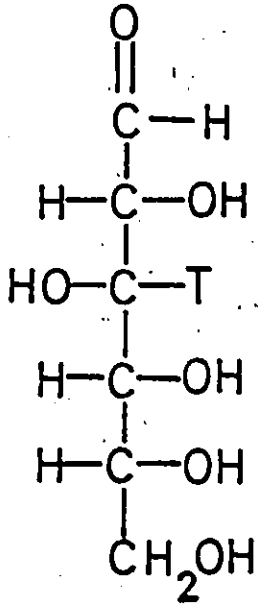
Locusts were injected with 6×10^6 dpm of either ^3H -D-glucose (12.4 mCi/mg) combined with 8 mg cold glucose in a volume of 30 μl , or with D-[^3H]-3FG combined with 8 mg cold 3FG in a final volume of 30 μl . $^3\text{H}_2\text{O}$ levels were determined as outlined in Materials and Methods. Errors are quoted as \pm S.E.M. The number in brackets represents the number of determinations.

Harvesting Time (hours)	Mean % yield of $^3\text{H}_2\text{O}$ from D-[^3H] 3FG	Mean % yield of $^3\text{H}_2\text{O}$ from D-[^3H]-glucose
4	0.53 ± 0.1 (4)	27.1 ± 3 (4)
24	2.75 ± 0.4 (4)	58 ± 5 (4)

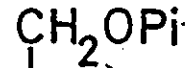
Figure 38

Stereochemistry of D-[3-³H]-glucose. TPI = triose phosphate isomerase.

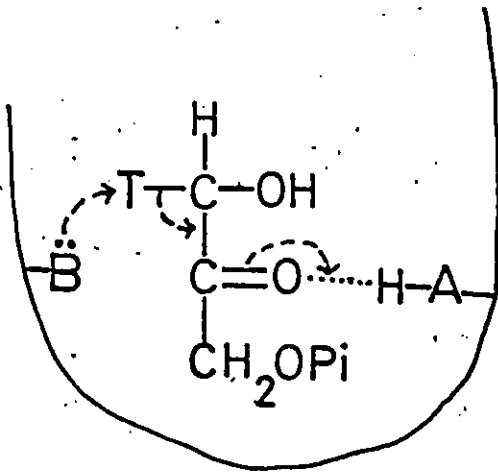
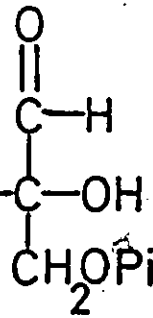
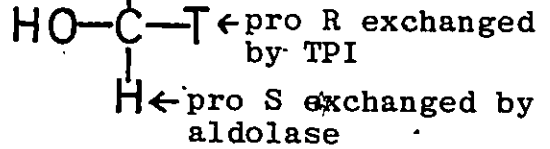
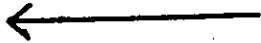
Figure 38



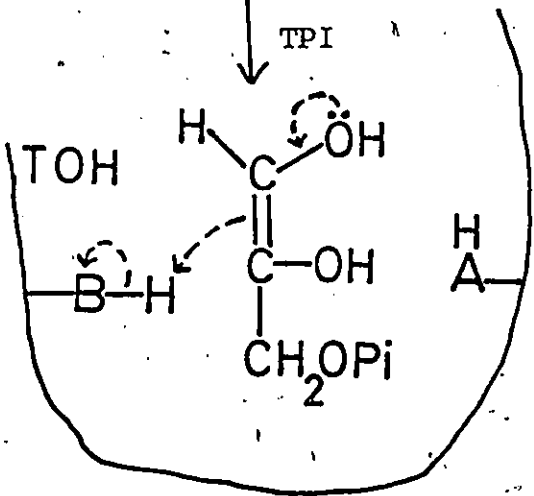
aldolase



TPI



TPI



D-[3-³H]-3FG or D-[3-³H]-glucose were contaminated with ³H₂O or that ³H₂O was released from these sugars upon incubation for 24 hours at 30°C in 0.1 M phosphate buffer pH 6.5 or 7.5. It seemed likely, therefore, that the slow rate of ³H₂O release in the case of 3FG was due to a kinetic factor, and that 3FG was indeed slowly metabolized as far as triose phosphate isomerase.

Based on the known mechanisms and stereochemistry of aldolase (113) and triose phosphate isomerase (114), it was thought that either of these two enzymes could have been a potential target for irreversible inactivation by a phosphorylated fluorometabolite (Figure 39). Fondy and co-workers have shown that fluoro-hydroxyacetone phosphate was an irreversible affinity label for triose phosphate isomerase. In order to test these possibilities, it was decided to examine the effect of 3FG on the tritium release of D-[3-³H]-glucose. An inhibition of ³H₂O release would suggest that one or both of these enzymes were inhibited. The results of this experiment are summarized in Table 7. The differences between the means were not statistically significant at either the 95% or 99% confidence limit based on the t test (115). Therefore, one could not say that a metabolite of 3FG resulted in a significant inhibition of either of the above enzymes, although

Table 7

Effects of 3FG and F⁻ on ³H₂O Release from D-[3-³H]-glucose

Control locusts were injected with 8 mg glucose plus D-[3-³H]-glucose, 3FG poisoned locusts were injected with 8 mg 3FG plus D-[3-³H]-glucose, and F⁻ poisoned locusts were injected with 25 µg F⁻ plus D-[3-³H]-glucose. Locusts were freeze clamped after 24 hours and ³H₂O levels determined as described in Materials and Methods. Error limits were expressed as ± S.E.M. Number in brackets is the # of determinations.

	Treatment		
	Glucose + Glucose*	3FG + Glucose*	F ⁻ + Glucose*
³ H ₂ O yields	42 ± 2.74% (4)	37 ± 2.11% (4)	43.5 ± 3.92% (4)

(Glucose * is radioactive glucose)

Statistical Analysis

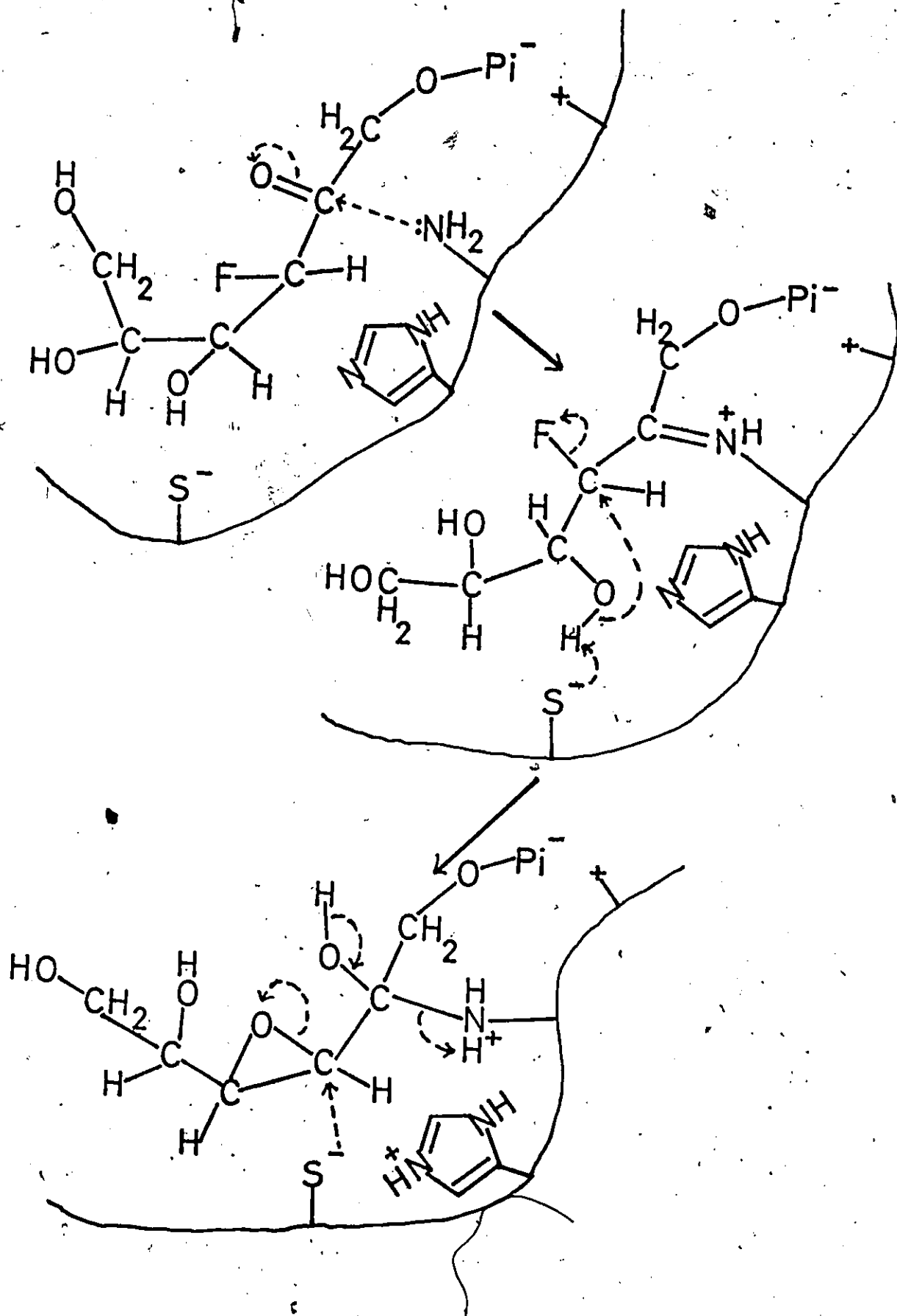
	3FG	Glucose	F ⁻
Sum of squares	53.4	90.3	184.2
Pooled Variance	24		45.75
Variance of differences	12	22.9	
S.E.M. of differences	3.46	4.79	
t value	1.445	0.313	

t values for 6 degrees of freedom at 95% confidence limit = 2.447,
at 99% confidence limit t = 3.707.

Figure 39

Hypothetical inactivation mechanism of aldolase by a metabolite of 3FG.

Figure 39



tritium release was slightly depressed. It may have been possible to evoke a significant effect by using higher doses of 3FG and harvesting locusts after longer periods of incubation with 3FG and radiolabel. It had been suggested by Rognstad and Katz that one of the problems associated with such a whole animal study was the possibility that the modifying agent only affected the metabolism of specific tissues and that the magnitude of the effect was obscured by $^3\text{H}_2\text{O}$ release from other tissues (108).

One possibility that occurred to us was the specific enzymic release of fluoride from a fluoro-metabolite. Previous studies in our lab had shown that the C-F bond of 3FG and 3FGL was extremely stable at physiological pH and only minute amounts of F^- were released upon exposure to basic conditions (59).

Subsequent investigations revealed that massive fluoride release had occurred in locust tissues (Table 8). Eight hours after an 8 mg dose of 3FG, the tissue fluoride levels increased about 100-fold. After 16 hours a 12 mg dose of 3FG which resulted in 67% mortality at the time of assay, resulted in a tissue fluoride increase of about 130-fold. A 60 μg dose of fluoride which resulted in 100% locust mortality within 13 hours increased tissue fluoride levels by almost 200-fold.

Table 8

Comparison of Tissue F⁻ levels in Control,
F⁻ Poisoned and 3FG Poisoned Locusts

Tissues were treated as described in Materials and Methods.

The numbers in brackets represent the number of determinations for each value, 3 locusts were used for each determination.

± error limits represent the standard error in the mean.

Control locusts were injected with sterile deionized H₂O plus a fluoride concentration equivalent to that present in the 3FG solution (this was usually less than 0.0005 mg F⁻/ml).

	Control	Treatment		
		F ⁻ Poisoned (60 µg/30 µl)	3FG (8 mg/30 µl)	3FG (12 mg/30 µl)
Time of assay (hrs after injection)	8,13,16	13	8	16
% death at time of assay	0%	100%	0%	67%
Approx. time to death (hrs)	-	10-13	48-72	13-20
Tissue (F ⁻)* mg/ml	25±2.5 x 10 ⁻⁵ (3)	47±1.8 x 10 ⁻³ (3)	22±1.8 x 10 ⁻³ (3)	32±2.3 x 10 ^{-3**} (3)

* Tissue F⁻ levels were calculated on the basis of the following rationale. Preliminary experiments indicated that no appreciable F⁻ loss due to excretion occurred during the period of investigation. Based on this observation the mean total aqueous volume of locusts was calculated to be 877 ± 50 µl/gm locust (3 determinations)

Table 8 (con'd)

by F^- dilution analysis. This value was used to approximate the tissue F^- levels.

**This value represented a fluoride yield of 3.2% when compared to the total fluoride available for release from 36 mg of 3FG injected into 3 locusts.

It seemed likely, therefore, that enzymic fluoride release from a fluoro-metabolite might have accounted for the toxicity of 3FG and 3FGL. The lower levels of fluoride responsible for death in the 12 mg 3FG dose group could be due to the intracellular release of fluoride, rather than the diffusion of extracellular F^- into locust tissues. There is not sufficient information available on locust anion transport to make any comment regarding the ease of cellular membrane penetration by fluoride (116).

Previous studies on sorbitol dehydrogenase discussed in this dissertation demonstrated no detectable release of fluoride from the action of this enzyme on 3FGL. It was suspected that fluoride was inhibiting the enzyme enolase (117)(118) due to the $^{14}CO_2$ respiratory patterns obtained with 6- ^{14}C -D-glucose and 1- ^{14}C -acetate. The potential inhibitory effects of fluoride on other Mg^{2+} dependent enzymes could not, however, be discounted (119). Wang and Himoe have shown that fluoride formed a strong enolase bound complex with Mg^{2+} and phosphate (118). With rabbit muscle enolase the apparent dissociation constant of fluoride from this complex was 50 μM . They suggested that fluoride formed a direct coordination complex with Mg^{2+} on the enzyme and inhibited the reaction by acting as an

analogue of OH^- ion, which was generated during the course of normal enolase-catalyzed reaction. The total body concentration of fluoride after 16 hours in locusts injected with 12 mg 3FG was estimated at about 1.7 mM (Table 8). This concentration is about 35 times higher than the apparent dissociation constant of fluoride from rabbit muscle enolase. If locust enolase had a similar susceptibility to fluoride, its complete inhibition could be accounted for by the levels of fluoride present.

In order to attempt the identification of a possible metabolite of 3FG which was susceptible to defluorination and/or detritiation, we conducted a phosphorylated metabolite scan based on the procedure of Newsholme (105). Since the majority of the tritium label in D-[$3\text{-}^3\text{H}$]-3FG was known to remain attached to a hydrocarbon skeleton, locusts were injected with 35×10^6 dpm of D-[$3\text{-}^3\text{H}$]-3FG, which was mixed with 10 mg of cold 3FG to help force the label into the glycolytic stream. A typical radiochromatographic scan is depicted in Figure 40. The majority of the ^3H counts were found in the region between glucose-6-phosphate and glyceraldehyde-3-phosphate. This radioactivity represented about 3% of the total radioactivity loaded onto the chromatographic plate. The majority of the radioactivity was

Figure 40

Sample chromatogram of locust phosphorylated metabolites on P.E.I. cellulose after injection of $D-[3\text{-}^3\text{H}]-3\text{FG}$. Solvent system, formic acid 2 N : lithium chloride 0.5 N, 1:1.

G1P = glucose-1-phosphate

F6P = fructose-6-phosphate

FDP = fructose-1,6-diphosphate

G6P = glucose-6-phosphate

PEP = phosphoenolpyruvate

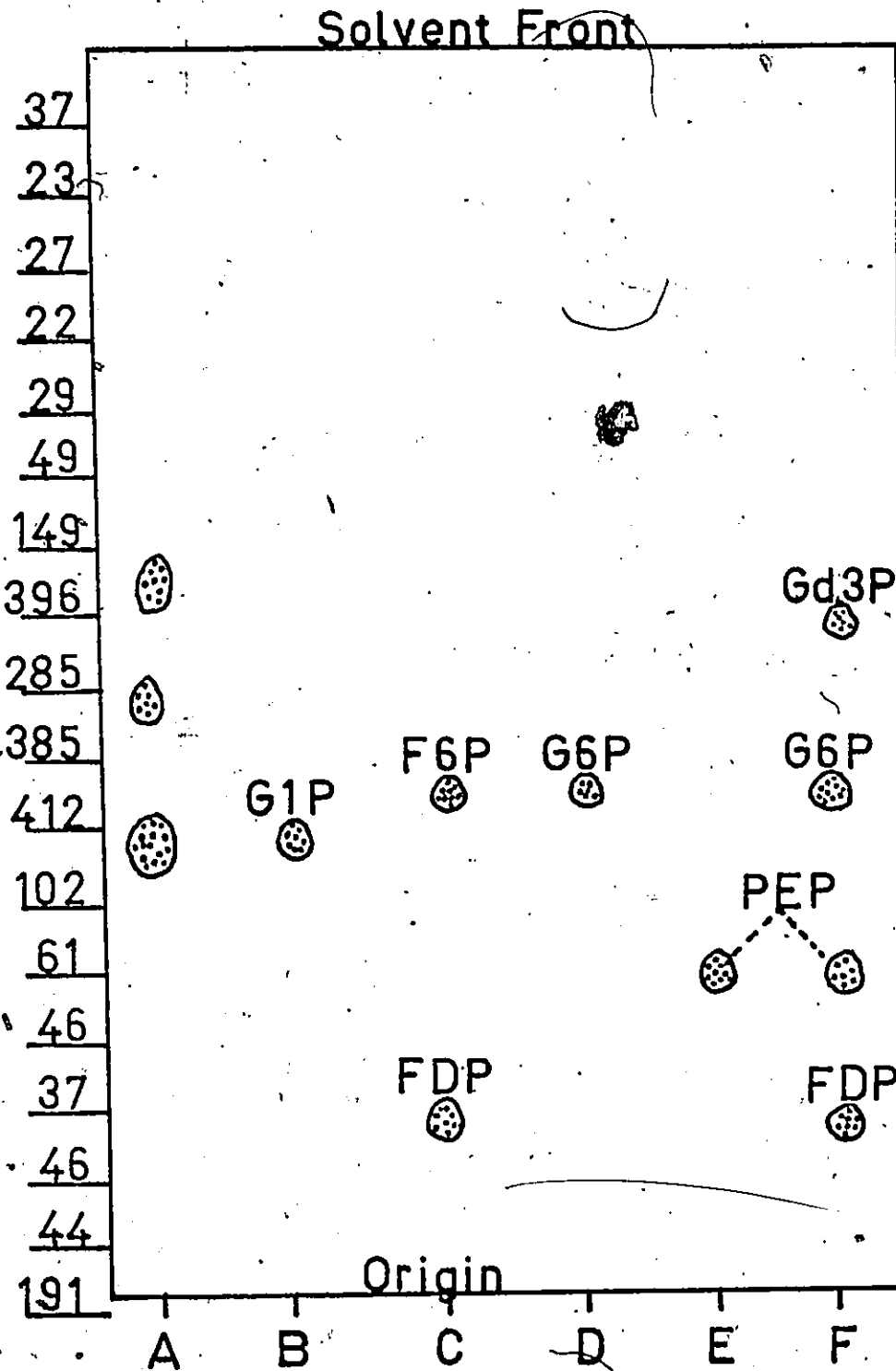
Gd3P = glyceraldehyde-3-phosphate

A = phosphorylated metabolites from $D-[3\text{-}^3\text{H}]-3\text{FG}$ treated locusts as detected by phosphate sensitive spray.

B→F = phosphorylated metabolite markers.

The numbers to the left of column A represent the ^3H counts per minute detected from 1 cm x 1 cm squares cut out of column A.

Figure 40



lost when the plates were washed with 95% methanol to remove non-phosphorylated material.

In order to determine whether organically-bound fluorine was present in the area marked by radioactivity on the P.E.I. cellulose plates, we separated the monophosphorylated metabolites from other locust tissue metabolites using the method of M.G. Clark (102)(103). The monophosphorylated-tritiated metabolites were concentrated to a volume of 1 ml and were subjected to Fourier transform ^{19}F NMR. Figure 41 depicts the spectrum obtained after 76,000 scans. The signal to noise ratio was about 3:1. Although no structural assignments can be proposed on the basis of this spectrum alone, it was obvious that the fluorine signal was due to an organically-bound fluorine present in a phosphorylated metabolite(s).

Thus far in the investigation of 3FG toxicity in Locusta migratoria, it appears likely that 3FG enters glycolysis via its conversion to 3-fluoro-fructose with subsequent phosphorylation of this compound by a hexo- or fructokinase. Since 3FF or its putative phosphorylated derivative are haloketones, these metabolites would be particularly susceptible to nucleophilic attack if correctly oriented and activated in an enzyme active site. Whether

Figure 41

^{19}F Fourier Transform NMR of a phosphorylated fluoro-metabolite from locusts after 3FG injection.

A = trifluoro-acetic acid 1 mM

B = metabolite

C = F^-

Conditions used for scans of A + B

offset = 29,776 Hz

O2 = 5,700

AQ = .0983

FW = 50,000

SI = 8

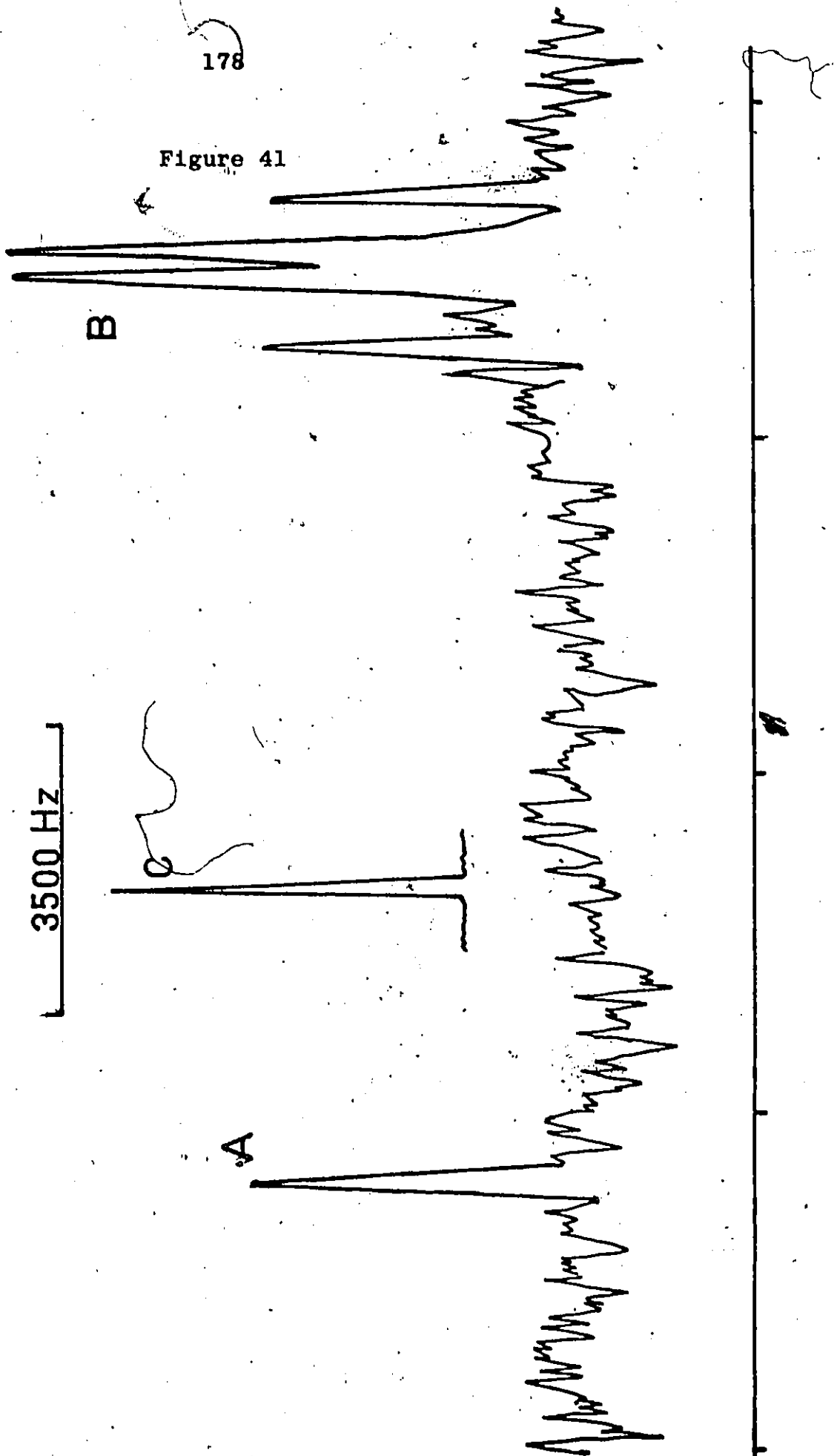
DW = 12

number of scans = 76,000

line broadening = 60 Hz

The broadness of the lines was attributed to the presence of a small concentration of para magnetic ion(s).

Figure 41



or not such enzyme action results in irreversible covalent alkylation remains to be elucidated. An example of fluoride release without enzyme inactivation has been described by Leung and Frey (120). They have demonstrated the release of fluoride from monofluoro-pyruvate by the first enzyme in the pyruvate dehydrogenase complex. It is evident, however, that a massive enzyme catalyzed release of fluoride from a 3FG metabolite occurs in locusts. This is likely responsible for locust death due to the irreversible inhibition of enolase.

It is believed that the most attractive target sites for fluoride release are aldolase or triose phosphate isomerase. Previous studies by Hartman have shown that haloacetol phosphates (Br, Cl, I) do not act as active site affinity agents for aldolase. This was a surprising finding since both aldolase and triose phosphate isomerase share a similar primary proton abstraction step in their reaction mechanisms. It is known, however, that monofluoro-hydroxyacetone phosphate both defluorinates and alkylates triose phosphate isomerase. The effect of this compound on aldolase has not been investigated. Since the tritium release experiments demonstrated that a small but significant amount of $^3\text{H}_2\text{O}$ is lost from D-[3- ^3H]-3FG, it is

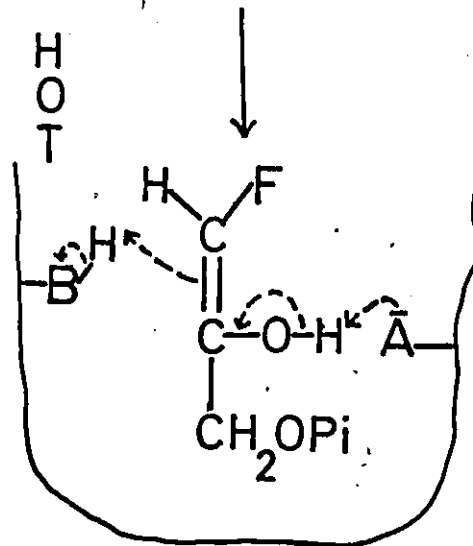
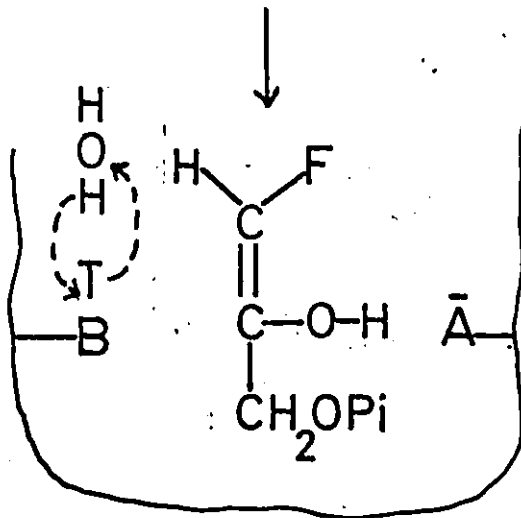
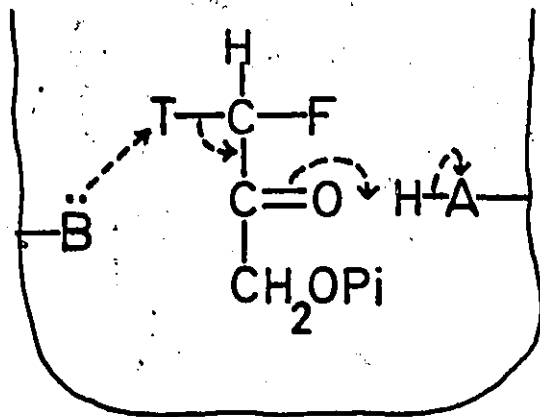
possible that pro-R-³H-monofluoro-hydroxyacetone phosphate is formed by aldolase and subsequently detritiated or defluorinated by triose phosphate isomerase. Such a mechanism is not unrealistic due to the outcome of similar experiments conducted by Meloche on 2-keto-3-deoxyphosphogluconate aldolase using ³H-labelled bromopyruvate. These experiments were discussed in the introduction of Part 1. No one has yet investigated the possible detritiation of pro-R-³H-monofluorohydroxyacetone phosphate by triose phosphate isomerase. It is thought that such a mechanism provides a good working hypothesis for the mechanism of tritium and fluoride release from D-[³H]-3FG (Figure 42). One cannot, however, exclude the possibility that detritiation and defluorination occur on separate enzymes.

Figure 42

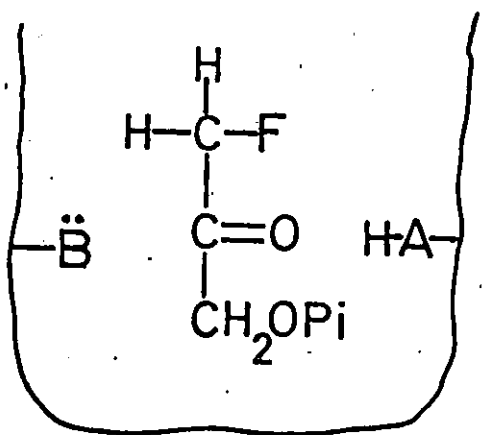
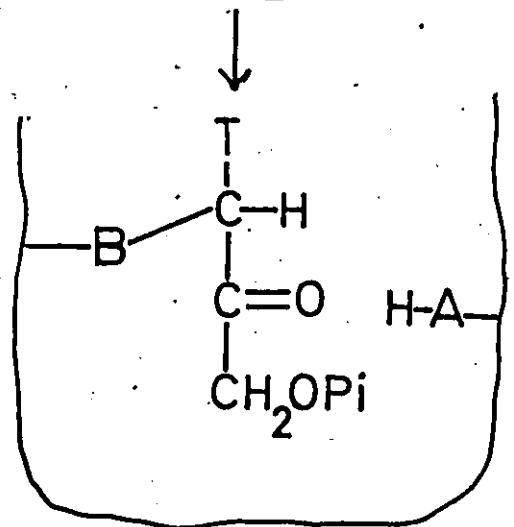
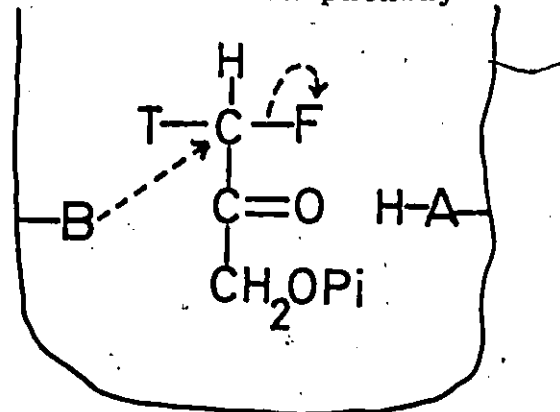
Proposed mechanism for concomitant detritiation and defluorination of pro-R-³H-monofluoro-hydroxyacetone phosphate by triose phosphate isomerase.

Figure 42

Tritium exchange pathway



Inactivation pathway



APPENDIX 1

Least Squares Method

All linear plots were analyzed by the least squares method. It was assumed that the set of experimental points fit the equation $y = a + bx$, where 'x' and 'y' are the dependent and independent variables, 'a' is the 'y' intercept and 'b' is the slope of the resulting line. This method chooses an 'a' and 'b' so that the average sum of the squares of the difference between the experimental 'y' values and the calculated 'y' values is at a minimum. The equations used to calculate 'a' and 'b' are

$$a = \frac{\sum_{n=1}^k x_n^2 \sum_{n=1}^k y_n - \sum_{n=1}^k x_n \sum_{n=1}^k (x_n y_n)}{\left[k \sum_{n=1}^k x_n^2 - \left(\sum_{n=1}^k x_n \right)^2 \right]} = Z$$

$$b = \frac{k \sum_{n=1}^k (x_n y_n) - \sum_{n=1}^k x_n \sum_{n=1}^k y_n}{Z}$$

Initial velocity equations were rearranged into reciprocal form, where

$$\frac{1}{v_i} = \frac{K_m}{V_{\max}} \left[\frac{1}{S} \right] + \frac{1}{V_{\max}}$$

$$\left[\frac{1}{S}\right] = x, \quad \text{and} \quad \frac{1}{v_i} = y$$

Sample calculation for uninhibited plot in Figure 15a, $k=6$

x	y	x·y	x ²
5	50.0	250	25
10	73.9	739	100
16.7	93.0	1,553	278.9
25	105.8	2,645	625
50	163.4	8,170	2,500
100	270.0	27,000	10,000
($\sum x$) 206.7	($\sum y$) 756.1	($\sum x \cdot y$) 40,357	($\sum x^2$) 13,528.9

$$a = \frac{(206.7)(40,357) - (13,529)(756.1)}{42,725 - 6(13,528.9)} = 49.1$$

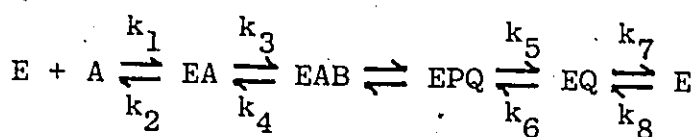
$$b = \frac{(206.7)(756.1) - 6(40,357)}{42725 - 6(13,528.9)} = 2.23$$

and $y = 49.1 + 2.23(x)$

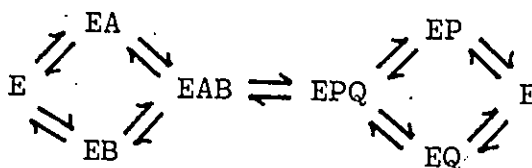
Mechanistic and Kinetic Aspects of Dehydrogenase Enzymes

Based upon twenty years of intense interest and research in the area of dehydrogenase enzyme mechanisms, it is now known that all the dehydrogenases studied fall into two general mechanistic categories (84). Those which follow an ordered binding mechanism, or those which follow a random mechanism. Various special cases exist in each category,

such as the Theorell-Chance, the rapid equilibrium random, partial random, and preferred pathway random. Of all the dehydrogenases studied, none have been found to exhibit a substituted enzyme (ping-pong) type of mechanism as is commonly found in transaminases.



(Ordered Mechanism)



(Random Mechanism)

E = Enzyme, A = NAD⁺ or NADP⁺, B = reduced substrate,
P = oxidized substrate, Q = NADH or NADPH

In all of the ordered cases studied NAD⁺ or NADH always add on first. The majority of the dehydrogenase enzyme mechanisms all give the same steady state initial velocity equation (84). In the following discussion, the Cleland notation will be used (78), although the Dalziel method is equally applicable (84). The steady state initial velocity equation is

$$v_i = \frac{V_1(A)(B)}{K_{ia}K_b + K_b(A) + K_a(B) + (B)(A)} \quad (\text{Cleland})$$

$$\frac{e}{v} = \phi_0 + \frac{\phi A}{A} + \frac{\phi B}{B} + \frac{\phi AB}{AB} \quad (\text{Dalziel})$$

Using the example of an ordered bi-bi mechanism, it can be shown that K_m (app)

$$= \frac{k_1(k_4 + k_5)k_7 \frac{k_2}{k_1(A)} + 1}{\frac{1}{k_1k_3(k_5 + k_7)} + k_3k_5k_7}$$

and in the case of a comparison of two K_m (app)'s

$$\frac{K_m'(\text{app})}{K_m(\text{app})} = \frac{\frac{k_4 + k_5}{\frac{1}{k_1k_3(k_5 + k_7)} + k_3k_5k_7}}{(k_4 + k_5)} \cdot \frac{\frac{1}{k_1k_3(k_5 + k_7)} + k_3k_5k_7}{\frac{1}{k_1k_3(k_5 + k_7)} + k_3k_5k_7}$$

where (A) is the same in each K_m (app).

This treatment assumes that the introduction of an alternative substrate only affects those rate constants associated directly

with the substrate.

In the case where one wishes to compare V_{\max} (app)'s, it can be shown for the same mechanism that


$$\frac{V'_{\max}(\text{app})}{V_{\max}(\text{app})} = \frac{k_5 [k_1(A)(k'_5 + k_7) + k'_5 k_7]}{k_5 [k_1(A)(k_5 + k_7) + \underbrace{k_5 k_7}]}$$

The preceding equations make it obvious that one cannot make rigorously valid remarks by comparing V_{\max} (app) or K_m (app) values on the basis of steady state information alone, since these parameters are complex functions of many individual kinetic rate constants. One further handicap in the case of steady state analysis of bireactant enzymes is the fact that initial velocity expressions do not directly reflect the rate constants which govern the interconversion of ternary complexes (80)(78). In order to make valid statements regarding the effects of substrate substituents on enzyme binding affinities and catalytic rate constants, one must employ fast kinetic techniques such as stop flow, temperature jump, etc. to give a direct measure of individual rate constants. By examining the effects of substrate substituents on individual rate constants, particularly in the catalytic step, one can then make justifiable statements

regarding the effects of substituents on free energy changes in the transition state. The validity of this statement may be easily demonstrated. If one considers the EAB complex as a unimolecular species, then transition state theory for a unimolecular reaction can be applied (85). The first order rate constant for a unimolecular reaction can be written as

$$k_1 = (kT/h) \exp(\Delta S^\ddagger/R) \exp(-\Delta H^\ddagger/RT)$$

where ΔS^\ddagger , ΔH^\ddagger are the entropy and enthalpy of activation. Comparison of the rate constants of ternary interconversions for a variety of substrates with different substituents can give valuable information regarding free energies in the transition state. Unfortunately, such studies are not easily performed in the case of dehydrogenase enzymes. Such studies, however, have been carried out on chymotrypsin and other serine proteases which have simpler kinetic schemes (86). These substituent studies when combined with binding studies have constituted the basis of verification for the Circé effect as proposed by Jencks (87).



APPENDIX 11

Calculation of Standard Errors in the Mean

The standard error in the mean (S.E.M.) was calculated using the relationship

$$\text{S.E.M.} = \sqrt{\frac{\sum(x - \bar{x})^2}{n(n-1)}}$$

and
$$\sum(x - \bar{x})^2 = \sum(x^2) - \frac{(\sum x)^2}{n} = s^2 \text{ (variance)}$$

A sample calculation for control $^{14}\text{CO}_2$ specific activity at 30 min from 1- ^{14}C -D-glucose (Figure 33) is given below:

\bar{x}	8.2×10^4
$\sum x$	24.5×10^4
$\sum(x^2)$	232.75×10^8
$\frac{(\sum x)^2}{n}$	200×10^8
s^2	16.4×10^8
s	4.04×10^4
S.E.M.	2.3×10^4

REFERENCES

1. Marais, J.S.C., Onderstepoort J. Vet. Sci. Anim. Ind. 18, 203, (1943).
2. Liebecq, C. and Peters, R.A., J. Physiol. (London), 108, 11P, (1948).
3. Liebecq, C., and Peters, R.A., Biochem. Biophys. Acta., 3, 215, (1949).
4. Peters, R.A., Wakelin, R.W., Buffa, P., Thomas, L.C., Proc. Royal Soc. London, B140, 497 (1953).
5. Peters, Sir R.A., "Biochemical Lesions and Lethal Synthesis", MacMillan Co., New York, (1963).
6. Peters, Sir R.A., in "Carbon Fluorine Compounds", CIBA Foundation Symposium, Elsevier North-Holland, Amsterdam, p. 55, (1972).
7. Brady, R.O., J. Biol. Chem., 217, 213, (1955).
8. Saunders, B.C., in "Carbon Fluorine Compounds", CIBA Foundation Symposium, Elsevier North-Holland, Amsterdam, p. 9, (1972).
9. Kun, E., in "The Citric Acid Cycle", edited by E. Lowenstein, Dekker Publishers, New York, p. 297, (1969).
10. Kun, E., Gottwald, L.K. and Fanshier, D.W., J. Biol. Chem., 237, 3588, (1962).
11. Gottwald, L.K., Fanshier, D.W., and Kun, E., J. Biol. Chem., 239, 424, (1963).
12. Dummel, R.J. and Kun, E., J. Biol. Chem., 244, 2966, (1969).
13. Carrel, H.L. and Glusker, J.P., Acta Crystallogr., 29, 4364, (1973).
14. Peters, Sir R.A., British Med. Bull., 25, 223, (1969).
15. Pattison, F.L.M. and Peters, Sir R.A., in "Handbook of Experimental Pharmacology", vol. XX, Springer Press, New York, p. 387, (1966).

16. Guarriera-Bobyleva, V., and Buffa, P., *Biochem. J.*, 113, 853, (1969).
17. Glusker, J.P., *J. Molec. Biol.*, 38, 149, (1968).
18. Carrel, H.L., Glusker, J.P., Villafranca, J.J., Mildvan, A.S., Dummel, R.J., and Kun, E., *Science*, 170, 1412, (1970).
19. Kun, E., in "Biochemistry Involving Carbon-Fluorine Bonds", ACS Symposium Series #28, edited by R. Filler, p. 1, (1976).
20. Eanes, R.Z., and Kun, E., *Molec. Pharmacol.*, 10, 130, (1974).
21. Kun, E., unpublished experiments.
22. Newsholme, E.A. and Start, C., in "Regulation in Metabolism", J. Wiley and Sons, Toronto, p. 13, (1973).
23. Eanes, R.Z., Skilliter, D.N. and Kun, E., *Biochem. Biophys. Res. Comm.* 46, 1618, (1972).
24. Chappel, J.B., *British Med. Bull.* 24, 150, (1968).
25. Brand, M.D., Evans, S.M., Mendes-Mourao, J., and Chappel, J.B. *Biochem. J.*, 134, 217, (1973).
26. Kirsten, E., Sharma, M.L. and Kun, E., *Molec. Pharmacol.*, 14, 172, (1978).
27. Kun, E., Kirsten, E., Sharma, M.L., *Proc. Natl. Acad. Sci., U.S.A.*, 74, 4942, (1977).
28. Silverman, R.B., and Abeles, R.H., *Biochemistry*, 16, 5515, (1977).
29. Walsh, C.T. and Wang, E., *Biochemistry*, 17, 1313, (1978).
30. Santi, D.V., McHenry, C.S. and Sommer, H., *Biochemistry*, 13, 471, (1974).
31. Wold, F., in "Methods in Enzymology", Vol. XLVI, edited by W.B. Jacoby and M. Wilchek, Academic Press, New York, p. 3, (1977).

32. Schoellmann, G. and Shaw, E., *Biochem. Biophys. Res. Comm.*, 7, 36, (1962), and *Biochemistry*, 2, 252, (1963).
33. Hartman, F.C. in "Methods in Enzymology", Vol. XLVI, edited by W.B. Jacoby and M. Wilchek, Academic Press, New York, p. 28, (1977).
34. Meloche, H.P., Luczak, M.A., and Wurster, J.M., *J. Biol. Chem.* 247, 4186, (1972).
35. Hartman, F.C., *J. Amer. Chem. Soc.*, 92, 2170, (1970).
36. Hartman, F.C., *Biochemistry*, 10, 146, (1971).
37. De La Mare, S., Coulson, A.F.W., Knowles, J.R., Priddle, J.D., and Offord, R.E., *Biochem. J.*, 129, 321, (1972).
38. Grazi, E., Meloche, H.P., Martinez, G., Wood, W.A., and Horecker, B.L., *Biochem. Biophys. Res. Comm.*, 10, 4, (1963).
39. Meloche, H.P., and Wood, W.A., *J. Biol. Chem.*, 239, 3511, (1964).
40. Meloche, H.P., *Biochem. Biophys. Res. Comm.*, 18, 277, (1965).
41. Meloche, H.P., *Biochemistry*, 6, 2273, (1967).
42. Meloche, H.P., Luczak, M.A. and Wurster, J.M., *J. Biol. Chem.*, 247, 4186, (1972).
43. Meloche, H.P., *Biochemistry*, 9, 5050, (1970).
44. Silverman, J.B., Babiarez, P., Mahajan, K., Buschek, J., and Fondy, T.P., *Biochemistry*, 14, 2252, (1975).
45. Pauling, L. in "The Nature of the Chemical Bond", Cornell University Press, Ithaca, New York, p.85, (1960).
46. Santi, D.V., and McHenry, C.S., *Proc. Natl. Acad. Sci. U.S.A.*, 69, 1855, (1972).

47. Santi, D.V., McHenry, C.S., and Sommer, H., *Biochemistry*, 13, 471, (1974).
48. Santi, D.V., in "Biochemistry Involving Carbon-Fluorine Bonds", ACS Symposium #28, edited by R. Filler, p. 57, (1976).
49. Rando, R.R., in "Methods in Enzymology", Vol. XLVI, edited by M. Wilchek and W.B. Jacoby, Academic Press, New York, p. 29, (1977).
50. Rando, R.R., *Accounts of Chemical Research*, 8, 281, (1975).
51. Kahan, F.M., and Jacobus, D.P., Abstract, Interscience Conference on Antimicrobial Agents and Chemotherapy, Abstracts 101-103, Washington, D.C., Sept. (1975).
52. Eisenthal, R.E., Harrison, R., Lloyd, W.J., and Taylor, N.F., *Biochem. J.*, 130, 199, (1972).
53. Taylor, N.F., Hill, L., and Eisenthal, R.E., *Can. J. Biochem.*, 53, 57, (1975).
54. Taylor, N.F. and Li-Yu Louie, *Can. J. Biochem.*, 55, 911, (1977).
55. Al-Jobore, A., PhD Dissertation, University of Windsor, (1978).
56. Taylor, N.F., Romaschin, A.D., and Smith, D.A., in "Biochemistry Involving Carbon-Fluorine Bonds" ACS Symposium #28, edited by R. Filler, p. 99, (1976).
57. Taylor, N.F. and Gagneja, G.L., in "Cell Surface Carbohydrate Chemistry", edited by R.E. Harmon, Academic Press, New York, p. 269, (1978).
58. Taylor, N.F. and Halton, D.M., submitted for publication, *J. Neurochemistry*, (1978).
59. Riley, G.J., PhD Dissertation, University of Bath, (1973).
60. Romaschin, A.D., Taylor, N.F., Smith, D.A. and Lopes, D., *Can. J. Biochem.*, 55, 369, (1977).

61. Smith, D.A., MSc Thesis, University of Bath, (1974).
62. Ford, W.C.L., and Candy, D.J., *Biochem. J.*, 133, 1101, (1972).
63. Chino, H., *Nature (London)*, 80, 606, (1957).
64. Handel, E.V., *Comp. Biochem. Physiol.*, 29, 1023, (1969).
65. Bailey, E., in "Insect Biochemistry and Function", edited by D.J. Candy and B.A. Kilby, Chapman and Hall, London, p. 90, (1975).
66. Sacktor, B., in "Insect Biochemistry and Function", edited by D.J. Candy and B. A. Kilby, Chapman and Hall, London, p. 3, (1975).
67. Crabtree, B., and Newsholme, E.A., in "Insect Muscle", edited by P.N.R. Usherwood, Academic Press, London, p. 405, (1975).
68. Sactor, B., *Biochem. Soc. Symp.*, 41, 111, (1976).
69. Newsholme, E.A. and Crabtree, B., *Biochem. Soc. Symp.* 41, 61, (1976).
70. Rees, H.H., "Insect Biochemistry", Chapman and Hall, London, (1977).
71. Brunt, R.V. and Taylor, N.F., *Biochem. J.*, 105, 41c, (1967).
72. Taylor, N.F., Hunt, B., Kent, P.W., and Dwek, R.A., *Carbohydr. Res.*, 22, 467, (1972).
73. Partridge, S.M., *Nature*, 164, 443, (1949).
74. Segal, I.H., "Enzyme Kinetics", John Wiley and Sons Inc., New York, p. 114, (1975).
75. McFadden, B.A. and Howes, W.V., *Anal. Biochem.*, 1, 240, (1960).
76. Romaschin, A.D., unpublished results.

77. Graves, D.J. and Wu Yun-Tai, in "Methods in Enzymology", Vol. XXXIV, edited by W.B. Jacoby and M. Wilchek, Academic Press, New York, p. 140, (1974).
78. Plowman, K.M., "Enzyme Kinetics", McGraw-Hill, New York, p. 132, (1972).
79. Newsholme, E.A. and Start, C., "Regulation in Metabolism", John Wiley and Sons, London, p. 13, (1973).
80. Cornish-Bowden, A., "Principles of Enzyme Kinetics", Butterworths, London, p. 21, (1976).
81. Laidler, K.J., Can. J. Chem., 33, 1614, (1955).
82. Gabbay, K.H. and Kinoshita, J.H. in "Methods in Enzymology" Vol. XLI, edited by H.G. Wood, Academic Press, New York, p. 164, (1975).
83. Moriyama, T., Tetsuya, K., Takao, W., Tatsumi, K., Katsuyasu, K., Yoshio K., and Kandru, S., J. Nara. Med. Assoc. (Japan), 24, 356, (1973).
84. Dalziel, K., in "The Enzymes", Third Edition, edited by P.D. Boyer, Academic Press, New York, p. 1, (1975).
85. Fersht, A., "Enzyme Structure and Mechanism", W.H. Freeman and Company, San Francisco, (1977).
86. Baumann, W.K., Bizzozero, S.A. and Dutler, H., F.E.B.S. Lett., 2, 257, (1970) and Eur. J. Biochem., 39, 381, (1973).
87. Jencks, W.P., in "Advances in Enzymology", Vol. 43, edited by A. Meister, Wiley-Interscience, New York, p. 219, (1975).
88. Eisenthal, R., Lloyd, W., and Harrison, R., Arch. Biochem. Biophys., 163, 185, (1974).
89. Silverman, J.B., Babiarez, P.S., Mahajan, K.P., Bushek, J., and Fondy, T.P., Biochemistry, 14, 2252, (1975).
90. Velle, W., in "Methods in Enzymology", Vol. XLI, edited by W.A. Wood, Academic Press, New York, p. 165, (1975).

91. Jones, J.B., in "Application of Biochemical Systems in Organic Chemistry", Part 1, edited by J.B. Jones, J. Wiley and Sons, New York, p. 236, (1976).
92. Prendergast, F.G. and Veneziale, C.M., J. Biol. Chem., 250, 1282, (1975).
93. Levine, G.A., Bissel, M.J., and Bissel, D.M., J. Biol. Chem., 253, 5985, (1978).
94. Chefurka, W., Horie, Y. and Robinson, J.R., Comp. Biochem. Physiol., 37, 143, (1970).
95. Silva, G.M., Doyle, W.P. and Wang, C.H., Nature, London, 182, 102, (1958).
96. Wood, H.G., Katz, J. and Landon, B.R., Biochem. J., 338, 809, (1963).
97. Ela, R., Chefurka, W., Robinson, J.R., J. Insect Physiol., 16, 2137, (1970).
98. Brand, H., and Hess, B., in "Methods of Enzymatic Analysis", Vol. 1, Second Edition, edited by H.U. Bergemeyer, Academic Press, London, p. 134, (1974).
99. "Worthington Enzymes Manual", Worthington Biochemical Corp., Freehold, N.J., p. 181, (1972).
100. Wang, C.H., Willis, D.L. and Loveland, W.D., "Radiotracer Methodology in the Biological Environmental and Physical Sciences", Prentice-Hall, Englewood Cliffs, N.J., p. 294, (1975).
101. Lopes, D.P., PhD Dissertation, University of Windsor, (1978).
102. Clark, M.G., Int. J. Biochem., 9, 17, (1978).
103. Clark, M.G., Bloxham, D.P., Holland, P.C. and Lardy, H.A., Biochem. J., 134, 589, (1973).
104. Boltz, D.F. and Holland, W.J., Chem. Anal., 8, 161, (1958).
105. Conyers, R.A.J., Newsholme, E.A., and Brand, K., Biochem. Soc. Trans., 4, (6), 1040, (1976).

106. Randerath, K. and Randerath, E., J. Chromatogr., 16, 111, (1964).
107. Hanes, C.S. and Isherwood, F.A., Nature, London, 164, 1107, (1949).
108. Rongstad, R. and Katz, J., in "Current Topics in Cellular Regulation", edited by Horecker and Stadtman, Academic Press, New York, p. 237, (1976).
109. Rose, I.A. and Reider, D.J., J. Amer. Chem. Soc., 77, 5764, (1955).
110. Rose, I.A. in "The Enzymes", Vol. 2, Third Edition, edited by P.D. Boyer, Academic Press, New York, p. 281, (1970).
111. Rose, I.A. and Reider, D., J. Biol. Chem., 234, 1007, (1959).
112. Hartman, F.C. and Ratrie, H., Biochem. Biophys. Res. Comm., 77, 746, (1977).
113. Lai, C.Y. and Horecker, B.L. in "Essays in Biochemistry", Vol. 8, edited by P.N. Campbell and F. Dickens, Academic Press, London, p. 149, (1972).
114. Rose, I.A., in "Advances in Enzymology", Vol. 43, edited by A. Meister, J. Wiley and Sons, London, p. 491, (1975).
115. Wood, E.C., in "Comprehensive Analytical Chemistry", edited by C.L. Wilson and D.W. Wilson, Elsevier, Amsterdam, p. 76, (1959).
116. Rees, H.H., in "Insect Biochemistry", Chapman and Hall, London, p. 25, (1977).
117. Warburg, O. and Christian, W., Biochem. Z., 310, 384, (1941).
118. Wang, T. and Himoe, A., J. Biol. Chem., 249, 3895, (1974).
119. Hewitt, E.J. and Nicholas, D.J.D., in "Metabolic Inhibitors", Vol. 2, edited by R.M. Hochester and J.H. Quastel, Academic Press, New York, p. 311, (1963).

120. Leung, H. and Frey, B., Biochem. Biophys. Res. Comm., 81, 274, (1978).
121. Warburg, O. and Christian, W., Biochem. Z., 310, 384, (1942).

20

NS

2

VITA AUCTORIS

Name: Alexander Dimitri Romaschin

Place of Birth: Toronto, Ontario

Date of Birth: May 25, 1951

Education:

BSc. - University of Toronto - 1974

Marital Status: Married